Development of Routes to Access and Functionalise [1,2,4]Triazolo[4,3-a]pyrazine Amides as New Antimalarial Compounds

A thesis submitted in partial fulfilment of the requirements for the degree of Bachelor of Science (Honours) in the School of Chemistry at The University of Sydney

Thomas Stuart Charles MacDonald

November 2014

Abstract

With drug resistance a growing concern in the treatment of malaria, new medicines are needed. This work focuses on the development of a new series of [1,2,4]triazolo[4,3-*a*]pyrazine antimalarials. These compounds are thought to target a sodium ion channel in the *Plasmodium falciparum* parasite, and have previously shown rapid clearance *in vivo*.

There are few literature reports of syntheses of [1,2,4]triazolo[4,3-*a*]pyrazines. Here, two distinct synthetic routes are used to access triazolopyrazine derivatives. In a four-step linear pathway, hypervalent iodine effected an oxidative cyclisation of prefunctionalised pyrazinylhydrazones to give the desired triazolopyrazine analogue compounds in good yields. Ten triazolopyrazine amide were prepared using this method, and demonstrated potencies against *P. falciparum* down to 234 nM.

Additionally, a new route was developed to small triazolopyrazine building blocks from hydrazinylpyrazines by Brønsted acid-catalysed condensation with triethyl orthoformate. These simple heterocyclic building blocks are commercially unavailable, and literature preparations are few and low-yielding. Regioselective brominations of these compounds were developed, with the resulting halotriazolopyrazines ideal substrates for cross-coupling based divergent synthetic strategies.

This work was carried out using an open-source science philosophy. Discussions and planning were carried out using open media such as GitHub and Twitter, and data were recorded using an electronic lab notebook. This lab notebook is freely and publicly accessible, and contains all raw data and observations obtained; these results are summarised on an open wiki. By facilitating input from outside contributors, this approach led to constructive discussions with participants from academia and industry.

Statement of Student Contribution

The initial direction of this project was provided by A/Prof. Matthew Todd.

Nuclear magnetic resonance spectroscopic data were obtained by me, initially with assistance from Dr. Ian Luck. Low resolution ESI mass spectrometry was carried out by myself. Low resolution APCI mass spectrometry was carried out by Mr. Marlowe Graham and Dr. Nick Proschogo. High resolution mass spectrometry was carried out by Dr. Nick Proschogo. Elemental analyses were carried out by Dr. Christopher McRae at Macquarie University.

Biological assays were carried out by SynGene, GSK Tres Cantos, and AstraZeneca.

As an open science project, results were discussed publicly over the internet on open platforms. Where input was received from the open scientific community, this has been explicitly acknowledged.

Proof reading was carried out by Dr. Alice Williamson, A/Prof. Matthew Todd, A/Prof. Peter Rutledge, and Mrs. Jane MacDonald. Advice on the structure of this thesis was given by Dr. Matthew Todd and Dr. Peter Rutledge. I certify that this document contains work carried out by myself, except where otherwise acknowledged.

<div align="center">
Thomas S. C. MacDonald
</div>

Acknowledgements

List of Abbreviations

1D	one-dimensional
2D	two-dimensional
Anal.	elemental analysis
AO	aldehyde oxidase
APCI	atmospheric pressure chemical ionisation
app	apparent
bp	boiling point
Calcd	calculated
Chloramine-T	*N*-chloro tosylamide sodium salt
CLogP	calculated water-octanol partition coefficient
CRO	contract research organisation
DCE	dichloroethane
dcpp	1,3-bis(dicyclohexylphosphino)propane
d	doublet
dd	doublet of doublets
ddd	doublet of doublets of doublets
DIPEA	*N,N*-diisopropylethylamine
DMF	dimethyl formamide
DMSO	dimethyl sulfoxide
EI	electron impact
ELN	electronic lab notebook
ESI	electrospray ionisation
FDA	Food and Drug Administration
FTIR	Fourier-transform infrared
g	gram
GSK	GlaxoSmithKline
h	hour(s)
hERG	human ether-à-go-go related gene
HMBC	heteronuclear multible bond correlation
HOMO	highest occupied molecular orbital
HRMS	high resolution mass spectrometry
HSQC	heteronuclear single quantum correlation
HTS	high-throughput screening
Hz	hertz

IC$_{50}$	concentration required for 50% inhibition
LUMO	lowest unoccupied molecular orbital
m	*meta*
m-CPBA	*meta* chloroperbenzoic acid
mg	milligram
MHz	megahertz
min	minute(s)
MMV	Medicines for Malaria Venture
mp	melting point
MS	mass spectrometry
nM	nanomolar
NMR	nuclear magnetic resonance
NOESY	nuclear Overhauser effect spectroscopy
o	*ortho*
OSM	Open Source Malaria
p	*para*
Pfal	*Plasmodium falciparum*
PIDA	phenyliodine diacetate
pK_a	-log acid dissociation constant
ppm	parts per million
PTFE	polytetrafluoroethylene
rt	room temperature
S$_E$Ar	electrophilic aromatic substitution
S$_N$Ar	nucleophilic aromatic substitution
S$_N$1	unimolecular nucleophilic substitution
S$_N$2	bimolecular nucleophilic substitution
t	triplet
T3P	propylphosphonic anhydride
TEA	triethylamine
THF	tetrahydrofuran
TLC	thin layer chromatography
TMS	trimethylsilane
TP	triazolopyrazine, specifically [1,2,4]triazolo[4,3-*a*]pyrazine
TsOH	*p*-toluenesulfonic acid
$\nu_{\max}$ (film)/cm^{-1}	absorption in wavenumbers

Contents

1

Introduction and Background

1.1 Malaria

Malaria is an infectious disease caused by parasitic *Plasmodium*-genus protozoans. Carried by mosquitoes and then transferred to humans by bites, symptoms include fever, vomiting, and headaches. Untreated infections can quickly become fatal. 2012 World Health Organisation (WHO) figures for malaria claim an estimated 207 million cases of infection leading to 627,000 deaths, mainly among young children in Sub-Saharan Africa[1]. More positively, the same report claims that increased funding for malaria control over the last decade has led to a 42% reduction in mortality rates since 2000.
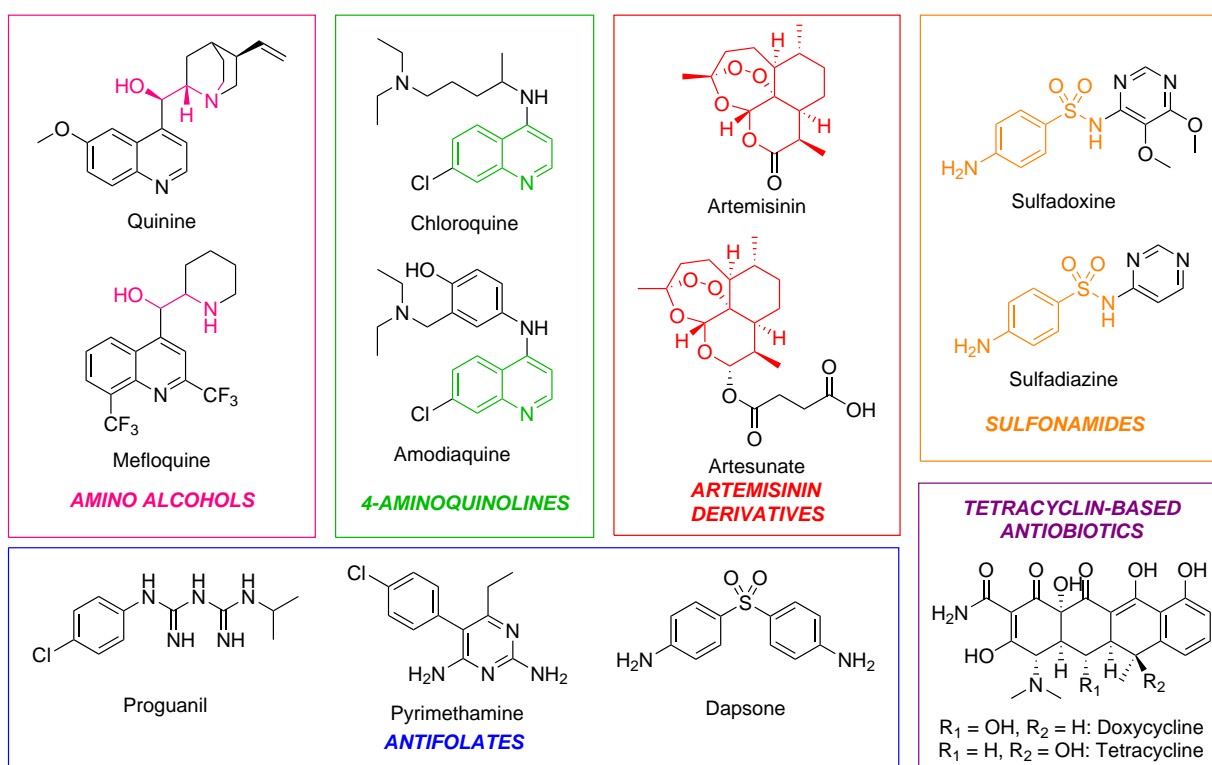
Figure 1.1: Some common classes of antimalarial drugs. The current best treatment is artemisinin combination therapy (ACT), consisting of an artemisinin together with other therapeutics.

Effective treatments for malaria have existed for centuries. The most familiar of these is likely

quinine, which has been used (as the ground bark of the cinchona tree) since the mid 16th century. Quinine remained the main treatment for malaria until the mid 20th century, when synthetic drugs such as chloroquine with fewer adverse side-effects were developed. Unfortunately, developing resistance to these synthetic drugs has rendered many of them ineffective as sole treatments[2]. Currently, the best available treatment involves artemisinin derivatives. Artemisinin is a natural product extracted from the qinghao plant, which was recorded in 340 AD as a treatment for fevers by the Chinese physician Ge Hong and found to possess antimalarial activity in 1971. To slow the development of resistance, artemisinin is generally administered in combination with other drugs as artemisinin-based combination therapy (ACT)[3]. Despite these efforts, over the last decade artemisinin-resistant strains of malaria have emerged in South-East Asia, particularly along the Thai-Cambodian border[4]. At this time, artemisinin-resistant malaria is largely confined to the Mekong delta region, and is still treatable with other medicines. However, the potential development of multi-drug resistant malaria demonstrates the need for research into new therapeutic treatments with new modes of action. Recent years have seen substantial increases in funding to combat malaria: the Bill and Melinda Gates foundation alone has committed over US$2 billion in grants towards a stated goal of the complete eradication of malaria[5].

One organisation that focuses on combating malaria is the Medicines for Malaria Venture (MMV). MMV was established in 1999 as a not-for-profit public-private partnership with the goal of discovering and developing new antimalarial drugs, and obtains funding from public and philanthropic sources. MMV does not itself conduct research, but coordinates the research efforts of partnered academic and industrial instutitions. In doing so, MMV funds a portfolio of activities ranging from early screening and lead-optimisation research through to clinical trials, and improving access to approved antimalarial medicines.

1.2 Open Source Malaria and open source research

1.2.1 Open Source Malaria

Open Source Malaria (OSM) is a project aimed at "...finding, improving and bringing to market new medicines"[6] for malaria by applying open source research. The concept of Open Source originates in software development, and is most familiar in this context. In general, projects are open to interested parties throughout their development, and barriers to participation are as low as possible. The results of this work are often then made freely available for others to

use, either as consumers or for further development. Successful open-source projects include the Linux operating system, the Firefox browser, the GIMP and Inkscape graphics editors, and the Texmaker editor used to prepare this document.

OSM aims to use these principles to accelerate the discovery of new medicines. All data and discussions are accessible to any interested parties online; anyone interested is welcome to participate at whatever level they are capable of, and results of this research will not be patented[6]. Raw data for in-progress experiments are published on an electronic lab notebook[7] (ELN), and discussed over open media such as Twitter and Google+. This methodology is particularly apt for tackling problems seen to lack commercial incentives, such as malaria and other tropical diseases (an Open Source tuberculosis project is also in development). Previously, OSM has worked on optimisation of three compound series identified and publicly released[8] by GlaxoSmithKline: an arylpyrrole series that showed good potency but could not be made metabolically stable, a triazolourea series, and an aminothienopyrimidine series that is still under investigation. OSM is currently actively investigating a fourth series, based on a core triazolopyrazine motif.

1.2.2 Series 4: the triazolopyrazine series
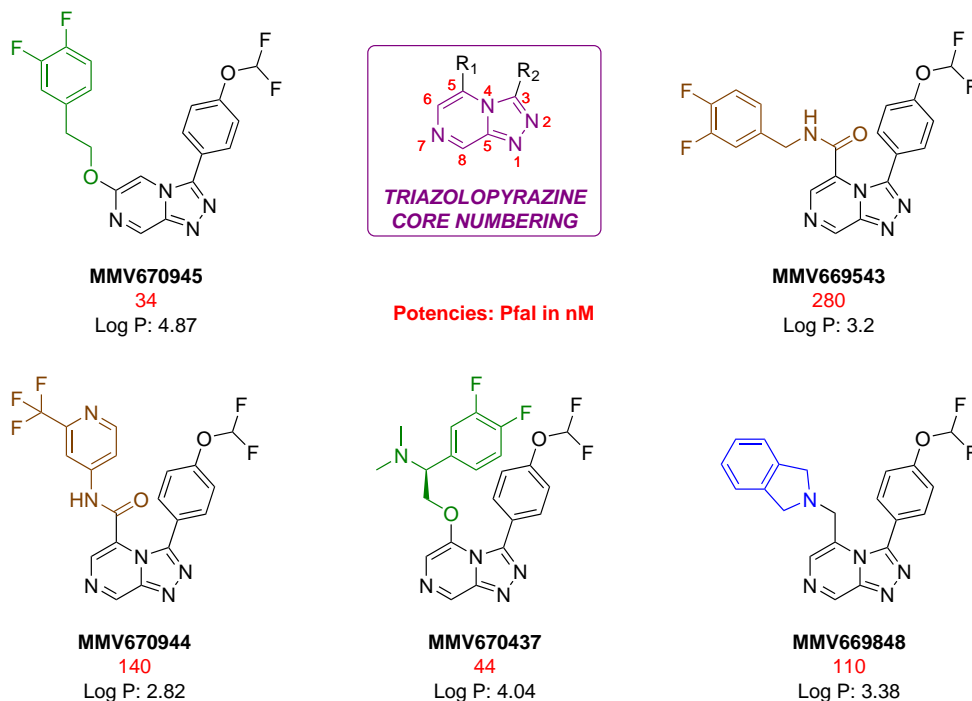
Figure 1.2: Some potent Series 4 compounds that were inherited by OSM from MMV. Inset: the numbering scheme for the TP core. Series 4 compounds generally substitute at the 3 and 5 positions, as shown.

The most recent series of molecules targeted by OSM is Series 4, also known as the triazolopyrazine (TP) series. These compounds consist of a [1,2,4]triazolo[4,3-a]pyrazine core, generally functionalised at the 3 and 5 positions (Figure 1.2). Announced in late 2013 by OSM[9] and MMV[10], Series 4 compounds are though to act by inhibiting the *Pf*ATP4 sodium pump, killing the *Plasmodium falciparum* parasite. The compounds were initially identified by high-throughput screening (HTS) of a Pfizer library (160,000 compounds), and passed through early optimisation first at Pfizer and then at a contract resarch organisation (CRO; this work funded by MMV) before being handed over to OSM for further research. These initial compounds had potencies down to 16 nM, but there were concerns regarding metabolic stability and solubility.

1.3 Nitrogen heterocycles in medicinal chemistry

1.3.1 Nitrogen heterocycles are common in biologically active small molecules

1. Piperidine 2. Pyridine 3. Piperazine 4. Cephem 5. Pyrrolidine 6. Thiazole 7. Imidazole 8. Penam 9. Indole 10. Tetrazole
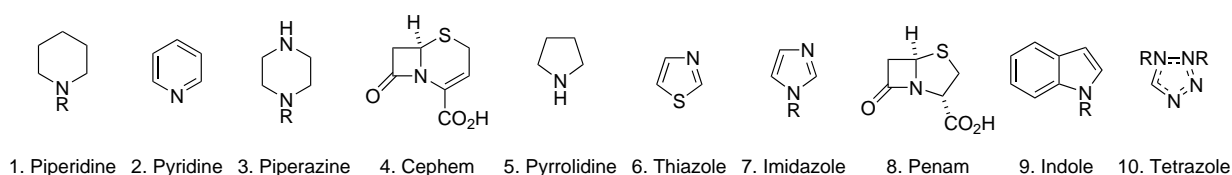
Figure 1.3: The ten most common heterocyclic motifs in approved pharmaceuticals, as found by Vitaku *et al.* [11]

A recent survey[11] of FDA-approved small-molecule pharmaceuticals found that 84% contain at least one nitrogen atom, and 59% at least one nitrogen heterocycle. The authors note that these heterocycles are thus far more common than the presence of sulfur (26%) and fluorine (13%) atoms. The ten most common of these heterocyclic motifs are shown in Figure 1.3.

Any discussion of nitrogen heterocycles in the context of antimalarials would be incomplete without mention of the original antimalarial compound, quinine. This molecule contains two heterocyclic motifs: the aromatic quinoline system, and the saturated bicyclic quinuclidine. Returning to the list of common treatments for malaria presented earlier (Figure 1.1), it can be seen that the quinoline has remained a common core for many newer antimalarial compounds.

As well as synthetic pharmaceuticals, it is worth briefly noting the importance of *N*-heterocyclic biomolecules. The purine and pyrimidine nucleoside bases (Figure 1.4) are perhaps the most familiar of these. As a structural isomer of the triazolopyrazines, the purine core is a particularly apt demonstration of the relevance of polyaza bridged heterocycles to biological systems.

4
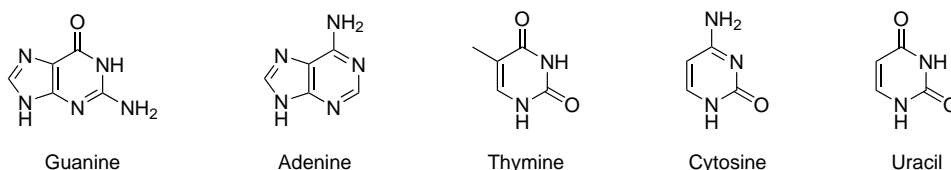
Figure 1.4: The five purine- and pyrimidine-derived nucleoside bases.

1.3.2 Aldehyde oxidase can metabolise azaheterocycles

Aldehyde oxidase (AO) is a molybdenum-containing enzyme that catalyses reactions of the form $C-H \longrightarrow C-OH$, where the carbon is either part of an aldehyde or part of a nitrogen heterocycle[12]. As other enzymes such as aldehyde dehydrogenase are more active at degrading aldehydes, oxidation of aldehydes is not (despite the name) thought to be a major function of AO[13]. Oxidation of heterocycles by AO is thought to follow from an initial nucleophilic attack on a cyclic carbon atom (Figure 1.5). It follows that heterocycles more prone to nucleophilic attack are more prone to oxidation by AO. The presence of electron-withdrawing motifs such as carbonyl derivatives, halogens, and basic centres that will be protonated at physiological pH are thus potentially problematic when combined with azaheterocycles.
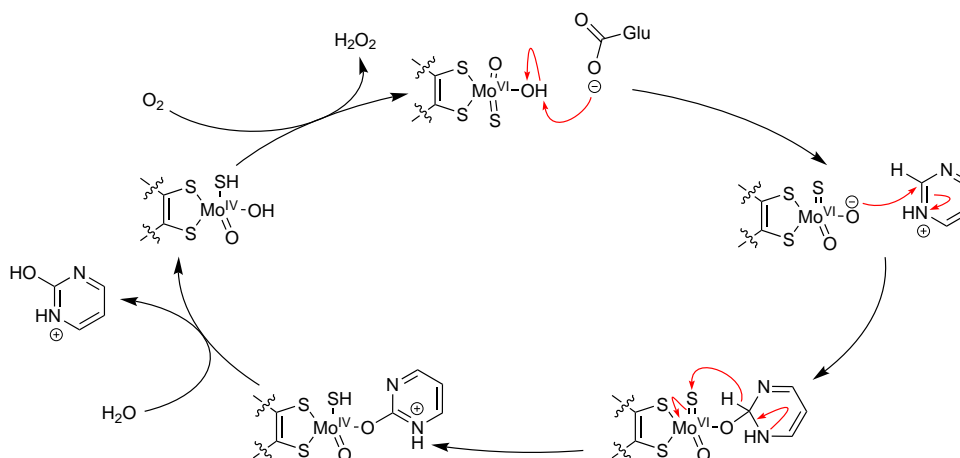
Figure 1.5: The proposed AO mechanism of action[14]. Nucleophilic attack by a Mo^{VI}-coordinated oxygen on a heterocyclic carbon leads to an oxidised heterocyclic species and a reduced Mo^{IV} centre. Hydrolysis releases the oxidised heterocycle, and the molybdenum centre is re-oxidised to Mo^{VI} by molecular oxygen, in the process forming hydrogen peroxide. The oxidation of heterocycles by AO requires an initial nucleophilic attack adjacent to a heteroatom. Heterocycles that are activated to nucleophilic attack, such as those possessing electron-withdrawing functional groups, are therefore more prone to oxidation by AO.

The broad substrate scope of AO combined with the prevalence of azaheterocycles in medicinal chemistry makes this enzyme a significant factor when considering the metabolic liability of drug candidates[15]. Further, significant variations in AO activities exist across mammalian species:

several drug candidates showing high bioavailability in mouse, rat, and dog models have been terminated in early clinical trials due to rapid metabolism by human AO[14]. A small selection of substrates known to be oxidised by AO is given in Figure 1.6, together with the core structure of a Series 4 amide. The similarities between the TP core and AO substrates are clear, and the substituted amide can only be expected to increase vulnerability to nucleophilic attack.
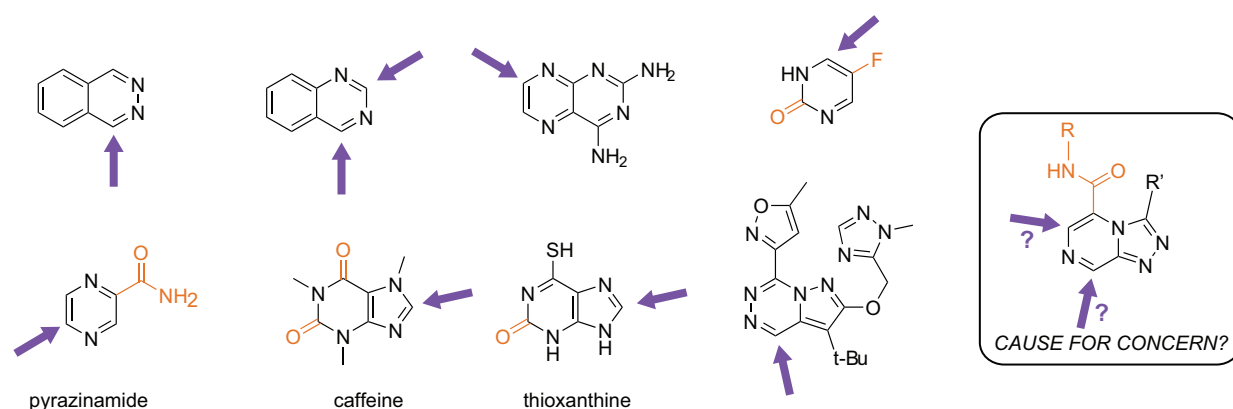
Figure 1.6: Some examples of azaheterocyclic substrates found to be oxidised by AO, selected from a list given by Pryde *et al.* [14]. Positions of attack and electron withdrawing substituents are noted. Inset: a triazolopyrazine amide, with potential positions of vulnerability.

Possible changes to improve metabolic stability against AO can include the addition of electron-donating functional groups (alcohols, ethers, carboxylates) to disfavour nucleophilic attack, or protecting at-risk carbon atoms by replacing hydrogen atoms with other functional groups, such as small halides. While AO susceptibility is hard to predict computationally, a 'litmus test' developed recently by the Baran group[16] might prove useful here. In this technique, a heteroaryl system is exposed to the nucleophilic $CHF_2^{\bullet}$ radical, generated from $Zn(SO_2CHF_2)_2$. AO-vulnerable substrates are difluoromethylated, which can be observed by LCMS as a characteristic M+50 peak.

1.4 Chemistry of heterocycles

1.4.1 Early heterocyclic chemistry

Heterocyclic compounds have been targets of synthetic chemistry since the beginning of modern chemistry. Appropriately enough, some of the earliest research was in attempts to produce synthetic quinine: armed with a chemical formula of $C_{20}H_{24}N_2O_2$ and little idea of the structure he was attempting to make, it was an 1856 attempt to synthesise quinine that led William Perkin to

serendipitously discover the first synthetic organic dye, which he named mauveine. The activity generated by the dye industry in its rush to develop and commercialise new compounds is often described as the beginning of industrial fine chemistry.
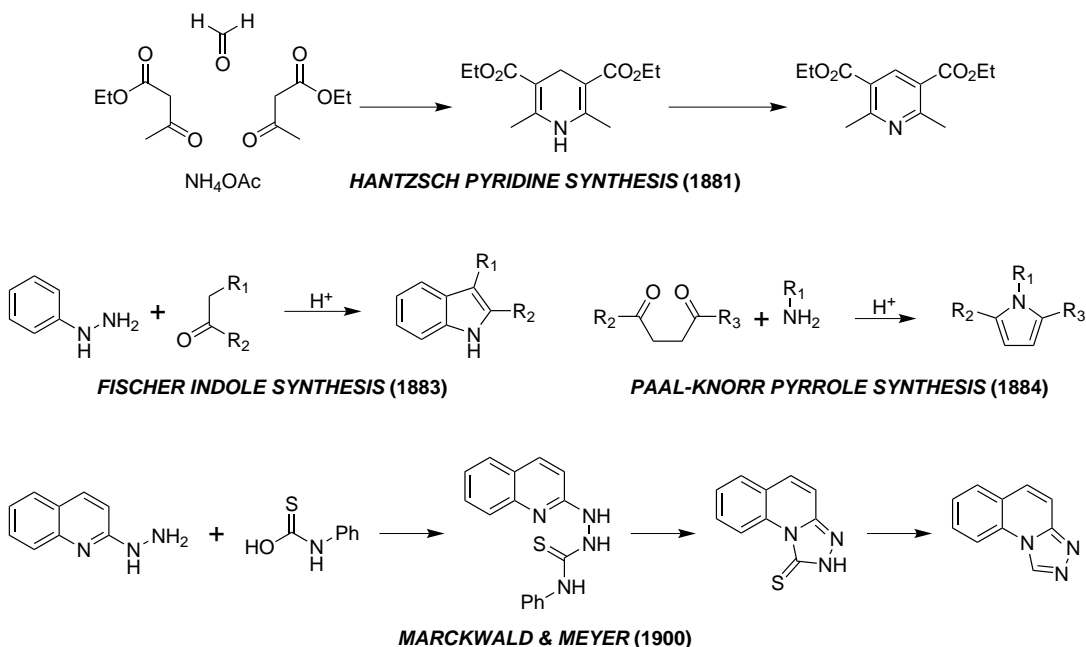
Scheme 1.1: Early techniques for the production of *N*-heterocycles[17,18,19,20]. This 1900 synthesis of a triazoloquinoline by Marckwald and Meyer[21] from the corresponding hydrazinylquinoline is an early demonstration of the types of reactions used to synthesise triazolopyrazines later in this work.

By the end of the 19th century, more systematic access to heterocyclic compounds had been developed. Functionalised pyridines[17], pyrroles[20], and indoles[18,19] were now accessible using the reactions shown in Scheme 1.1. These reactions often proceed from acid-catalysed condensations, with thermodynamically-stable aromatic systems the eventual products. A synthesis of a triazoloquinoline reported by Marckwald and Meyer[21] in 1900 (Scheme 1.1) shows an application of some of these techniques, and is similar to the methods used to access triazolopyrazine cores later in this work.

1.4.2 Divergent synthesis

A characteristic shared by all of these early routes to heterocycles is the use of prefunctionalised starting materials to give functionalised products. Preparing a single compound by these routes is relatively straightforward from appropriate starting materials. However, as the route to each individual compound proceeds linearly from the initial starting materials, there is no efficiency to be found in preparing structurally similar analogues. Preparing a library of compounds will
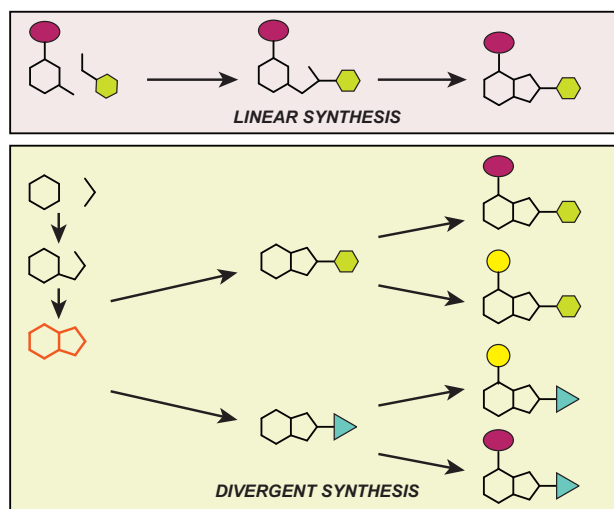
Figure 1.7: Linear and divergent synthetic strategies. In this example, the linear strategy gives a desired bifunctionalised bicyclic compound in two steps, with functional groups determined by the initial reagents. An alternate divergent strategy begins by creating a common core (orange) which is then functionalised. Each individual product of the divergent strategy requires more synthetic steps to access, but when synthesising large numbers of compounds this approach is more efficient overall.

therefore require many repetitive cyclisations from many different starting materials.

A different approach to the *linear* synthesis model would be to sequentially add diversifying substituents to some common core compound. The diversifying reactions would then be the ultimate steps in the route to analogues, and the overall number of reactions performed could be significantly reduced. A diagrammatic example of this *divergent* synthetic strategy is given in Figure 1.7.

Divergent synthetic strategies of the sort described here rely on the ability to create core intermediates posessing 'handles' which can be converted to functional groups. As an example, an alcohol might be transformed into an ether by reaction with alkyl halides, or a carboxylate derivative might be reacted with amines to give diverse amides. Within recent years, these methods have been significantly supplemented by the use of transition metals to catalyse new reactions. A particularly important class of these reactions for medicinal chemistry is the palladium catalysed cross-coupling reactions.

1.5 Palladium catalysis in organic chemistry

The past fifty years have seen homogeneous transition metal catalysts become increasingly important in organic chemistry. In particular, palladium catalysed cross-coupling reactions have

become invaluable tools in the construction of carbon-carbon bonds. In these reactions, a halide-functionalised sp^2 carbon centre is coupled with a nucleophilic carbon partner. Named variants exist for many different nucleophilic carbon centres: boronates (Suzuki[22]), alkenes (Heck[23]), organozincs (Negishi[24]), organotins (Stille[25]), and alkynes (Sonogashira[22]) to name a few. Some of these named reactions are shown in (Figure 1.8.
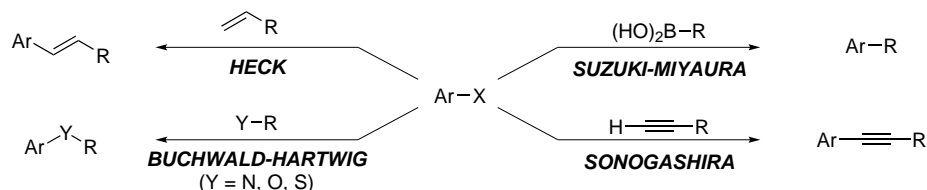
Figure 1.8: Some common palladium-catalysed cross-coupling reactions, where X = I, Br, Cl, or a pseudohalide.

Palladium catalysed cross-couplings are thought to proceed from coordinatively unsaturated palladium(0) complexes. These active compounds are capable of *oxidative insertion* into a carbon-halide bond. As an example, the $Pd^0(PPh_3)_2$ species formed from $Pd^0(PPh_3)_4$ by ligand dissociation is a $14e^-$ complex, and thus highly nucleophilic; by oxidative insertion into an Ar$-$Br bond, a more stable coordinatively saturated $ArPd^{II}(PPh_3)_2Br$ $16e^-$ complex is formed. To favour ligand dissociation and thus production of the active palladium species, sterically bulky electron-rich phosphine ligands are often used, some of which are shown in Figure 1.9.
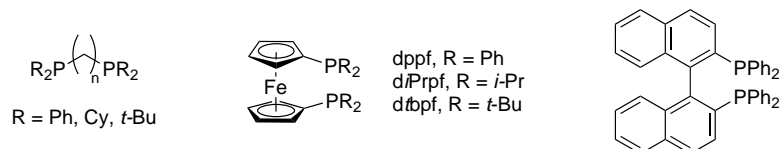
Figure 1.9: A selection of bidentate phosphine ligands commonly used together with palladium catalysts.

As Pd^{II} complexes are electrophilic, nucleophilic coupling partners are needed for reactions. For C$-$C bond-forming reactions, organometallic reagents are used as sources of nucleophilic carbon. These compounds can participate in transmetallation reactions with the palladium complex, transferring the coupling partner onto the palladium centre and removing the coordinated halogen to form a stable metal halide. With two organic functionalities now coordinated to the palladium complex, reorganisation can lead to C$-$C bond formation, and loss of the coupled product. This *reductive elimination* of the product regenerates the Pd^0L_2 active species, completing the catalytic cycle. This mechanism as applied to the Sonogashira reaction between an aryl halide and an alkyne is shown in Figure 1.10.

9
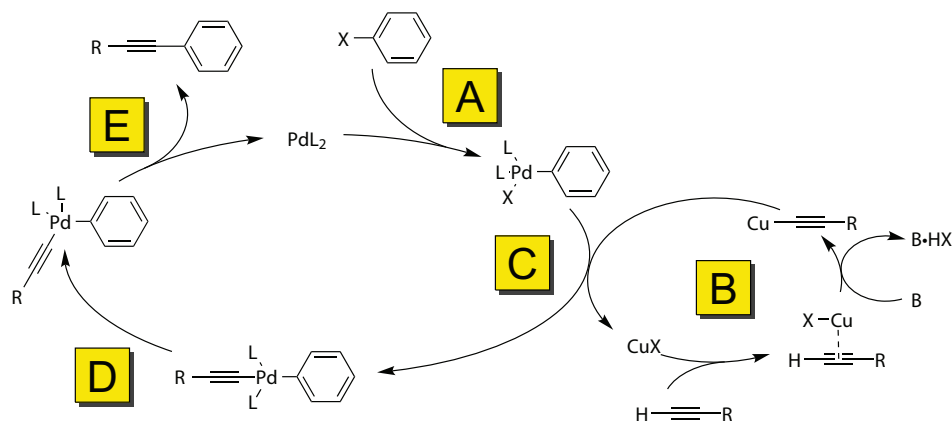
Figure 1.10: The Sonogashira reaction [22] is an example of a palladium catalysed cross-coupling reaction. **A**: the active Pd^0 species oxidatively inserts into an aryl-halide bond, forming an aryl palladium complex. **B**: a separate catalytic cycle generates a copper acetylide by deprotonating an alkyne *via* a copper complex. **C**: the copper acetylide is transferred to the palladium centre in a transmetallation reaction, expelling a copper halide. **D**: the *trans* palladium complex formed earlier isomerises to a *cis* complex. **E**: reductive elimination of the palladium centre, leaving an aryl alkyne species. All of these steps are reversible equilibria.

1.6 Carbonylative coupling reactions

1.6.1 Palladium-catalysed carbonylations

Carbonylative palladium-catalysed couplings were first explored by Heck and coworkers in the early 1970s. While Heck is best known for the palladium-catalysed coupling of aryl halides and alkenes, he also published a number of reports of cross-couplings featuring the incorporation of a carbonyl unit [26,27]. In these reactions, aryl or vinyl halides were reacted with carbon monoxide under catalytic conditions to form acylpalladium complexes, which were then intercepted by nucleophiles to produce the relevant amides, esters, or aldehydes. Mechanistically, this can be understood as a simple extension on the catalytic cycles shown earlier, and a generalised mechanism for this form of coupling is given in Figure 1.11.

Carbonylative variations of palladium-catalysed couplings are not new chemistry, but they are generally less used by academic researchers [29]. These reactions can be technically challenging to conduct: toxic and flammable carbon monoxide is the most commonly used carbonyl source, and many procedures call for long reaction times under significant pressures. However, recent advances in this chemistry remove or at least reduce these difficulties. Improved catalyst-ligand systems allow reactions to proceed at atmospheric pressure [30,31], removing the need for specialist high-pressure equipment. Use of gaseous CO can be minimised to the substoichiometric level by *in-situ* generation [32], or replaced entirely by the use of metal carbonyls [33] as solid, non-volatile
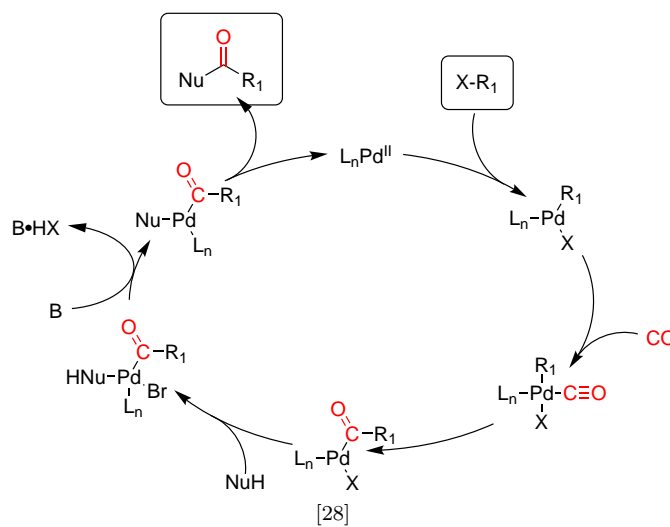
Figure 1.11: A palladium-catalysed carbonylative coupling. The nucleophile can be an alcohol or water (hydroxycarbonylation), an amine (aminocarbonylation), or various organometallics as carbonylative variations on standard coupling reactions.

sources of carbonyl ligands. In an interesting and recent development, it has been reported that the use of molybdenum hexacarbonyl as a CO source allows reactions not only in the absence of carbon monoxide, but also the absence of palladium[34,35,36].

1.7 Project aims

The aims of this project can be divided into three broad areas:

1. Develop a synthetic route to the Series 4 TP amides, and apply to the synthesis of Series 4 analogues. Screen these newly synthesises analogues in various biological assays, learn about structural-activity relations for *P. falciparum* potency, metabolic liabilities, and any unwanted off-target effects.

2. Investigate the fundamental chemistry required to synthesise and functionalise triazolopyrazine heterocycles, and apply any findings to improving the synthetic accessibility of Series 4 compounds.

3. Use an open science philosophy and methodology to help achieve the first two aims by sharing, discussing, and seeking comment on the work being performed in the public sphere.

2

Results and Discussion Part 1:

Synthesis and activities of antimalarial triazolopyrazine amides

2.1 Synthesis of triazolopyrazine amides for anti-malarial screening

Following early CRO research into the triazolopyrazine (TP) series, it was found that substitution at the 3- and 5- positions (generally with two aryl pendant groups) gave compounds with the greatest antimalarial potencies. At the 3- position, monosubstituted aryl groups directly linked to the TP core were preferred, with 4-difluoromethoxyphenyl a representative potent choice. At the 5- position, substituents linked by a heteroatom were found to be most potent (Figure 2.1). The majority of potent compounds investigated carried an ether linkage, but a small number of potent amides were also discovered[37].
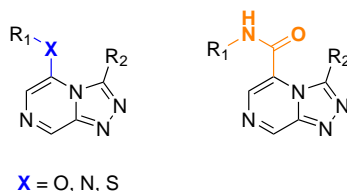
Figure 2.1: Series 4 TPs currently under active investigation. The central triazolopyrazine core is functionalised with two pendant groups at the 3- and 5- positions: the 3- substituent *via* a carbon-carbon bond, and the 5- substituent attached *via* a heteroatom linker. This work focuses exclusively on TPs featuring an amide linker at the 5- position.

Many of the ether compounds synthesised, while active, were disappointingly insoluble. It was hoped that use of the more polar amide linkage could improve solubility: one way of estimating this is CLogP, the calculated octanol-water partition coefficient. A high CLogP indicates a more lipophilic compound, less soluble in an aqueous biological environment. Unfortunately, while some experimental data for the synthesis of the ether compounds were provided by the CRO, these were not provided for the amide-series triazolopyrazines. Development of a route to the triazolopyrazine amides was needed.

2.1.1 Synthetic planning for TP amides
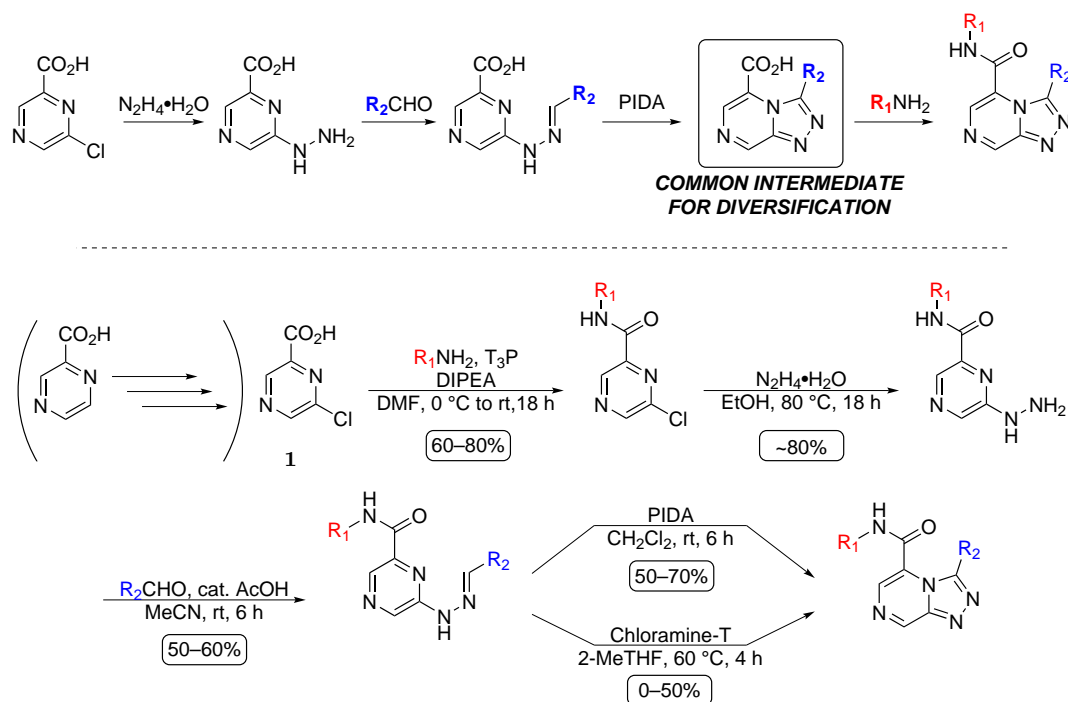
Scheme 2.1: Synthetic routes to triazolopyrazine amides. Top: scheme proposed during initial discussions on GitHub[38]. Later work found the bare carboxylic acid group to be incompatible with hydrazine addition. Bottom: scheme as used in this work, together with representative yields. Chloramine-T was initially used for the final cyclisation reaction, but later replaced by a simpler and more effective PIDA protocol. Both schemes require access to chloropyrazinecarboxylic acid **1**: this compound is commercially available, but expensive. A more affordable source was found in a literature preparation of **1** from pyrazinecarboxylic acid[39].

In late 2013 a route to the desired TP amides was suggested during discussions on GitHub, one of the online platforms used by OSM to plan research[38] (Scheme 2.1). It was hoped that pyrazine carboxylic acid **1** could be used as a starting material to synthesise a functionalised triazolopyrazine-5-carboxylic acid. This compound could act as a common intermediate for rapid synthesis of diverse amides in a final amide coupling reaction. However, early work by Dr Alice E. Williamson found that displacement of the pyrazinyl chloride with hydrazine failed to proceed under the literature conditions[21] of refluxing ethanol. It seems plausible that under these reaction conditions, the carboxylic acid would deprotonate to a carboxylate, which could inductively lower the electrophilicity of the conjugated pyrazine ring and thus prevent the $S_N Ar$ reaction.

Thus, an alternate route was proposed. Instead of carrying through an unprotected carboxylic acid for functionalisation in a final reaction, the amide could be formed in the initial reaction. This amide would not longer disfavour $S_N Ar$ substitution, facilitating the subsequent steps.

2.1.2 Synthetic chemistry
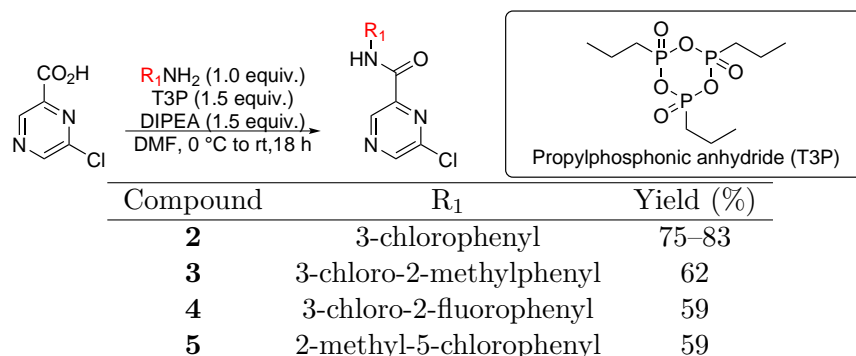
Scheme 2.2: Pyrazine amides were prepared by the coupling of anilines with pyrazinecarboxylic acid **1**. Propylphosphonic anhydride (T3P) was used as a coupling reagent: the reaction is driven by the formation of stable P−O bonds, with the alkyl phosphate byproducts easily removed during an aqueous workup.

The first step in the proposed route was coupling of pyrazinecarboxylic acid **1** and an appropriate amine to give a pyrazine amide. Peptide chemistry provides a vast number of mild and effective protocols for amide formation[40]. Propanephosphonic anhydride (T3P) was found to be satisfactory, with yields of over 50% obtained for all reactions after purification by flash chromatography (Scheme 2.2).
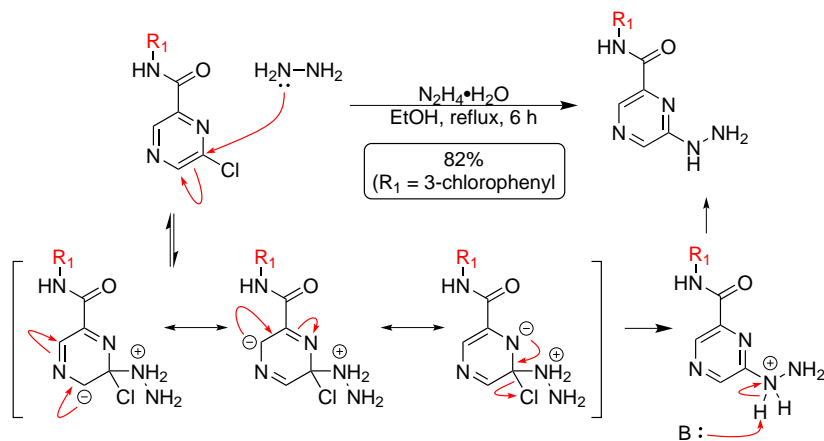
Scheme 2.3: Hydrazinylpyrazines were formed by the nucleophilic displacement of chlorine by hydrazine. Nucleophilic aromatic substitution is favoured by the presence of nitrogen heteroatoms in the ring system capable of stabilising the anionic Meisenheimer intermediate: of the three resonance forms shown, the most significant contributor carries the negative charge on a nitrogen atom. Initially, crude material was carried forward from this reaction without a known yield, but an improved workup was later developed to give pure product. 3-chloroanilide hydrazine **6** was prepared from **2** using this procedure in 82% isolated yield.

Hydrazinyl pyrazines were obtained by nucleophilic aromatic displacement of the chlorine with hydrazine hydrate in refluxing ethanol. Nucleophilic aromatic substitution, generally less

common than electrophilic substitution for aromatic systems, is here favoured by the ability of the heterocyclic nitrogen atoms to stabilise the negatively charged Meisenheimer intermediate through resonance (Scheme 2.3). Initially, compounds were carried forward from this reaction into the following condensation without further purification, but a workup was subsequently developed in which residual hydrazine was washed away from a solution of the crude product in ethyl acetate to give the pure hydrazinylpyrazine. This modification improved yields, and an isolated yield of 82% was achieved for 3-chloroanilide derivative **6**.

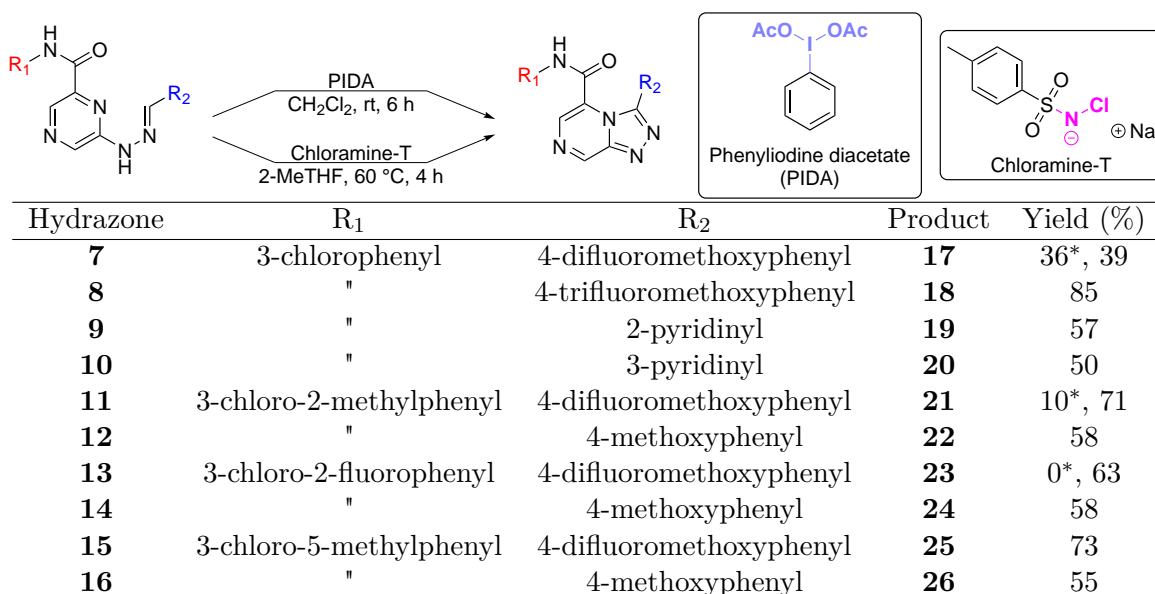| R_1	R_2	Product	Yield (%)
3-chlorophenyl	4-difluoromethoxyphenyl	**7**	46
"	4-trifluoromethoxyphenyl	**8**	94
"	2-pyridinyl	**9**	44
"	3-pyridinyl	**10**	57
3-chloro-2-methylphenyl	4-difluoromethoxyphenyl	**11**	56
"	4-methoxyphenyl	**12**	63
3-chloro-2-fluorophenyl	4-difluoromethoxyphenyl	**13**	56
"	4-methoxyphenyl	**14**	55
3-chloro-5-methylphenyl	4-difluoromethoxyphenyl	**15**	58
"	4-methoxyphenyl	**16**	50
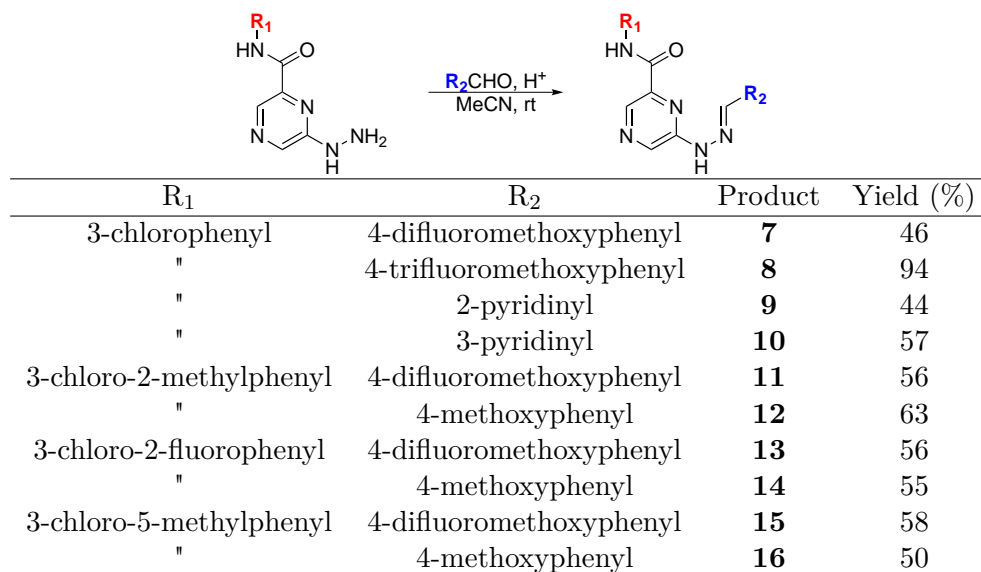
Scheme 2.4: Synthesis of hydrazones by acid-catalysed condensation between hydrazinylpyrazines and an aryl aldehyde; yields are after purification by flash chromatography.

The penultimate step in this sequence was the acid-catalysed condensation of the hydrazinylpyrazine with an aromatic aldehyde, to give diversified hydrazones capable of undergoing oxidative cyclisation to give the desired TP final products. Yields varied greatly (Scheme 2.4), with **8** anomalously high compared to a general range of 50–60%. Crude products were purified by column chromatography before being carried forward, using ethyl acetate in hexanes on silica. A 1% triethylamine additive was used for pyridinylhydrazones **9** and **10**, as these basic compounds were found to protonate and streak under normal solvent conditions.

Finally, the hydrazones were transformed to triazolopyrazines by oxidative cyclisation. Following the literature, two oxidising agents were investigated: phenyliodine diacetate (PIDA)[41], and chloramine-T[42]. Chloramine-T gave consistently low yields, with large amounts of starting material recovered under the literature conditions. Cyclisation with PIDA generally gave acceptable yields, and was a simpler reaction to run: stirring at rt and removal of solvent gave crude

Hydrazone	R$_1$	R$_2$	Product	Yield (%)
7	3-chlorophenyl	4-difluoromethoxyphenyl	**17**	36*, 39
8	"	4-trifluoromethoxyphenyl	**18**	85
9	"	2-pyridinyl	**19**	57
10	"	3-pyridinyl	**20**	50
11	3-chloro-2-methylphenyl	4-difluoromethoxyphenyl	**21**	10*, 71
12	"	4-methoxyphenyl	**22**	58
13	3-chloro-2-fluorophenyl	4-difluoromethoxyphenyl	**23**	0*, 63
14	"	4-methoxyphenyl	**24**	58
15	3-chloro-5-methylphenyl	4-difluoromethoxyphenyl	**25**	73
16	"	4-methoxyphenyl	**26**	55

Scheme 2.5: Oxidative cyclisation of hydrazones to the bicyclic triazolopyrazines. Initially, chloramine-T was used as an oxidising agent, but was later replaced by hypervalent iodine in the form of phenyliodine diacetate (PIDA). Yields are given after isolation and purification by flash chromatography. Yields marked with * refer to the chloramine-T cylisation protocol; all other yields refer to the use of PIDA.

product, as opposed to the reflux and workup involved in the chloramine-T reaction. In both cases, purification by flash chromatography (silica, ethyl acetate/hexanes) gave the desired products. Yields after purification for reactions with PIDA and the small number using chloramine-T are presented in Scheme 2.5.

2.2 Synthesis of key starting material 6-chloro-2-pyrazinecarboxylic acid

The synthetic route to series 4 TP amides (Scheme 2.1) required 6-chloro-2-pyrazinecarboxylic acid **1** as a starting material. While commercially available material was initially used to validate the reactions detailed above, this compound is expensive (>\$50 per gram). A literature route for the preparation of **1** starting from inexpensive and commercially available pyrazine carboxylic acid by esterification, formation of a pyrazine *N*-oxide, nucleophilic chlorination, and finally hydrolysis[39] was investigated (Scheme 2.6). All reagents used were relatively inexpensive, and no purifications by chromatography were reported.

Methyl ester **30** was obtained in quantitative yield from acid-catalysed esterification in refluxing methanol. Treatment of **27** with m-CPBA in refluxing dichloroethane achieved oxidation
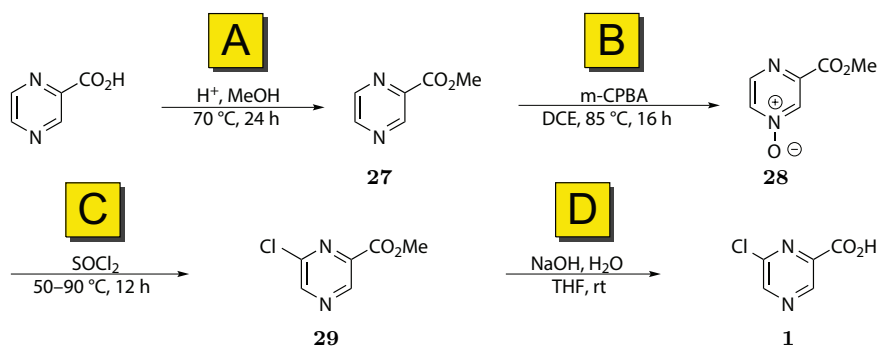
Scheme 2.6: Key starting material **1** was prepared from inexpensive pyrazinecarboxylic acid in four steps. **A**: The carboxylate group was protected as a methyl ester **27** by acid-catalysed esterification. **B**: The pyrazine was oxidised to give *N* oxide **28** by *m*-chloroperbenzoic acid (*m*-CPBA) in refluxing dichloroethane. **C**: The pyrazine *N* oxide was chlorinated with thionyl chloride, to give the desired 6-chloropyrazine system **29**. **D**: The chloropyrazine ester was hydrolysed to give carboxylic acid **1** by the action of aqueous sodium hydroxide in THF.

to the *N*-oxide, but removal of the chlorobenzoic acid byproduct proved surprisingly challenging. Dilution of the reaction mixture with CH_2Cl_2 caused some (but not all) of the chlorobenzoic acid to precipitate. Attempts to purify by concentrating under reduced pressure, cooling the concentrated solution over ice, removing the formed precipitate and repeating never gave product of more than ∼60% purity. An alternate workup involving extraction from a basic ($NaHCO_3$ or Na_2CO_3) aqueous solution with CH_2Cl_2 was attempted, but the highly polar pyrazine *N*-oxide could not be recovered from the aqueous layer. Finally, it was decided to carry the crude product on without further purification. Yield by NMR integration was ca. 70%.

Chlorination to give chloropyrazine **29** was achieved in refluxing thionyl chloride. An exotherm and vigorous bubbling were observed on heating to 50 °C. Exclusive regioselectivity was shown by ^{1}H NMR *J*-coupling analysis: $J = 0.6$ Hz coupling between both observed peaks is consistent only with $^4J_{HH}$, as expected. It is interesting to note that while heterocyclic *N*-oxides generally activate nucleophilic aromatic substitution at positions *ortho* and *para* relative to the *N*-oxide, eventual chlorination here occurs at the *meta* position. This selectivity can be explained by the proposed mechanism given in Scheme 2.7: following initial attack at the 5-position, a second chloride anion attacks the pyrazine at the 6-position rather than acting as a base to abstract H_5, and give the 5-chloro product along with loss of SO_2. The inductively withdrawing ester carbonyl then aids abstraction of H_6, with the loss of Cl_5 returning aromaticity. Following removal of residual thionyl chloride under reduced pressure, the crude product was quenched with water and sodium carbonate solution and re-extracted with CH_2Cl_2 to give a brown oil. By NMR, this crude product consisted of **29**, **27** (presumably from incomplete conversion in the prior oxidation
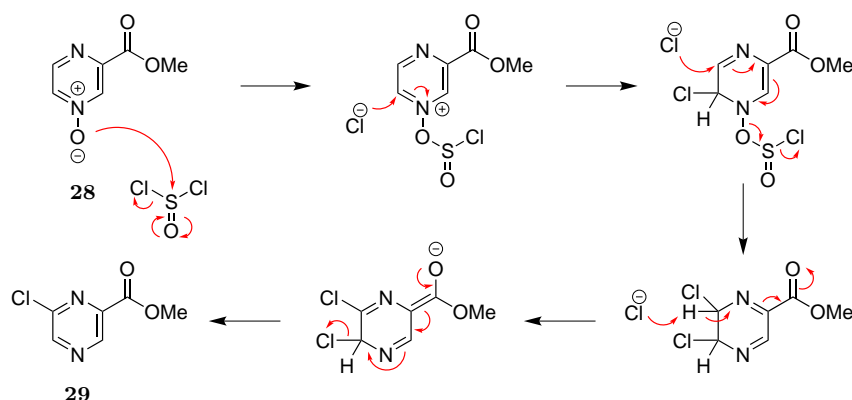
Scheme 2.7: Proposed mechanism for regioselective chlorination of *N* oxide **28** to give chloropyrazine species **29**. Neat thionyl chloride acts both as a nucleophile and source of chloride anions. While nucleophilic substitutions of *N* oxides normally proceed *ortho* or *para* to the oxidised nitrogen, here *meta* selectivity is observed. This is explained by the presence of the electron-withdrawing ester group: deprotonation is favoured at the 6 position, followed by loss of the 5-position chlorine to give **29**.

reaction), and some derivative of remaining *m*-chlorobenzoic acid. The latter was distinguishable by its distinct ^{1}H multiplicities, but the exact chemical species was not identified (an acid chloride or acid anhydride seem likely). A standard flash chromatography separation (hexanes, ethyl acetate, silica) recovered around 60% by mass of the crude product as pure **29**, a yellow oil that solidified to a waxy substance below 20 ℃.
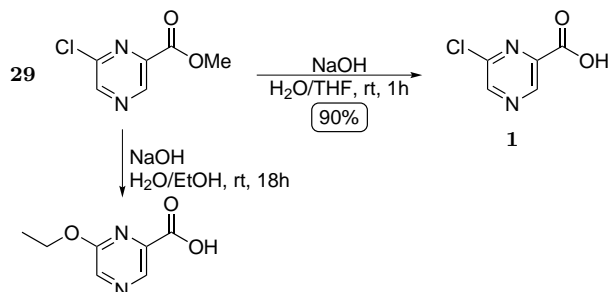
Scheme 2.8: Base-catalysed hydrolysis of **29** to give **1**. Ethanol as a solvent led to incomplete conversion of starting material, and an undesired side reaction giving the ethoxy-substituted product. The use of THF as a solvent gave good yields, and removed the possibility of nucleophilic attack on the pyrazinyl chlorine.

Finally, the desired product **1** was obtained by basic hydrolysis of **29** (Scheme 2.8). The literature[39] reports the used of NaOH in ethanol, but when trialled these conditions led to displacement of the chlorine by ethanol, giving an undesired 6-ethoxy product. After this was established, non-nucleophilic THF was used instead as solvent, giving quantitative formation of **1** within 1.5 h. The brown solid obtained was ∼95% pure by NMR, with minor contamination by persistent *m*-chlorobenzoic acid. As these two organic acids were not easily separable by column chromatography, this was judged acceptable as the amides prepared as the first step towards TP

compounds could be purified far more easily.

2.3 NMR characterisations of triazolopyrazine amides

While several TP analogues had previously been synthesised in this project, no structural assignments had been made by NMR. With little idea of where to find core triazolopyrazine ^{13}C peaks, this made interpreting the spectra of new compounds challenging. Full structural assignment of a model compound would simplify this by providing a starting reference from which the influences of different substituents could more easily be observed.

By using 2D NMR heteronuclear correlation experiments, proton and carbon chemical shifts were completely assigned for model triazolopyrazine compound **17** and its intermediates hydrazone **7**, hydrazine **6**, and amide **2**. These assignments are shown in Figure 2.2.
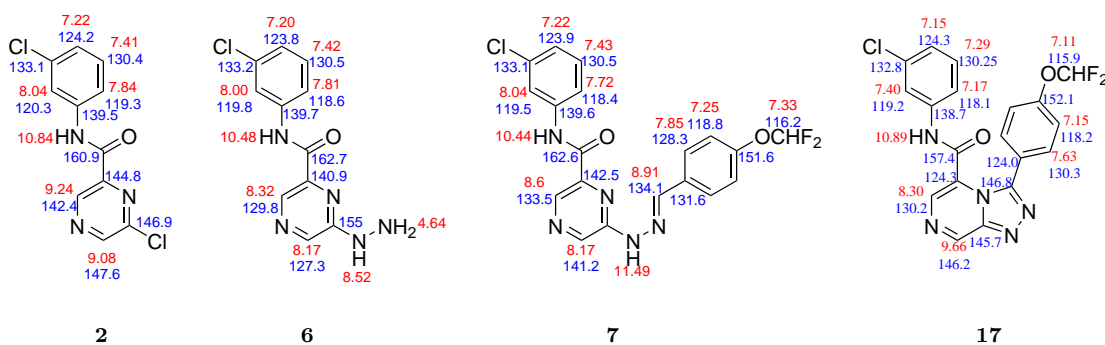

Figure 2.2: Using 2D correlation experiments, NMR spectra were fully assigned for the compounds leading to and including **17**. Proton shifts are in red, carbon shifts in blue. All spectra recorded in DMSO$-$d$_6$ at 400/125 MHz.

As an example of the processes involved, the assignment of the proton and carbon spectra of **2** using the ^{1}H, ^{13}C, HSQC, and HMBC spectra shown in Figure 2.3 follows. The same logic was used to assign spectra of compounds **6**, **7**, and **17**.

Considering first ^{1}H data chemical shifts, there are three distinct areas. Firstly, the lone signal at 10.84 ppm must be assigned to amide proton 6. The two singlets at 9.24 and 9.08 ppm presumably belong to the two pyrazinyl protons, and below that lie the four signals making up the 3-chloroanilide group. Now considering coupling constants, the fine triplet at 8.04 ppm is unambiguously proton 8, and the broad triplet at 7.41 ppm proton 11. The two doublets at 7.22 and 7.84 ppm can be assigned to protons 10 and 12, in unknown order.

Now consulting the 2D data, amide proton 6 is correlated through multiple bonds with carbon signals at 160.9 ppm (unambiguously carbonyl 5), 119.3, and 120.3 ppm. These latter two signals
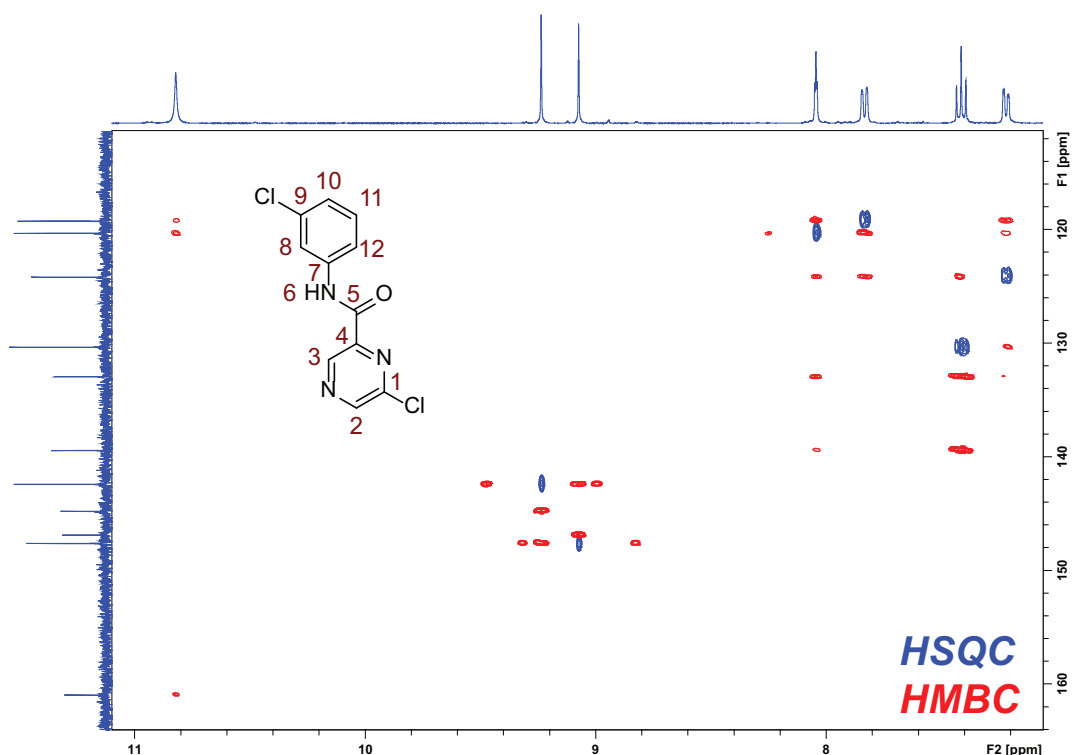
Figure 2.3: Overlaid HSQC (blue) and HMBC (red) spectra for amide **2**. By considering chemical shifts and through-bond correlations, proton and carbon shifts can be assigned to each nucleus present.

have single-bond correlations with protons at 8.04 (already assigned to position 8) and 7.84 ppm; the last of which must therefore be position 12. It follows that the other doublet proton signal at 7.22 ppm and the HSQC-correlated carbon signal at 124.2 ppm must be at position 10. Two other carbon signals at 139.5 and 133.1 ppm show multiple bond correlations to the protons of this aromatic ring: these must correspond to positions 7 and 9. The chemical shift of the carbon bonded to the amide nitrogen might be expected to be slightly higher, and this together with correlation between the signal at 133.1 ppm and proton 10 allows us to assign these two peaks, completing the assignment of this aromatic system.

The two pyrazinyl protons are clearly correlated to four carbon signals: 142.4, 144.8, 146.8, and 147.6 ppm. From the data presented here, it is not possible these signals definitively. However, it seems likely that the through-space deshielding effects of the carbonyl group would shift the nearly adjacent pyrazinyl proton downfield, suggesting that the peak at 9.24/142.4 ppm is in fact 3. From this, the correlated quaternary carbon at 144.8 ppm must be at position 4, the other pyrazinyl proton at 9.08/147.6 ppm at 2, and the final carbon signal at 146.8 ppm at 1. Comparison to the ^{1}H shifts of the final triazolopyrazine **17** supports this: in **17**, long-range correlations can be

observed between the proton marked here as 2, and the quaternary triazole carbon.

Using these reference spectra, the analysis of products of new reactions was made significantly easier. In particular, for compounds with significant $C-F$ splitting such as **23** the discrimination of split carbon signals from multiple single signals was aided by an understanding of approximately where single peaks could be expected to occur.

2.4 Biological screening of synthesised triazolopyrazine amides

2.4.1 *P. falciparum* inhibition

The ten TP amide analogues synthesised were screened against the NF54 (sensitive to all known drugs) strain of the asexual form of *P. falciparum* by SynGene. Activity of the parasite is measured by uptake of radiolabeled hypoxanthine[43] at various concentrations of the compound assayed. Potencies of assayed compounds are expressed as IC_{50}, the molar concentration required for 50% inhibition of activity. The results obtained are given in Figure 2.4.

It is clear that the 3-chloro monosubstituted anilides are superior to the other amides investigated. Further substitutions on the anilidic ring dramatically lower activity: for the 4-difluoromethoxyphenyl-substituted compounds, replacing the 2-hydrogen of **17** with a fluorine atom in **23** triples the IC_{50}. Replacing the fluorine with a bulkier methyl group as in **21** removes potency completely. One exception is the 2-methyl-5-chloro compound **25**, retaining a relatively high potency at 391 nM. These results suggest a very tight binding interaction involving the 3-chlorophenyl, which can easily be disrupted by the presence of additional functional groups near the chlorine.

Considering the $C-C$ linked pendant group, it is unfortunate that the two pyridinyl compounds synthesised were inactive, as this would have been an easy way to lower LogP and increase solubility of future compounds. Otherwise, the di- and trifluoromethoxy groups show similar potencies, while the p-anisole appears to dramatically lower potencies.

2.4.2 Possible off-target inhibition of hERG

When developing new medicines, off-target effects are always a concern. A potent compound may cause unacceptable risks when administered *in vivo*, leading to expensive and embarrassing failures in pre-clinical trials. One protein recognised as being particularly vulnerable to small-molecule drug interaction is hERG (the protein expressed by the human ether-à-go-go related
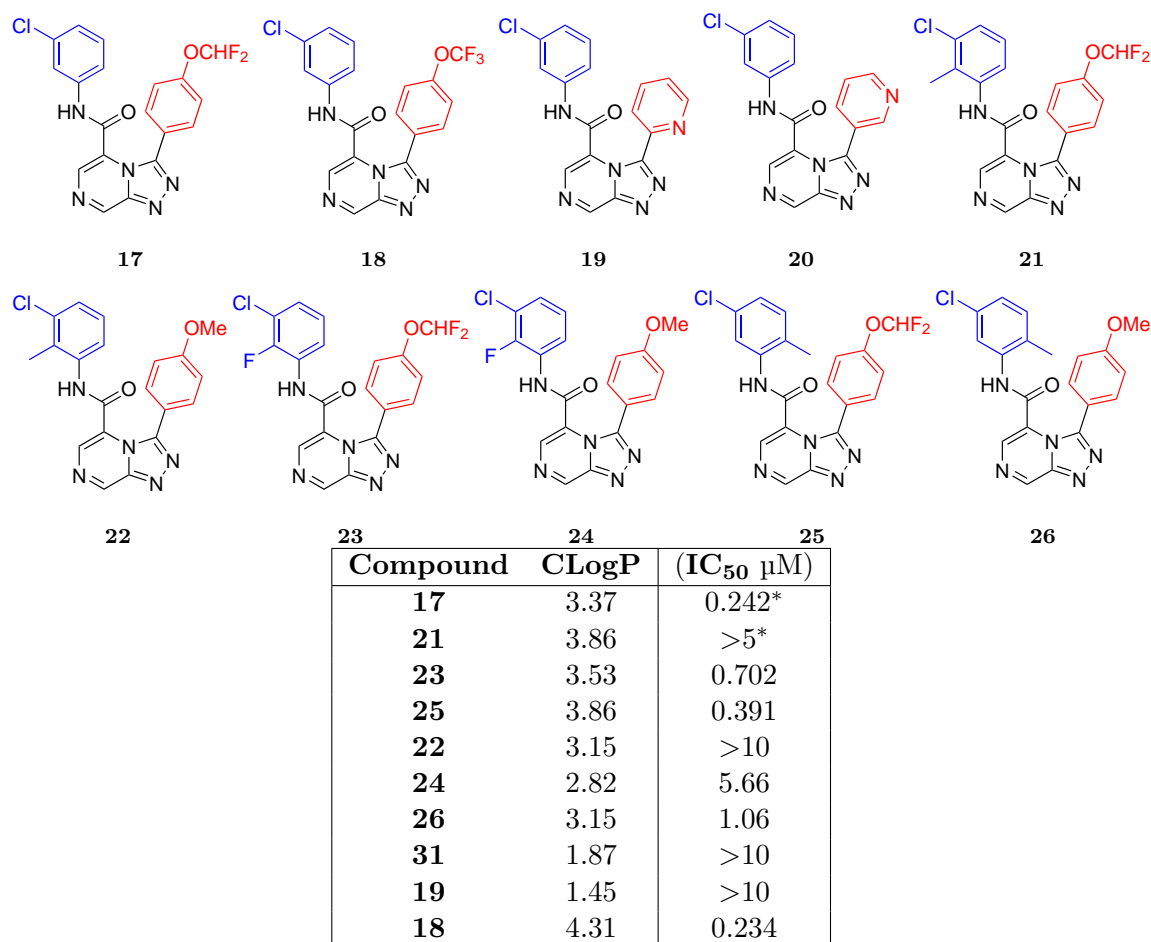
Figure 2.4: Potencies of evaluated compounds against *P. falciparum*, as IC$_{50}$. * denotes compounds evaluated by GSK Tres Cantos; all other assays were performed by SynGene.

Compound	CLogP	(IC$_{50}$ μM)
17	3.37	0.242*
21	3.86	>5*
23	3.53	0.702
25	3.86	0.391
22	3.15	>10
24	2.82	5.66
26	3.15	1.06
31	1.87	>10
19	1.45	>10
18	4.31	0.234

gene), a potassium ion channel involved in controlling cardiac action potential[44]. Binding to hERG risks cardiac arrhythmia, and potentially sudden death[45]. As such, early screening for hERG interactions is now a standard procedure in drug discovery. To investigate potential hERG interactions of Series 4 compounds, a selection were sent for screening using a 'medium-throughput electrophysiology-based hERG assay using IonWorks™ HT' at AstraZeneca[46]. Results are provided in Figure 2.5.

All compounds assayed show hERG binding, with the amides appearing to show slightly higher hERG binding than the ethers. Since any real-world dosage of these compounds would depend on the activity against *P. falciparum*, a more useful comparison is the difference in potencies between hERG and Pfal inhibitions: a highly potent compound with relatively high hERG binding might be usable in low enough concentrations to be safer than a less potent compound with lower hERG binding. Comparing these results, the ether compounds generally show a selectivity for Pfal over
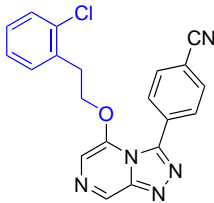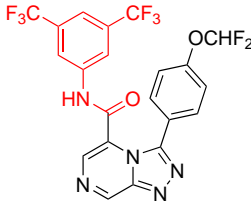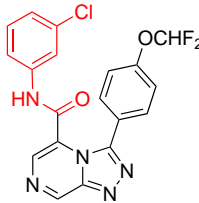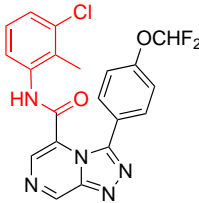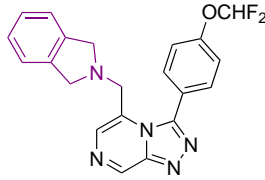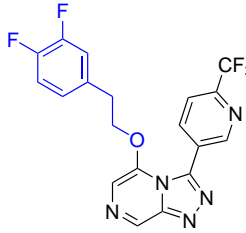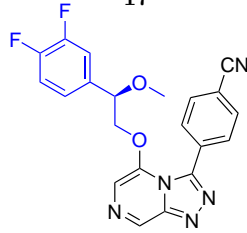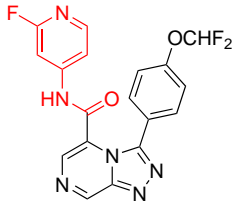
Figure 2.5: A selection of Series 4 compounds screened for hERG activity by AstraZeneca. hERG activity is given as -pIC$_{50}$, the negative logarithm of molar IC$_{50}$. Pfal activity is given in nM and -pIC$_{50}$. A measure of the selectivity of the screened compounds for Pfal inhibition over hERG inhibition can be found by taking the difference in -pIC$_{50}$ values for Pfal and hERG.

Compound	hERG -pIC$_{50}$	Pfal (IC$_{50}$, nM)	PFal -pIC$_{50}$	Relative affinity for Pfal
MMV639725	>4.48	309	6.51	2.03
MMV675719	5.24	309	6.51	1.27
MMV669542(**17**)	4.89	242	6.62	1.73
MMV675718 (**21**)	5.12	>5000	<5.30	<0.18
MMV669848	>4.53	110	6.96	2.43
MMV670936	>4.48	262	6.58	2.10
MMV669844	5.20	40	7.40	2.20
MMV670944	5.60	140	6.85	1.25

hERG of >2 orders of magnitude, while the best amide has a difference of 1.73.

Overall, the Series 4 TP amides synthesised show promising but not exceptional potency, and a concerning level of hERG inhibition. More, and more diverse, analogues are required to probe these areas further. While the linear synthetic route developed here could be used to access these future compounds, more efficient chemistry would be desirable. A divergent strategy with late-stage amide diversification would greatly assist the preparation of new compounds: in particular, this could be used to investigate the relationship between TP amides and high hERG binding.

3

Results and Discussion Part 2: Development of a route towards triazolopyrazine building blocks for further functionalisation

3.1 Planning a divergent strategy to improve synthetic access to Series 4 compounds
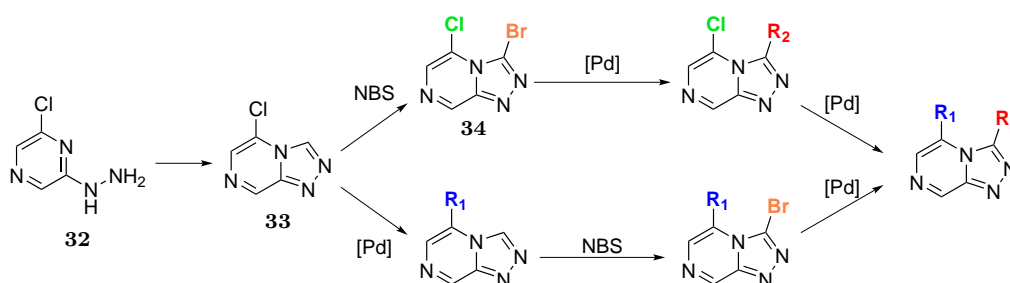
**Scheme 3.1:** Possible diversification from triazolopyrazine building block **33**. Regioselective bromination at the 3- position is combined with well-established cross-coupling reactions to give bifunctionalised triazolopyrazines. Combined with access to large quantities of **12** the two pathways shown would allow rapid synthesis of Series 4 analogues, while allowing easy variation of both R_1 and R_2 from penultimate intermediates.

The scheme used for synthesis of TP amide analogues has a serious shortcoming: diversity is introduced very early, so repetitive linear chemistry (hydrazine addition and oxidative cyclisation steps) is needed to build a library of compounds. In particular, the scheme is not well suited to investigating varying amides. To address these shortcomings, and in the process explore some relatively uncharted chemistry, an alternate scheme was proposed (Scheme 3.1). 5-Chlorotriazolopyrazine **33** would be used as a common core to access 3,5 bifunctionalised TP derivatives. It was thought that the more electron-rich triazole ring would direct electrophilic halogenation at this position, allowing access to the 3-bromo derivative. If achieved, this would open two possible paths to diversified triazolopyrazines: either a cross-coupling with the heterocyclic chlorine, followed by bromination and then a second cross-coupling, or an initial bromination followed by two consecutive selective cross-coupling reactions. As oxidative insertion of a palladium species into the carbon-bromine bond is known to proceed far more easily with than the

carbon-chlorine bond, selectivity in these reaction was not expected to be a significant concern.

These cross coupling reactions could give access to a wide range of possible derivatives, as discussed earlier. Ideally, carbonylative coupling reactions with either oxygen or nitrogen nucleophiles could be applied to these halo-triazolopyrazines to give either amides or carboxylates (which could be converted to amides in one further step). If this could be successfully applied, then the desired divergent route from a common intermediate to TP amides would be achieved.
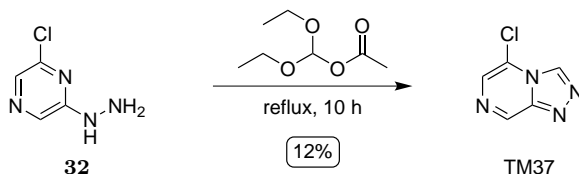
Scheme 3.2: Preparation of **33** from **32** in low yield, as reported by Bradac *et al.* [47].

The first step in this process was ensuring that compound **33** could be accessed in reasonable quantities. Only one preparation is reported in the literature: 2-chloro-6-hydrazinylpyrazine **32** reacted with diethoxy methyl acetate, to give **33** in 12% yield[47] (Scheme 3.2). The authors of this paper note failed attempts to cyclise **32** using triethyl orthoformate, and a mix of triethyl orthoformate and acetic anhydride. This is in conflict with the earlier work of Nelson and Potts[48], which reports effective cyclisations of hydrazinylpyrazines using alkyl orthoesters in xylene. Both of these papers note the failure of conditions successfully used to cyclise hydrazinyl pyridines, pyrimidines, and pyridazines when applied to pyrazine systems. Further, Nelson and Potts[48] found that functionalisation of pyrazine with electron donating groups had no effect on the ease of cyclisation. From these comments, it appeared that the formation of [1,2,4]triazolo[4,3-a]pyrazine building blocks presents unusual challenges that warranted further study.

3.1.1 The effect of Brønsted acid catalysis on orthoester-mediated annulation
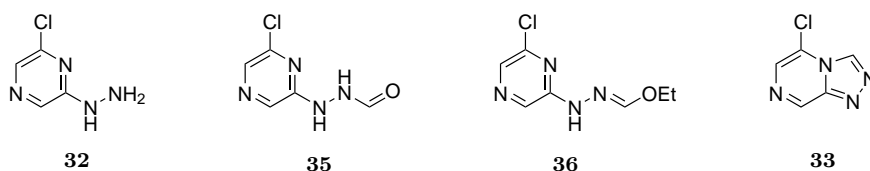

Figure 3.1: Products obtained from various attempts to form **33** by the cyclisation of **32** with formic acid and triethyl orthoformate.

Despite the unpromising literature cited above, it was decided to attempt cyclisation with formic acid and triethyl orthoformate. As a starting point, literature conditions[49] reported for

the cyclisation of hydrazinylpyrimidine with a mixture of formic acid and triethyl orthoformate were used, on hydrazine **32**. **32** was prepared on a large scale (20 g; >90% yield) from commercially available 2,6-dicholopyrazine by reaction with hydrazine hydrate in refluxing ethanol. No cyclisation was observed for the reaction between **32** and triethyl orthoformate in formic acid. Instead, formylated hydrazone **35** was obtained, its identity established by ^{1}H NMR and LCQ-MS. This is a plausible intermediate towards the formation of **33**, but under these conditions no evidence of the required acid-catalysed dehydrative cyclisation was observed. Further, isolation of **35** raises the question of whether the orthoester is required in the reaction at all. To probe this further, additional reactions were conducted, using neat formic acid and neat triethyl orthoformate. The reaction in formic acid yielded **35** as before; the orthoester reaction gave uncyclised ethoxyhydrazone product **36** analogous to the formylated **35** (Figure 3.1). The results from these and all further test reactions are summarised in Table 3.1.

As no evidence of desired product **33** had been observed at this point, the problem was considered mechanistically. In the reaction between **32** and triethyl orthoformate, it seemed clear that each step towards **33** would involve the loss of one molecule of ethanol. Further, as the EtO$^-$ anion is a strong base and therefore poor leaving group, any such mechanism would likely first involve the protonation of an ethoxy group to form an oxonium or oxocarbenium cation. A proposed mechanism is based on these lines of thought is given in Scheme 3.3.

For cyclisation to occur, the pyrazinyl nitrogen lone pair HOMO must be able to overlap a LUMO covering the soon-to-be triazole carbon. In the language of Baldwin's rules for ring closure[50,51], this is a 5-trig reaction, as a 5-membered ring is to be formed by nucleophilic addition to a trigonal carbon centre. Additionally, the cyclisation must be described as either *exo* (in which the breaking bond is exocyclic to the formed ring), or *endo* (in which the breaking bond is endocyclic). In Baldwin's original formulation, a 5-*exo*-trig cyclisation is favoured, while a 5-*endo*-trig cyclisation is disfavoured. This follows from consideration of the Bürgi-Dunitz trajectory[52,53] required as the nucleophile approaches the π^* LUMO of the trigonal system: for an endocyclic ring formation, it is conformationally challenging for this interaction to develop.

The cyclisation here could be considered to proceed by either *exo* (with the oxygen as an electrophile) or *endo* (with the nitrogen filling this role) pathways. The relevant conformations are shown in Scheme 3.3: the conformational difficulty of **36** cyclising is apparent. However, the conformation required for the *exo* cyclisation is not entirely straightforward. All five ring-forming atoms possess sp^2 character, giving a barrier to the rotations required to access the oxocarbenium
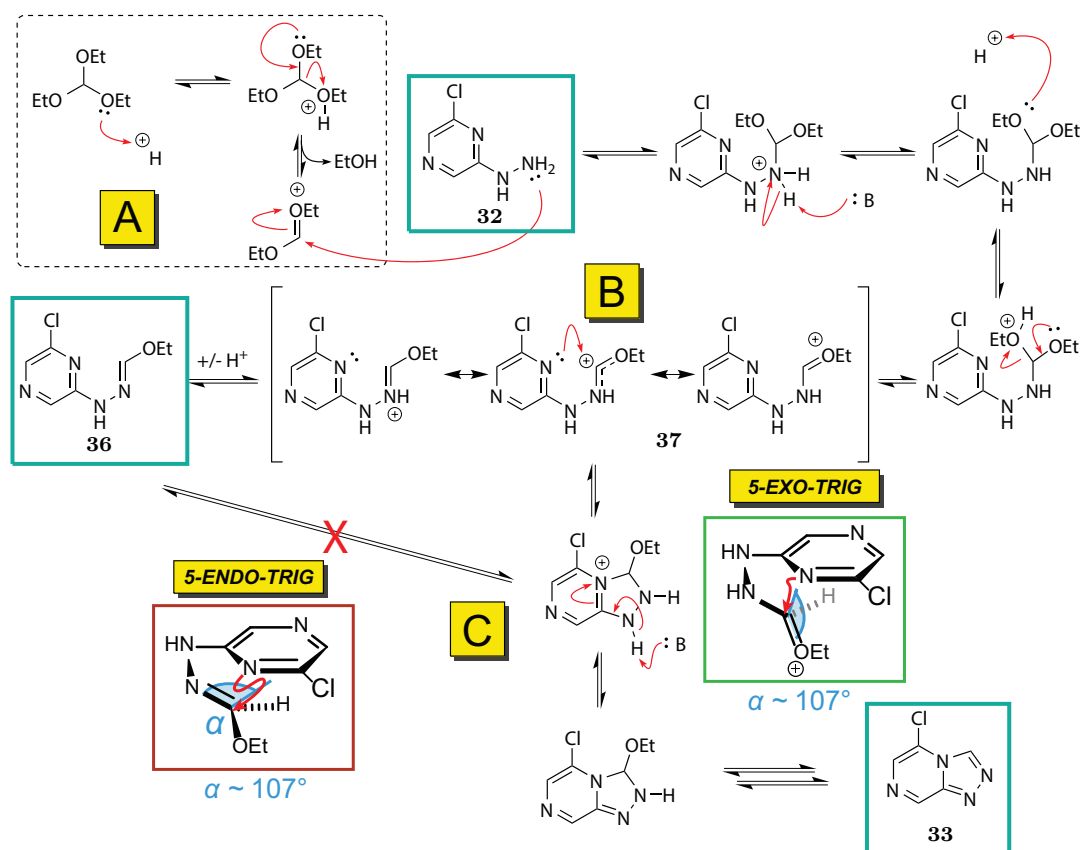
Scheme 3.3: Proposed mechanism for the formation of **33** from **32**. **A**: *Via* an acid-catalysed mechanism, triethyl orthoformate is in equilibrium with an oxocarbenium species. Nucleophilic attack by **32**, proton abstraction by a base, and protonation of a second ethoxy group is followed by electron donation from one of the lone pair-carrying neighbouring heteroatoms to drive off ethanol and give resonance-stabilised carbenium species **37** (**B**). **37** can either be deprotonated to form thermodynamically stable **36**, or cyclise to give the bicyclic compound shown at **C**. Stable intermediate **36** could conceivably cyclise in a 5-endo-trig reaction. However, this is geometrically disallowed[50,51] due to the inability of the nitrogen lone pair to access the π^* imine/iminium LUMO along the required Bürgi-Dunitz angle of $\sim107°$[52,53]. For the 5-exo-trig cyclisation of the carbenium species, this orbital overlap is possible but is likely hindered by the rotational barriers around the extended sp^2 network making the required out-of-plane conformation difficult to achieve. **C**: after cyclisation, deprotonation and loss of ethanol (not shown) will proceed rapidly to give thermodynamically stable **33**.

π^* orbital at the $\sim107°$ Bürgi-Dunitz angle. From this it might be expected that long reaction times and high temperatures would be required to give good yields of **33**.

From this proposed mechanism, formation of **33** could be expected to require catalysis with a strong Brønsted acid, and long reaction times at elevated temperatures. Perhaps surprisingly, there appears to be no suggestion in the literature of this mechanism or use of catalytic acid to effect this reaction. A test reaction using 15 mol % p-toluenesulfonic acid (TsOH) in refluxing neat $HC(OEt)_3$ was attempted, and for the first time **33** was obtained in 17% isolated yield. However, large amounts of **36** were also recovered. While it was unclear if **36** was a stable intermediate on the way to forming **33** or a competing byproduct, the challenge was now to optimise the yield of **33** relative to **36**. To simplify this, ^1H NMR was used to estimate yields from the crude reaction product by comparing the integrations of the aromatic-region signals from **33** present at 9.70, 9.45, and 8.16 ppm to those of **36** present at 10.02, 8.27, 7.90, and 6.97 ppm. The results of various reaction conditions are presented in Table 3.1.

Table 3.1: Investigations into cyclisation of **32** to give **33** using formic acid and triethyl orthoformate. Isolated yields after purification by chromatography are marked by †. Other yields were compared by ^1H NMR integrations comparing the presence of **33** and **36** (see Figure 3.1 for structures): yields given for attempts 5–9 given as ratios refer to the presence of **36** relative to cyclised **33**, respectively.

No.	Reagent	Solvent	Reaction conditions	Yield
1	1 equiv. $HC(OEt)_3$	HCO_2H	reflux, 6 h	formylhydrazone
2	excess HCO_2H	—	reflux, 18 h	formylhydrazone
3	excess $HC(OEt)_3$	—	reflux, 8 h	ethoxyhydrazone
4	"	—	15% TsOH, 18 h	16% †
5	2 equiv. $HC(OEt)_3$	xylene	reflux, 4 h, 18 h	1:7
6	"	—	125℃, 30 h	1:4
7	"	—	15% TsOH, 125℃, 30 h	1.3:1
8	"	toluene	110℃, 30 h	1:20
9	"	"	15% TsOH, 110℃, 30 h	4:1
10	"	"	10% TsOH, 110℃, 40 h	Full cyclisation
11	"	"	20% TsOH, 110℃, 40 h	Full cyclisation
12	"	"	10% TsOH, 110℃, 24 h	49% †
13	"	"	10% TsOH, 110℃, 24 h, 8 g scale	62% †

Although there is scope for further optimisation, yields of over 50% were deemed adequate given the ease and affordability of preparation. It seems reasonable that these conditions could be applied to a range of prefunctionalised chloropyrazine compounds to give simple triazolopyrazine building blocks, although this was not explored further in this work. A brief search using eMolecules found no [1,2,4]triazolo[4,3-a]pyrazine derivatives commercially available for less than $\sim$\$200 per gram, while 2-chloropyrazine derivatives typically cost well under \$1 g per gram. The

acid-catalysed route presented here thus gives inexpensive access to previously unavailable building blocks.

3.2 Functionalising the triazolopyrazine core compounds
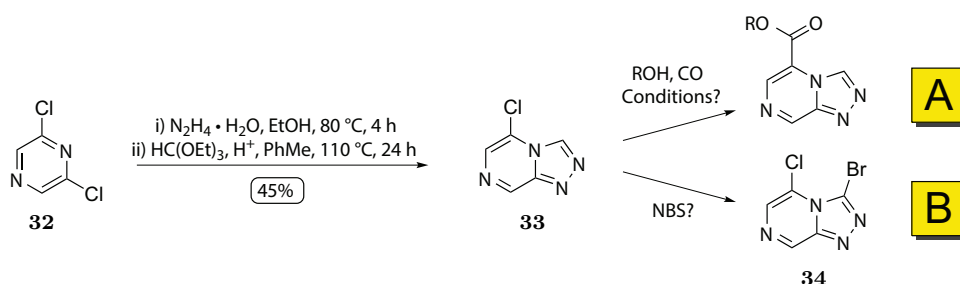
Scheme 3.4: Reactions required to functionalise **33**. **A**: To form the desired Series 4 amides, a carbonylation reaction would be needed. Aminocarbonylations could potentially form desired amides in one step. Alternately, alkoxycarbonylations could be used to form esters or carboxylic acids, which could then be reacted with amines using peptide coupling reagents. **B**: Cross-coupling at the 3- position requires the presence of a halide. Literature reactions with similar triazolopyrimidine compounds[49] suggested that nucleophilic bromonium released by *N*-bromosuccinimide would react to give desired compound **34** in reasonable yield and exclusive regioselectivity.

With **33** now in hand, reactions to functionalise this core were needed. With an eventual goal of Series 4 amide compounds, three chemical transformations were needed (Scheme 3.1). First, carbonylative coupling at the 5- position leading towards amides. Secondly, regioselective bromination at the 3-position to give a handle for functionalisation. Thirdly, the coupling of useful groups with the brominated triazolopyrazine. While the order of these operations may vary, all three needed to be achieved to access the desired compounds. Two strands of investigation were instigated in parallel, working towards cabonylative cross-couplings and regioselective bromination (Scheme 3.4).

3.2.1 Regioselective bromination
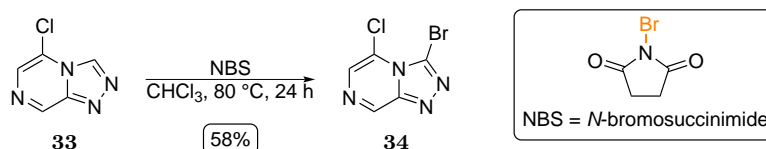
Scheme 3.5: 33 is brominated to give **34**, using NBS as source of electrophilic Br^+. Selectivity presumably arises from the more electron-rich triazole portion of the bicyclic TP system being more prone to electrophilic attack.

While **34** is novel to the literature and this reaction has not been reported in triazolopyrazines, precedent exists for regioselective bromination of analogous triazolopyrimidine compounds with N-bromosuccinimide (NBS) in refluxing chloroform[49]. When these conditions were applied to **33**, the desired **34** was obtained in 58% yield (Scheme 3.5), with the characteristic isotopic splitting pattern confirmed by APCI MS.
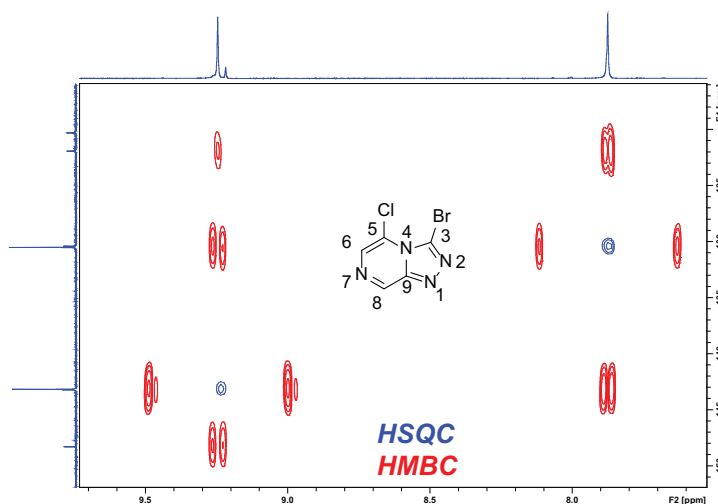

Figure 3.2: Long-range heteronuclear correlations demonstrating regioisomerism of **34** (400 MHz, CDCl$_3$). One carbon signal at 120.27 ppm shows no correlation with either proton signal, confirming that 5-substitution has indeed taken place.

By NMR, one regioisomer was obtained exclusively. Two proton signals were present, which resolved as two 0.6 Hz doublets at 500 MHz. This would seem to support the desired isomer, and was confirmed by the use of 2D heteronuclear correlation experiments (Figure 3.2).

These two proton signals correlate with four carbon signals, while a fifth signal at 120.27 ppm does not correlate with either proton. This is only consistent with the 3,5 substitution pattern expected, with C$_3$ too distant from both H$_6$ and H$_8$ for coupling.
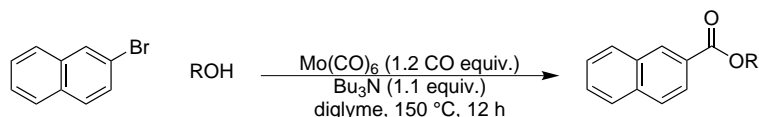
3.3 Carbonylative coupling reactions

Effective carbonylation of the halo-triazolopyrazines synthesised was expected to be the most challenging, and most synthetically interesting, part of the planned reaction scheme. This chemistry is not as well developed as other palladium-catalysed couplings, and heterocyclic substrates are seen as particularly challenging[54]. Here, this chemistry is required to transform the previously obtained halotriazolopyrazines into triazolopyrazine amides. More generally, use of these reactions allows future aryl carbonyl-derived functional groups to be 'masked' as relatively inert aryl halides

until needed.

3.3.1 Molybdenum hexacarbonyl mediated carbonylation

In 2002, the first example of a gas-free carbonylative reaction was reported[55] in which a transition metal carbonyl complex was used as the CO source. While metal carbonyls are also toxic, the convenience of using an air-stable solid instead of gaseous CO is significant. More recently, Ren and Yamane[36] have found that in addition to acting as a CO source (as in $Mo(CO)_6$), Mo^0 can itself act as a catalyst for the carbonylation reaction in the absence of palladium. This chemistry is new and little explored: at the time of writing, no published work from outside the Yamane group has replicated it. Before attempting to apply it to the triazolopyrazine substrate **33**, a model reaction was trialled from the most recent Yamane publication (Scheme 3.6).


Scheme 3.6: A palladium-free, gas-free alkoxycarbonylation as reported by Ren *et al.* [35]. The $Mo^{(0)}(CO)_6$ complex acts as both a carbonyl source, and a coordinating metal centre to catalyse the coupling reaction.

Phenol and water were chosen as two substantially different oxygen nucleophiles for initial testing. Initial reactions were conducted at 150 ℃ in diglyme under a nitrogen atmosphere, but no conversion of starting material was seen by TLC. As the phenol and water seemed to be leaving the solution and condensing on the upper sides of the reaction vessel, the reactions were repeated in sealed tubes. The reaction with phenol gave complete recovery of starting material, but under these conditions a new spot was observed for the reaction with water. Purification by flash chromatography (ethyl acetate, hexanes, silica) gave the desired 2-naphthoic acid in 15% yield (by ^{1}H NMR, compared to a known sample of 2-naphthoic acid). However, attempts to repeat this finding and to prepare the phenyl-2-naphthoate ester were unsuccessful. Email correspondence with A/Prof Yamane confirmed that temperatures above the 162 ℃ boiling point of diglyme and sealed tubes were indeed the best way to achieve good yields, but due to an inability to consistently replicate model conditions, this approach was not pursued further.

3.3.2 Palladium-catalysed alkoxycarbonylation at atmospheric pressure

With the failure of $Mo(CO)_6$ as a carbonyl source, reactions involving gaseous carbon monoxide were considered. The literature reports few reaction conditions that avoid high pressures, high-boiling solvents, or obscure and overly expensive catalyst/ligand systems. The most promising, described by Watson *et al.* [31], reports high yields for the carbonylative coupling between oxygen nucleophiles and various aryl chlorides. One of the heterocyclic substrates used in the paper was chosen to attempt to replicate the reaction (Scheme 3.7). Methyl and ethyl nicotinate were
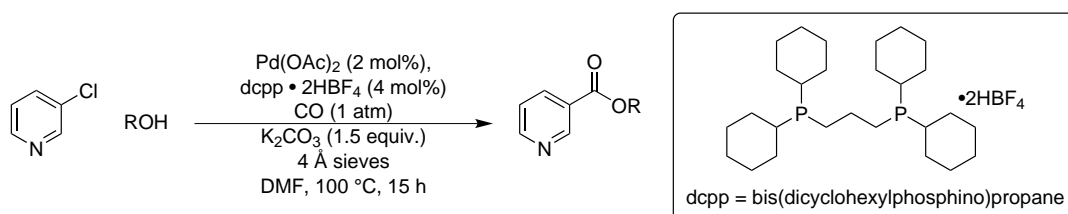
Scheme 3.7: Preparation of nicotinate compounds from 3-chloropyridine and atmospheric pressure CO, as reported by Watson *et al.* [31]. Unlike many gaseous carbonylations, no elevated pressures are required.

obtained from 3-chloropyridine in 62% and 53% yield respectively after only 5 hours. With this replication of the original results, these conditions were applied to attempt carbonylative coupling between **33** and phenol. After 3 h, a new spot was observed by TLC, so the reaction was worked up and purified by column chromatography. By ESI MS the mass was 28 less than expected, which can be explained by formation of a triazolopyrazine phenol ether, as shown in Scheme 3.8. Presumably, this occurs by a S_NAr mechanism involving the phenoxide anion: with a pK_a of 9.95, phenol would be significantly deprotonated by K_2CO_3 (HCO_3^- $pK_a = 10.83$). Repeating this reaction without palladium or ligand gave the same results, showing this to be a standard nucleophilic displacement without metal catalysis. As formation of the phenol ether occurred
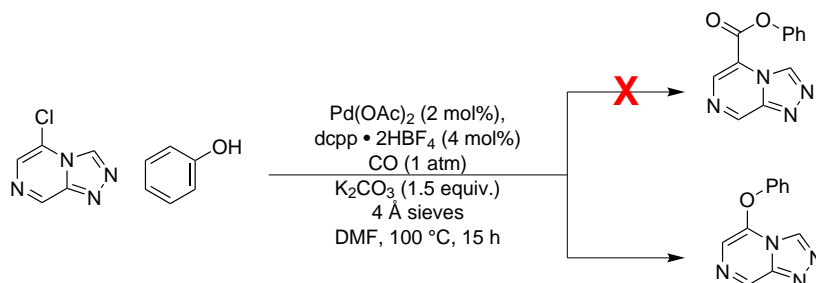
Scheme 3.8: Attempted alkoxycarbonylation of **33** with phenol. Instead of the desired ester, a phenolic ether was formed.

far more quickly than the 10–15 h reaction times reported for this reaction, a less active oxygen

nucleophile was needed. With pK_as of 15.5 and 15.9 respectively, methanol and ethanol seemed appropriate candidates, and were used for all further reactions.

Repeating the conditions of Scheme 3.8 but with methanol or ethanol as nucleophile, no conversion of starting material was observed by TLC. Further, after heating for half an hour the reaction mixture became brown and murky. For palladium-catalysed reactions this generally means that the catalyst has been inactivated, either by formation of palladium oxide or aggregation to form palladium black. This is almost inevitable over time in homogeneous transition metal catalysis, and so the hope is that a reaction can go to completion before the catalyst is inactivated. Repeating the reactions again sparging the solution with argon prior to heating and multiple evacuation-refills (first with nitrogen, then argon, then finally CO) gave no improvement and no conversion of starting material. The DMF solvent was replaced with DMSO (another solvent reported in the Buchwald paper), and $Pd(OAc)_2$ was replaced with more active Pd^0 sources $Pd(PPh_3)$ and $Pd(dba)_2$, but none of these changes brought any improvements.

3.3.3 Preparation of more active halo-triazolopyrazines

Palladium-catalysed reactions involving aryl halides are known to begin with oxidative insertion of Pd^0 into the aryl halide C–X bond. As this involves breaking of the bond, some halides (or pseudohalides) are significantly easier to react with than others. Generally, this order of reactivity is I > Br > Cl. With the failure to perform alkoxycarbonylation on chlorotriazolopyrazine, it was thought that the bromo- or iodo- derivatives might be more active. A literature route to 5-bromotriazolopyrazine **38** from triazolopyrazine **39** was found[47]. As **39** could presumably be prepared using the cyclisation protocol developed earlier, the route shown in Scheme 3.9 was proposed. Formation of **39** proceeded as expected using the conditions developed earlier. On addition
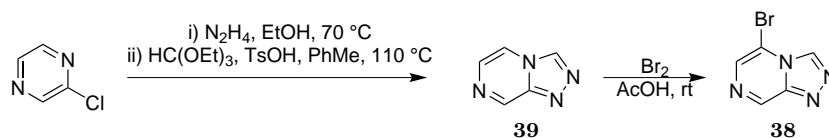

Scheme 3.9: Synthesis of 5-bromo triazolopyrazine **38**. Unfunctionalised triazolopyrazine **39** was prepared from chloropyrazine in two steps according to the protocol developed earlier, then reacted with Br_2 in acetic acid to give **38**.

of stoichiometric bromine to a solution of **39** in acetic acid, a yellow-orange precipitate formed. This precipitate was isolated by filtration, washed with sodium carbonate solution to remove the

hydrogen bromide byproduct, and extracted with CH_2Cl_2 to give **38** in 97% yield. Only one product was obtained, with ^{1}H NMR shifts in agreement with the literature[47]. The high yield and ease of preparation make this a simple and effective route to the desired 5-bromotriazolopyrazine. Unfortunately, due to time constraints and having exhausted supplies of the ligand required, no attempts could be made to carbonylate this material.

Two attempts were made to prepare the 5-iodo compound **40** by nucleophilic displacement from **33** using a Finkelstein reaction[56], a well-known protocol for halogen exchange. Originally reported for primary alkyl halides, a system is set up where an organohalide is in equilibrium with a different halide from a mineral source *via* an S_N2 mechanism. By choosing an appropriate solvent that only some of these compounds are soluble in, the equilibrium can be pushed to completion. A common example is acetone, in which sodium iodide is soluble but sodium chloride is not. Thus reaction between sodium iodide and an alkyl halide in acetone, while slow, can lead to formation of the alkyl iodide with precipitation of sodium chloride. As aromatic systems are not generally prone
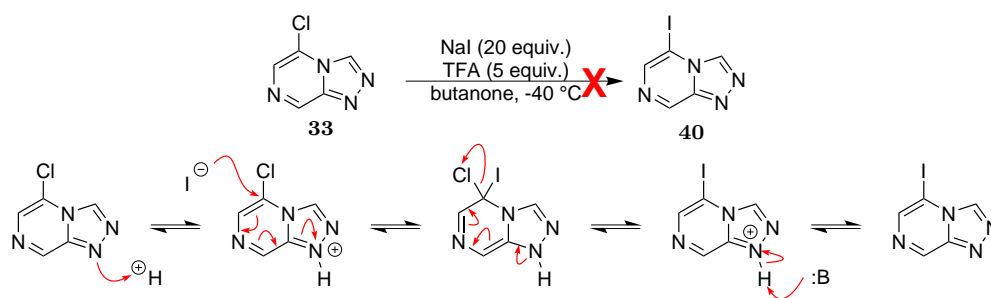
Scheme 3.10: Acid-catalysed Finkelstein reaction, using the conditions of Liu *et al.* [57]. A protonated triazolopyrazine species withdraws electron density from the 5-position, and stabilises the non-aromatic Meisenheimer intermediate. Precipitation of insoluble sodium chloride from the solution drives the equilibrium to the right.

to nucleophilic attack, this reaction is limited in scope, although a recent advance uses a copper catalyst to promote halogen exchange[58]. However, given how prone to nucleophilic substitution the triazolopyrazine compounds have already been found to be, the reaction was attempted under a more traditional set of conditions. Liu *et al.* [57] use trifluoroacetic acid and sodium iodide to convert chloropurine nucleosides into iodopurines, with butanone used as a solvent at -35 ℃ for the reason of relative solubilities mentioned previously. The authors suggest that the protonated purine species is activated to nucleophilic attack, thus creating the equilibrium conditions needed. A route using these conditions, together with a suggested mechanism, is given in Scheme 3.10.

Unfortunately, after 5 h no precipitate was observed to form, and no new spots were observed by TLC. The mechanism seems plausible and warrants further investigation; however, this was

not possible due to time constraints. One other attempt was made to obtain **40** by heating sodium iodide and **33** at reflux in acetone for 24 h. Again, no product was observed.

4

Conclusions and Future Work

While routes toward some triazolopyrazine building blocks were developed, due to time constraints these compounds were not functionalised. These simple compounds are not themselves medically useful, but could be utilised in future attempts to develop triazolopyrazine-based medicinal compounds.
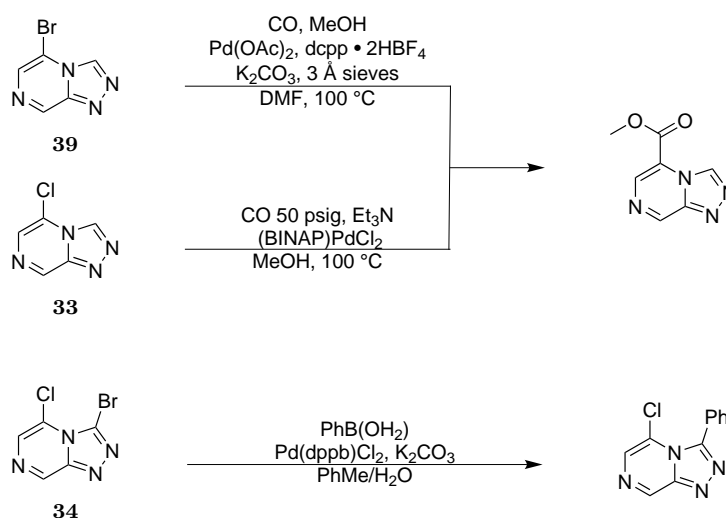
Scheme 4.1: Future reactions to be trialled. Carbonylation of the bromotriazolopyrazine **39** should be attempted used the conditions applied unsuccessfully. Carbonylation of chlorotriazolopyrazine **33** could be attempted using more traditional high-pressure CO conditions, such as those reported by Albaneze-Walker *et al.* [59] Functionalisation of the 3 position should be demonstrated using a model substrate, such as this phenylboronic acid Suzuki coupling.

The next step in this work towards TP compounds should be subjecting **33**, **34**, and **39** to different coupling conditions. Three early reactions to be trialled are shown in Scheme 4.1. Moving towards Series 4 amides, more work should be put into trying to successfully carbonylate at the 5 position: the atmospheric pressure conditions unsuccessfully applied to **33** should be attempted on bromotriazolopyrazine substrate **39**. Further attempts to carbonylate **33** could also look toward reactions involving high-pressure gaseous CO, such as those reported by Albaneze-Walker *et al.* [59].

C−C bond forming couplings should be investigated to functionalise at the 3 position. Compound **34** should be subjected to a test Suzuki coupling with a model substrate such as phenylboronic acid. Success in this area could be followed by the use of other couplings to explore

different new TP compounds: alkyne-substituted triazolopyrazines prepared using Sonogashira conditions could be an interesting scaffold to explore, as would triazole derivatives prepared from these compounds through click chemistry.

Ten triazolopyrazine amides were synthesised as part of OSM Series 4. These compounds were prepared in four steps starting from 6-chloro-2-pyrazinecarboxylic acid, and showed activity against the *Plasmodium falciparum* parasite down to 234 nM. It appears that potencies are very sensitive to small changes in the substitution patterns of the aryl amides used. Moving from a 3-chloroanilide to a 3-chloro-2-fluoroanilide dramatically lowered potency, and replacing the fluorine atom with a methyl group removed activity almost entirely.

Two of these compounds were screened for hERG activity, and showed concerningly high inhibitions. Notably, while hERG binding is a concern for all Series 4 compounds, the relative affinity for *P. falciparum* over hERG appears to be lower for Series 4 amides than for other compounds in the series. More research into this is needed: as it stands, the Series 4 amides show unacceptably high hERG inhibition. Without a way to lower hERG binding, these compounds will never escape the laboratory. hERG binding is known to be strongly correlated with lipophilicity[60]: a potential strategy to reduce this liability might thus be the incorporation of more polar/hydrophilic functional groups.
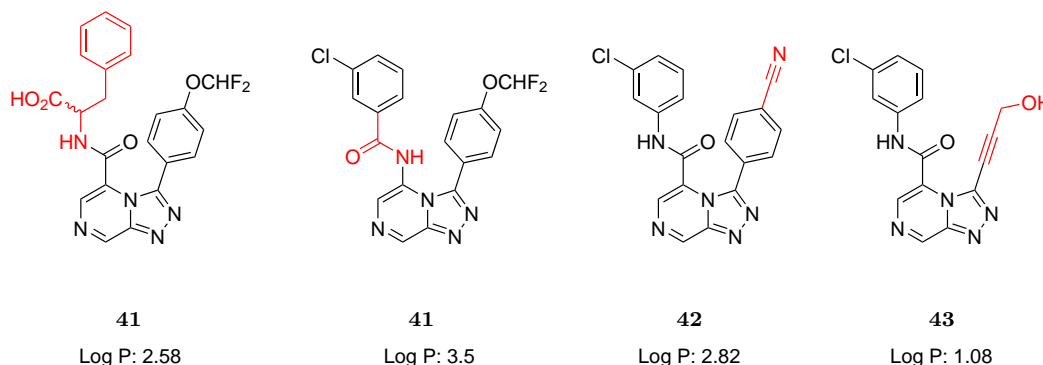

Figure 4.1: Some triazolopyrazine amides incorporating new functional motifs (in red) that could be targeted in future.

Synthesis of future TP amides could aim to lower LogP for the reasons stated above, and should also explore new functional groups. A selection of four different compounds that might be of interest is presented in Figure 4.1. Compound **44** is a chiral amino acid-derived amide with a carboxylic acid functionality. Compound **41** is an inverse amide based on the successful 3-chlorophenyl/4-difluoromethoxyphenyl combination of functional groups, and could be prepared

from an initial 5-chlorotriazolopyrazine core *via* reaction with a nitrogen nucleophile (difficult, but with precedent[61]) followed by coupling with a benzoic acid. Compound **42** reduces lipophilicity by incorporation of a nitrile group on the 3- substituent. Compound **43** dramatically lowers LogP through use of a propargylic alcohol. This could be accessed from a halotriazolopyrazine core (prepared using the methods developed here) by Sonogashira coupling, and would represent the first alkyne in Series 4.

One area of concern that has not been discussed so far is potential clearance by aldehyde oxidase, and thus low bioavailability, of the Series 4 compounds. At the time of writing, a selection of these compounds is being assayed for AO metabolic stability. When these data are available, protecting the triazolopyrazine core from AO metabolism may become a further concern to reckon with.

This work was aided by an open science approach. At various stages of the project, contributors pointed out topical publications[62], suggested new conditions for reactions[63], and ran computational studies[64]. As all the data obtained are in the public domain, any researcher who wishes to continue this work will have full access to the successes, failures, and unresolved questions that made up this project.

5

Experimental Details

5.1   General experimental details

Reagents were purchased from Sigma Aldrich, Alfa Aesar, A & K Scientific, Merck, Fisher Scientific, or Ajax. Unless specified, all reagents were used as supplied and without further purification. Molecular sieves were activated in a microwave then cooled under vacuum prior to use. High temperature reactions were carried out in silicone oil baths or metal heating blocks, controlled by temperature probes. Reduced pressure means 50–900 mbar under rotary evaporation at 40–50 ℃. Thin layer chromatography was performed on Merck Silica Gel 60 F_{254} aluminium plates and visualised under 254 nm UV light. Flash chromatography was performed by a Biotage Isolera Spektra automatic purification flash chromatography system using Grace Davison 40–63 μm (230–400 mesh) silica gel.

5.2   General analytical details

Melting points were taken using a Stanford Research Systems OptiMelt apparatus. Crude measurements were taken with 30 degree per minute ramp rates, then precise measurements with 3 degree per minute ramp rates. Infrared spectroscopy was carried out using a Bruker Alpha-E with atmospheric compensation, and processed using OPUS 6.5 software. Samples were prepared as thin films by evaporation of a concentrated acetone solution. Nuclear magnetic resonance spectroscopy was carried out at 300 K using Bruker spectrometers: either an AVANCE 300 (^{1}H at 300 MHz, ^{13}C at 75 MHz), AVANCE III 400 (^{1}H at 400 MHz, ^{13}C at 101 MHz), or AVANCE III 500 (^{1}H at 500 MHz, ^{13}C at 126 MHz). Spectra were processed using Topspin. Deuterated solvents (DMSO$-$d$_6$, CDCl$_3$, CD$_3$CN) were obtained from Cambridge Isotope Laboratories. ^{1}H and ^{13}C chemical shifts are reported in parts per million (ppm) with respect to TMS at 0.0. The chemical shifts of the spectra were calibrated to the residual solvent peaks: DMSO$-$d$_6$ 2.50, CDCl$_3$ 7.26, CD$_3$CN 1.94 for ^{1}H spectroscopy, and DMSO$-$d$_6$ 39.52, CDCl$_3$ 77.16 for ^{13}C. Signal splitting was reported as: s = singlet, d = doublet, t = triplet, m = multiplet. Multiple couplings were reported as a combination of these letters, for example dd = doublet of doublets, td = triplet of doublets.

Coupling constants J are reported in Hertz (Hz). Integrals are relative. A multiplicity followed by $_{app}$ = apparent, used when multiplicity was not entirely resolved (generally for non first-order coupling). Low resolution mass spectrometry (m/z) was carried out with Finnigan LCQ-MS in methanol using electrospray ionisation (ESI) or atmospheric-pressure chemical ionisation (APCI). High resolution mass spectrometry (HRMS) was carried out with a Bruker 7T FT-ICR using ESI or APCI. Positive or negative detection is shown by the charge on the ion, *e.g.* $[M+H]^+$ for a protonated positive ion.

5.3 General procedure 1: preparation of amides
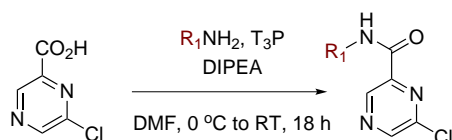
This procedure was adapted from the literature[65]. 6-chloropyrazine-2-carboxylic acid **1** (1 equiv.), appropriate amine (1 equiv.), and DIPEA (1.5 equiv.) were dissolved in DMF (1 M solution). The reaction mixture was cooled to 0 ℃ over ice, T3P (1.5 equiv., as 50% solution in EtOAc) was added dropwise with stirring, and the reaction mixture was then stirred for 18 h at rt. The reaction mixture was then diluted with EtOAc, and washed with aqueous NaHCO$_3$ solution (3 x). The aqueous portions were then combined and re-extracted with EtOAc (2 x). The organic portions were combined and washed with water and brine, then concentrated under reduced pressure to give the crude amide. The crude was purified by automated flash chromatography (10 to 50% EtOAc in hexanes; silica; $\lambda_{max} \sim$260 nm) to give the pure amide.

### 5.3.1 6-Chloro-N-(3-chlorophenyl)pyrazine-2-carboxamide 2

This compound is known to the literature, but not fully characterised[66,67]. Prepared according to general procedure 1 from **1** (1.50 g). Light brown solid, 1.90 g, 75%; mp 101–102 ℃ (lit.[67] 107–108 ℃); ν_{max} (film)/cm^{-1} 3362, 1691, 1593, 1533, 1300; δ_H (400 MHz, DMSO$-$d$_6$) 10.82 (s, 1 H), 9.24 (s, 1 H), 9.07 (s, 1 H), 8.04 (t, J = 1.9 Hz, 1 H), 7.83 (dd, J = 8.2, 1.1 Hz, 1 H), 7.41 (t, J = 8.1 Hz, 1 H), 7.22 (dd, J = 7.9, 1.3 Hz, 1 H); δ_C (100 MHz, DMSO$-$d$_6$) 160.94, 147.60, 146.86, 144.77, 142.40, 139.42, 132.93, 130.33, 124.16, 120.31, 119.23; m/z (EI) 267 ([M]$^+$); Anal. Calcd. for C$_{11}$H$_7$Cl$_2$N$_3$O: C, 49.28; H, 2.63; N, 15.67. Found: C, 49.73; H, 2.42; N, 15.22.

### 5.3.2 6-Chloro-N-(3-chloro-2-methylphenyl)pyrazine-2-carboxamide 3
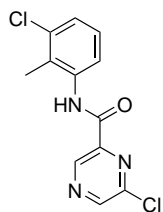
Prepared according to general procedure 1 from **1** (530 mg, 3.35 mmol). Crystalline beige solid (580 mg, 2.10 mmol, 62%); mp 155–156 ℃; ν_{max} (film)/cm^{-1} 3367, 1701, 1579, 1542, 1436; δ_H (400 MHz, CDCl$_3$) 9.44 (s, 1 H), 9.40 (s, 1 H), 8.84 (s, 1 H), 7.98 (dd, J = 1.18, 7.97 Hz, 1 H), 7.27 (dd, J = 1.28, 8.24 Hz, 1 H), 7.21 (t, J = 8.02 Hz, 1 H), 2.44 (s, 3 H);re δ_C (100 MHz, CDCl$_3$) 159.69, 147.91, 147.69, 144.05, 142.41, 136.15, 135.20, 127.93, 127.36, 126.82, 121.29, 14.62; m/z (APCI) 282 ([M + H]$^+$), (EI) 281 ([M]$^+$).

5.3.3 6-Chloro-N-(3-chloro-2-fluorophenyl)pyrazine-2-carboxamide 4
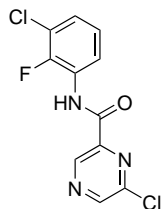
Prepared according to general procedure 1 from **1** (560 mg, 3.54 mmol). Off-white solid, 602 mg, 2.10 mmol, 59%; mp 107–109 ℃; ν_{max} (film)/cm^{-1} 3359, 1703, 1609, 1533, 1454; δ_H (400 MHz, CDCl$_3$) 9.71 (s, 1 H), 9.38 (s, 1 H), 8.84 (s, 1 H), 8.41 (ddd, J = 8.2, 6.8, 1.6 Hz, 1 H), 7.21 (ddd, J = 8.2, 6.6, 1.7 Hz, 1 H), 7.15 (dd, J = 8.2, 1.3 Hz, 1 H); δ_C (100 MHz, CDCl$_3$) 159.79, 149.07 (d, J = 247 Hz), 148.18, 147.88, 143.58, 142.33, 127.00 (d, J = 10 Hz), 126.14, 125.03 (d, J = 5 Hz), 121.19 (d, J = 16 Hz), 120.00; m/z (EI) 285 ([M]$^+$).

5.3.4 6-Chloro-N-(5-chloro-2-methylphenyl)pyrazine-2-carboxamide 5
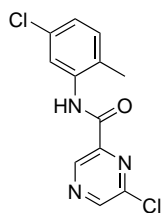
Prepared according to general procedure 1 from **1** (515 mg, 3.26 mmol). Beige powder, 545 mg, 1.9 mmol, 59%; mp 161–162 ℃; ν_{max} (film)/cm^{-1} 3373, 1698, 1587, 1537; δ_H (400 MHz, CDCl$_3$) 9.43 (s, 1 H), 9.40 (s, 1 H), 8.83 (s, 1 H), 8.28 (d, J = 2.1 Hz, 1 H), 7.17 (d, J = 8.2 Hz, 1 H), 7.11 (dd, J = 8.1, 2.1 Hz, 1 H), 2.37 (s, 3 H); δ_C (100 MHz, CDCl$_3$) 159.45, 147.94, 147.67, 144.02, 142.39, 136.05, 132.61, 131.59, 126.61, 125.50, 121.72, 17.27; m/z (APCI) 282 ([M + H]$^+$), (EI) 281 ([M]$^+$).

5.4 General procedure 2: preparation of hydrazinylpyrazines
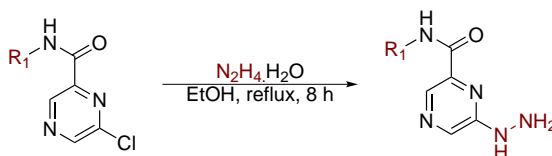
This procedure was adapted from the literature[68,21]. An appropriate chloropyrazine amide (1 eq) was placed in EtOH (0.45 M solution), hydrazine hydrate (3 eq) added, and the reaction mixture refluxed for 8 h. Volatiles were removed under reduced pressure to give a crude material (still containing some hydrazine and water). Initially, hydrazines were carried forward from this crude without further purification or isolation, but an improved workup was later developed:

The crude material was suspended in water, and ethyl acetate with added with vigorous shaking until all solid was dissolved. The layers were separated, and the aqueous portion re-extracted with ethyl acetate (4 x). The combined organic portions were washed with brine, then concentrated under reduced pressure to give the desired hydrazinylpyrazine with no further purification required.

5.4.1 N-(3-chlorophenyl)-6-hydrazinylpyrazine-2-carboxamide 6
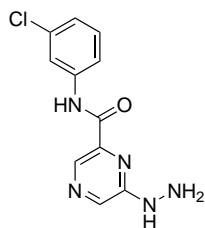
Prepared according to general procedure 2 from **2** (1.80 g, 6.70 mmol), with ethyl acetate workup. Drab yellow solid (1.46 g, 5.5 mmol, 82%); mp 187 ℃; ν_{max} (film)/cm^{-1} 3234, 1675, 1585, 1516, 1422; δ_H (400 MHz, DMSO$-$d$_6$) 10.47 (s, 1 H), 8.52 (s, 1 H), 8.32 (s, 1 H), 8.19 (s, 1 H), 8.00 (t, J = 2.0 Hz, 1 H), 7.81 (dd, J = 8.0, 1.6 Hz, 1 H), 7.42 (t, J = 8.1 Hz, 1 H), 7.20 (dd, J = 7.9, 1.9 Hz, 1 H), 4.64 (s, 2 H); δ_C (100 MHz, DMSO$-$d$_6$) 162.58, 154.96, 140.80, 139.58, 135.71, 133.04, 130.43, 129.74, 123.76, 119.72, 118.66; m/z (ESI) 264 ([M$+$H]$^+$).

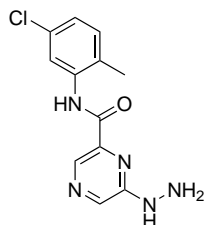### 5.4.2 N-(3-chloro-2-methylphenyl)-6-hydrazinylpyrazine-2-carboxamide 45
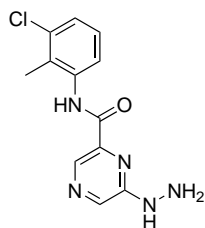
Prepared from **3** (525 mg, 1.86 mmol) according to general procedure 2 prior to development of ethyl acetate workup. Yellow solid (525 mg, >100%: residual hydrazine), carried forward without purification or full characterisation; ν_{max} (film)/cm^{-1} 2914, 1672, 1579, 1516, 1429; δ_H (400 MHz, DMSO$-$d$_6$) 10.15 (s, 1 H), 9.83 (s, 1 H), 8.65 (s, 1 H), 8.54 (s, 1 H), 7.69 (d, J = 7.0 Hz, 1 H), 7.34

(dd, J = 7.9, 1.4 Hz, 1 H), 7.27 (t, J = 7.8 Hz, 1 H), 4.37 (s, 2 H), 2.33 (s, 3 H); m/z (ESI) 278 ($[M+H]^+$).

5.4.3 *N*-(5-chloro-2-methylphenyl)-6-hydrazinylpyrazine-2-carboxamide 46

Prepared from **5** (495 mg, 1.75 mmol) according to general procedure 2 prior to development of ethyl acetate workup. Yellow solid (621 mg, >100%: residual hydrazine). Carried forward without further purification or full characterisation; ν_{max} (film)/cm^{-1} 3351, 1686, 1581, 1517, 1430; δ_{H} (400 MHz, DMSO$-$d$_6$) 10.22 (s, 1 H), 8.59 (s, 1 H), 8.33 (s, 1 H), 8.26 (s, 1 H), 7.96 (d, J = 2.2 Hz, 1 H), 7.32 (d, J = 8.4 Hz, 1 H), 7.18 (d, J = 8.2, 2.2 Hz, 1 H), 4.55 (s, 2 H), 2.32 (s, 3 H); m/z (ESI) 278 ($[M+H]^+$).

5.4.4 *N*-(3-chloro-2-fluorophenyl)-6-hydrazinylpyrazine-2-carboxamide 47
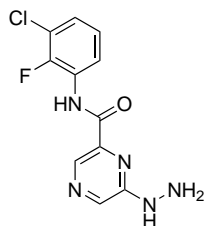
Prepared from **4** (200 mg, 0.70 mmol) according to general procedure 2 prior to development of ethyl acetate workup. Yellow solid (225 mg, 0.80 mmol, >100%: residual hydrazine). Carried forward without further purification or full characterisation; δ_{H} (400 MHz, DMSO$-$d$_6$) 10.38 (s, 1 H), 8.56 (s, 1 H), 8.32 (s, 1 H), 8.26 (s, 1 H), 7.88 (ddd, J = 8.3, 6.9, 1.5 Hz, 1 H), 7.45 (ddd, J = 8.4, 6.8, 1.6 Hz, 1 H), 7.29 (td, J = 8.3, 1.7 Hz, 1 H), 4.56 (s, 2 H); m/z (ESI) 282 ($[M+H]^+$).

## 5.5   General procedure 3: preparation of hydrazones
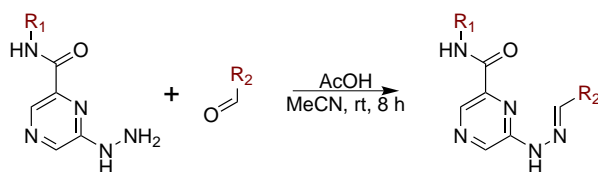
To a solution of the appropriate hydrazinyl pyrazine (1 equiv.) in acetonitrile (to 0.2 M) was added an appropriate aldehyde (1 equiv.) and acetic acid (catalytic, one small drop). The reaction mixture was stirred at rt until no starting material was observed by TLC (4–8 h); volatiles were removed under vacuum, and the crude product obtained was purified by automated flash chromatography (5 to 100% EtOAc in hexanes; silica; λ_{max} ~320 nm).

5.5.1 *N*-(3-chlorophenyl)-6-(2-(4-(difluoromethoxy)benzylidene)hydrazinyl) pyrazine-2-carboxamide 7
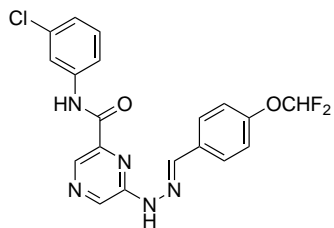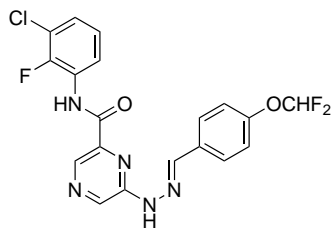
Prepared according to general procedure 3, from **6** (300 mg, 1.14 mmol). Pale yellow powder (217 mg, 0.52 mmol, 46%), mp 229–230 °C; ν_{max} (film)/cm^{-1} 3250, 1671, 1578, 1432, 1243, 1157; δ_H (400 MHz, DMSO−d$_6$) 11.48 (s, 1 H), 10.43 (s, 1 H), 8.89 (s, 1 H), 8.59 (s, 1 H), 8.16 (s, 1 H), 8.02 (t, J = 2.0 Hz, 1 H), 7.84 (d$_{app}$, J = 8.8 Hz, 2 H), 7.71 (ddd, J = 8.1, 1.7, 0.6 Hz, 1 H), 7.42 (t, J = 8.1 Hz, 1 H), 7.31 (t, J = 73.9 Hz, 1 H), 7.24 (d$_{app}$, J = 8.6 Hz, 2 H), 7.21 (ddd, J = 8.0, 2.0, 0.8 Hz, 1 H); δ_C (100 MHz, DMSO−d$_6$) 162.60, 151.55 (t, J = 3.2 Hz), 151.19, 142.33, 141.14, 139.63, 134.03, 133.41, 133.13, 131.60, 130.54, 128.26 (2 C), 123.84, 119.46, 118.82 (2 C), 118.43, 116.17 (t, J = 257.8 Hz); m/z (APCI) 418 ([M + H]$^+$); HRMS (APCI) 418.08770 ([M + H]$^+$) calcd. for $C_{19}H_{15}ClF_2N_5O_2^+$ 418.08769; Anal. Calcd. for $C_{19}H_{14}ClF_2N_5O_2$: C, 54.62; H, 3.38; N, 16.76. Found: C, 54.56; H, 3.11; N, 16.65.

## 5.5.2 *N*-(3-chloro-2-methylphenyl)-6-(2-(4-(difluoromethoxy)benzylidene) hydrazinyl)pyrazine-2-carboxamide 11
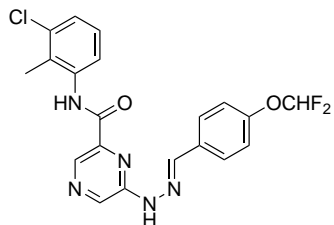
Prepared by general procedure 3 from **45** (300 mg, 1.08 mmol). Bright yellow flakes (265 mg, 0.61 mmol, 56%); mp 209 °C; ν_{max} (film)/cm^{-1} 2174, 1674, 1577, 1508, 1421, 1226, 1112; δ_H (400 MHz, DMSO−d$_6$) 11.48 (s, 1 H), 10.06 (s, 1 H), 8.87 (s, 1 H), 8.62 (s, 1 H), 8.17 (s, 1 H), 7.84 (d$_{app}$, J = 8.8 Hz, 2 H), 7.79 (dd, J = 7.9, 1.6 Hz, 1 H), 7.34 (dd, J = 8.1, 1.7 Hz, 1 H), 7.32 (t, J = 73.9 Hz, 1 H), 7.29(t, J = 7.9 Hz, 1 H), 7.24 (d$_{app}$, J = 8.7 Hz, 2 H), 2.37 (s, 3 H); δ_C (100 MHz, DMSO−d$_6$) 161.91, 151.62 (t, J = 3.1 Hz), 151.02, 141.61, 141.32, 137.26, 134.51, 133.78, 133.20, 131.65, 128.95, 128.32 (2 C), 127.27, 126.07, 122.54, 118.84 (2 C), 116.23 (t, J = 257.8 Hz); m/z (APCI) 432 ([M + H]$^+$); HRMS (APCI) 432.10329 ([M + H]$^+$) calcd. for $C_{20}H_{17}ClF_2N_5O_2^+$ 432.10334.

5.5.3 *N*-(3-chloro-2-fluorophenyl)-6-(2-(4-(difluoromethoxy)benzylidene) hydrazinyl)pyrazine-2-carboxamide 13
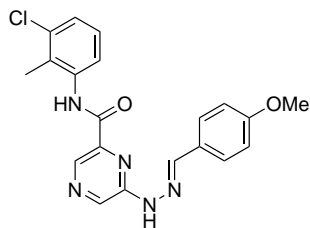
Prepared according to general procedure 3 from **47** (300 mg, 1.06 mmol). Lemon yellow flakes (256 mg, 0.59 mmol, 56%); mp 215–217 °C; ν_{max} (film)/cm^{-1} 1680, 1511, 1454, 1423, 1226, 1114; δ_H (400 MHz, DMSO−d$_6$) 11.54 (s, 1 H), 10.09 (sre , 1 H), 8.89 (s, 1 H), 8.63 (s, 1 H), 8.16 (s, 1 H), 8.13 (ddd, J = 8.3, 6.8, 1.4 Hz, 1 H), 7.84 (d, J = 8.7 Hz, 2 H), 7.41 (ddd, J = 8.3, 6.8, 1.4 Hz, 1 H), 7.31 (t, J = 73.9 Hz, 1 H), 7.29 (td, J = 8.1, 1.3 Hz, 1 H), 7.23 (d, J = 8.6 Hz, 2 H); δ_C (100 MHz, DMSO−d$_6$) 161.76, 151.59, 150.97, 150.46, 148.01, 141.39, 140.77, 134.85, 133.14, 131.59, 130.19, 128.27 (2 C), 127.05 (d, J = 10.6 Hz), 125.95, 125.31 (d, J = 4.8 Hz), 121.73, 119.83 (d, J = 15.9 Hz), 118.80 (2 C), 118.68, 116.17 (t, J = 258.0 Hz); m/z (APCI) 436 ($[M+H]^+$); HRMS (APCI) 436.07825 ($[M+H]^+$) calcd. for $C_{19}H_{14}ClF_3N_5O_2^+$ 436.07826.

5.5.4 *N*-(5-chloro-2-methylphenyl)-6-(2-(4-(difluoromethoxy)benzylidene) hydrazinyl)pyrazine-2-carboxamide 15
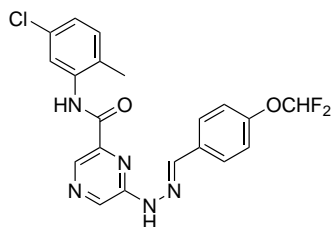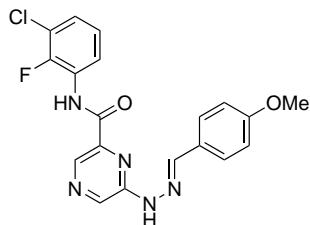
Prepared according to general procedure 3 from **46** (300 mg, 1.08 mmol). Bright yellow flakes (271 mg, 0.63 mmol, 58%); mp 212 °C; ν_{max} (film)/cm^{-1} 3342, 3247, 1689, 1583, 1523, 1430; δ_H (400 MHz, DMSO−d$_6$) 11.47 (s, 1 H), 9.94 (s, 1 H), 8.85 (s, 1 H), 8.64 (s, 1 H), 8.18 (s, 1 H), 8.14 (d, J = 2.3 Hz, 1 H), 7.84 (d$_{app}$, J = 8.9 Hz, 2 H), 7.33 (dd, J = 8.1, 0.7 Hz, 1 H), 7.31 (t, J = 73.8 Hz, 1 H), 7.25 (d$_{app}$, J = 8.8 Hz, 2 H), 7.18 (dd, J = 8.1, 2.3 Hz, 1 H), 2.38 (s, 3 H); δ_C (100 MHz, DMSO−d$_6$) 161.42, 151.60, 150.79, 141.44, 141.09, 136.92, 134.80, 132.99, 131.84, 131.61, 130.46, 130.19, 128.26 (2 C), 127.75, 124.36, 120.90, 118.83 (2 C), 116.17 (t, J = 258.0 Hz), 16.76; m/z (APCI) 432 ($[M+H]^+$); HRMS (APCI) 432.10331 ($[M+H]^+$) calcd. for $C_{20}H_{17}ClF_2N_5O_2^+$ 432.10334.

### 5.5.5 *N*-(3-chloro-2-methylphenyl)-6-(2-(4-methoxybenzylidene)hydrazinyl) pyrazine-2-carboxamide 12

Prepared according to general procedure 3 from **45** (250 mg, 0.90 mmol). Dark yellow solid (224 mg, 0.57 mmol, 63%); mp 192.9–193.4 °C; $\nu_{\max}$ (film)/cm^{-1} 3353, 3238, 1685, 1579, 1513, 1427, 1250; δ_H (500 MHz, DMSO$-$d$_6$) 11.29 (s, 1 H), 10.04 (s, 1 H), 8.82 (s, 1 H), 8.58 (s, 1 H), 8.13 (s, 1 H), 7.81 (d, J = 8.5 Hz, 1 H), 7.72 (d, J = 7.2 Hz, 2 H), 7.34 (d, J = 8.5 Hz, 1 H), 7.28 (t, J = 8.6 Hz, 1 H), 7.01 (d, J = 7.3 Hz, 2 H), 3,81 (s, 3 H), 2.38 (s, 3 H); δ_C (126 MHz, DMSO$-$d$_6$) 161.88, 160.32, 151.06, 142.48, 141.52, 137.23, 131.34, 133.73, 132.70, 128.74, 128.13 (2 C), 127.21, 128.94, 122.33, 114.27 (2 C), 55.26, 14.59; m/z (APCI) 396 ([M+H]$^+$); HRMS 396.12217 ([M+H]$^+$) calcd. for $C_{20}H_{19}ClN_5O_2^+$ 396.12218.

5.5.6 *N*-(3-chloro-2-fluorophenyl)-6-(2-(4-methoxybenzylidene)hydrazinyl) pyrazine-2-carboxamide 14
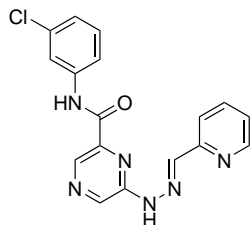
Prepared according to general procedure 3 from **47** (250 mg, 0.90 mmol). Fine yellow crystals (198 mg, 0.50 mmol, 55%); mp 195–196 °C; $\nu_{\max}$ (film)/cm^{-1} 3352, 1691, 1608, 1515, 1456, 1251; δ_H (500 MHz, DMSO$-$d$_6$) 11.38 (s, 1 H), 10.09 (s, 1 H), 8.85 (s, 1 H), 8.60 (s, 1 H), 8.14 (t$_{app}$, J = 6.8 Hz, 1 H), 8.12 (s, 1 H), 7.72 (d$_{app}$, J = 7.5 Hz, 2 H), 7.42 (t$_{app}$, J = 7.8 Hz, 1 H), 7.29 (t$_{app}$, J = 8.0 Hz, 1 H), 7.00 (d$_{app}$, J = 7.4 Hz, 2 H), 3.81 (s, 3 H); δ_C (126 MHz, DMSO$-$d$_6$) 161.84, 160.33, 151.07, 149.23 (d, J = 246.6 Hz), 142.56, 140.77, 134.73, 132.71, 128.16 (2 C), 127.17, 127.08 (d, J = 10.3 Hz), 125.95, 125.33 (d, J = 4.6 Hz), 121.74, 119.89, 119.76, 114.26, 55.25; m/z (APCI) 400 ([M+H]$^+$); HRMS 400.09711 ([M+H]$^+$) calcd. for $C_{19}H_{16}ClFN_5O_2^+$ 400.09711.

5.5.7 *N*-(5-chloro-2-methylphenyl)-6-(2-(4-methoxybenzylidene)hydrazinyl) pyrazine-2-carboxamide 16
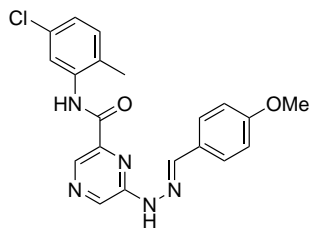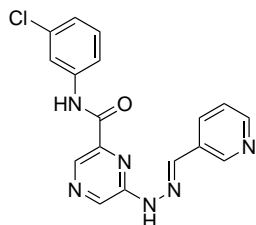
Prepared according to general procedure 3 from **46** (250 mg, 0.90 mmol). Turmeric-yellow solid (180 mg, 0.45 mmol, 50%); mp 226–227 °C; ν_{max} (film)/cm^{-1} 1691, 1605, 1515, 1431, 1252; δ_H (500 MHz, DMSO−d$_6$) 11.31 (s, 1 H), 9.95 (s, 1 H), 8.81 (s, 1 H), 8.60 (s, 1 H), 8.15 (s, 1 H), 8.13 (s, 1 H), 7.72 (s, $J = 8.8$ Hz, 2 H), 7.33 (d, $J = 8.0$ Hz, 1 H), 7.18 (d, $J = 8.25$ Hz, 1 H), 7.01 (d, $J = 8.8$ Hz, 2 H), 3.81 (s, 3 H), 2.38 (s, 3 H); δ_C (126 MHz, DMSO−d$_6$) 161.48, 160.35, 150.88, 142.61, 141.06, 136.94, 132.54, 131.86, 130.47, 128.14 (2 C), 127.68, 127.18, 124.32, 120.81, 114.28 (2 C), 55.27, 16.76; m/z (ESI) 396 ([M + H]$^+$), 418 ([M + Na]$^+$), (APCI) 396 ([M + H]$^+$); HRMS 396.12224 ([M + H]$^+$) cacld. for C$_{20}$H$_{19}$ClN$_5$O$_2$ 391.12218.

### 5.5.8 *N*-(5-chloro-2-methylphenyl)-6-(2-(pyridin-2-ylmethylene)hydrazinyl) pyrazine-2-carboxamide 9

Prepared according to general procedure 3 from **6** (200 mg, 0.76 mmol). Yellow solid (117 mg, 0.33 mmol, 44%); mp 252–254 °C; ν_{max} (film)/cm^{-1} 3355, 2925, 1693, 1579, 1527, 1429; δ_H (400 MHz, DMSO−d$_6$) 11.74 (s, 1 H), 10.49 (s, 1 H), 8.96 (s, 1 H), 8.64 (s, 1 H), 8.58 (ddd, $J = 4.8, 1.6, 1.2$ Hz, 1 H), 8.21 (s, 1 H), 8.13 (dt, $J = 7.8, 1.0$ Hz, 1 H), 8.04 (t, $J = 2.1$ Hz, 1 H), 7.86 (td, $J = 7.8, 1.7$ Hz, 1 H), 7.72 (ddd, $J = 8.2, 2.1, 0.8$ Hz, 1 H), 7.42 (t, $J = 8.1$ Hz, 1 H), 7.37 (ddd, $J = 7.5, 4.8, 1.0$ Hz, 1 H), 7.21 (ddd, $J = 8.0, 2.1, 0.7$ Hz, 1 H); δ_C (100 MHz, DMSO−d$_6$) 162.64, 153.52, 150.98, 149.39, 142.64, 142.48, 139.71, 136.74, 134.16, 134.05, 133.16, 130.60, 123.90, 123.74, 119.62, 119.48, 118.48; m/z (APCI) 353 ([M + H]$^+$); HRMS (APCI) 353.09121 calcd. for C$_{17}$H$_{14}$ClN$_6$O$^+$ 353.09121.

5.5.9 *N*-(5-chloro-2-methylphenyl)-6-(2-(pyridin-3-ylmethylene)hydrazinyl) pyrazine-2-carboxamide 10

Prepared according to general procedure 3 from **6** (200 mg, 0.76 mmol). Yellow solid (152 mg, 0.43 mmol, 57%); mp 241–242.0 ℃; ν_{max} (film)/cm^{-1} 3028, 1677, 1581, 1414; δ_H (400 MHz, DMSO−d$_6$) 11.67 (s, 1 H), 10.46 (s, 1 H), 8.95 (s, 1 H), 8.91 (d, J = 2.3 Hz, 1 H), 8.62 (s, 1 H), 8.57 (dd, J = 4.8, 1.8 Hz, 1 H), 8.22 (dt, J = 8.0, 2.0 Hz, 1 H), 8.19 (s, 1 H), 8.03 (t, J = 2.1 Hz, 1 H), 7.71 (dd, J = 8.2, 2.1 Hz, 1 H), 7.46 (dd, J = 8.1, 4.9 Hz, 1 H), 7.42 (t, J = 8.2 Hz, 1 H), 7.21 (dd, J = 8.0, 2.2 Hz, 1 H); δ_C (100 MHz, DMSO−d$_6$) 163.09, 151.56, 150.40, 148.68, 142.85, 140.13, 139.67, 134.68, 134.24, 133.61, 133.56, 131.05, 130.99, 124.38, 124.34, 119.93, 118.92; m/z (APCI) 353 ([M + H]$^+$) ; HRMS (APCI) 353.09131 ([M + H]$^+$) calcd. for C$_{17}$H$_{14}$ClN$_6$O$^+$ 353.09121

5.5.10 *N*-(3-chlorophenyl)-6-(2-(4-(trifluoromethoxy)benzylidene)hydrazinyl) pyrazine-2-carboxamide 8
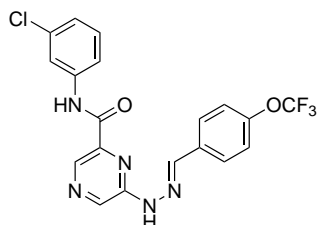
Prepared according to general procedure 3 from **6** (200 mg, 0.76 mmol). Pale yellow solid (312 mg, 0.72 mmol, 94%); mp 250.2–250.5 ℃; ν_{max} (film)/cm^{-1} 3322, 3257, 1671, 1577, 1432, 1310, 1144; δ_H (400 MHz, DMSO−d$_6$) 11.60 (s, 1 H), 10.46 (s, 1 H), 8.91 (s, 1 H), 8.60 (s, 1 H), 8.18 (s, 1 H), 8.03 (t, J = 2.0 Hz, 1 H), 7.92 (d$_{app}$, J = 8.8 Hz, 2 H), 7.71 (dd, J = 8.2, 2.1 Hz, 1 H), 7.42 (d$_{app}$, J = 8.7 Hz, 2 H), 7.42 (t, J = 8.1 Hz, 1 H), 7.21 (dd, J = 8.0, 2.1 Hz, 1 H; δ_C (125 MHz, DMSO−d$_6$) 162.59, 151.14, 148.69, 142.37, 140.57, 139.63, 134.08, 133.94, 133.63, 133.13, 130.55, 128.37, 123.85, 121.30, 119.46, 118.44; m/z (ESI) 436 ([M + H]$^+$); HRMS (APCI) 436.07823 ([M + H]$^+$) calcd. for C$_{19}$H$_{14}$ClF$_3$N$_5$O$_2^+$ 436.07826.

## 5.6 General procedure 4: preparation of triazolopyrazines
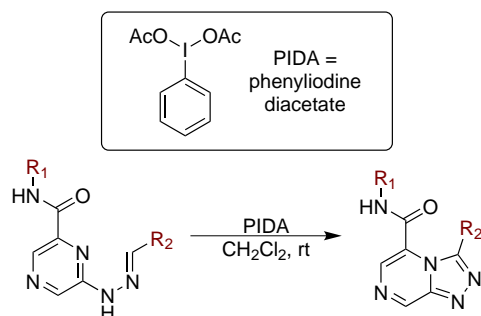
This procedure was adapted from the literature[41]. An appropriate hydrazone (1 equiv) was placed in CH_2Cl_2 (to 50 mM), and phenyliodine diacetate (PIDA) (1 equiv) added. The reaction mixture was stirred at rt for 12 h, then neutralised with an aqueous solution of saturated $NaHCO_3$. The mixture was extracted with CH_2Cl_2, the combined organic portions dried with brine, and concentrated under reduced pressure. The crude product was purified by flash chromatography on silica (automated chromatography: 20 to 100% EtOAc in hexanes; $\lambda_{max} \sim$230 nm) to give the desired [1,2,4]triazolo[4,3-a]pyrazine.

5.6.1 *N*-(3-chlorophenyl)-3-(4-(difluoromethoxy)phenyl)-[1,2,4]triazolo[4,3-a]pyrazine-5-carboxamide 17

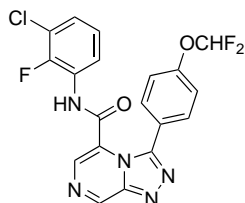Prepared according to general procedure 4, from **7** (150 mg, 0.36 mmol). Pearlescent white powder (60 mg, 39%); mp 257–258 °C; ν_{max} (film)/cm^{-1} 3053, 1671, 1591, 1536, 1465; δ_H (400 MHz, DMSO$-$d$_6$) 10.88 (s, 1 H), 9.66 (s, 1 H), 8.30 (s, 1 H), 7.63 (d$_{app}$, $J = 8.7$ Hz, 2 H), 7.40 (t, $J = 1.9$ Hz, 1 H), 7.29 (t, $J = 8.1$ Hz, 1 H) 7.17 (d, $J = 7.9$ Hz, 1 H), 7.15 (d, $J = 7.9$ Hz, 1 H), 7.15 (d, $J = 8.6$ Hz, 2 H), 7.11 (t, $J = 73.6$ Hz, 1 H); δ_C (100 MHz, DMSO$-$d$_6$) 157.35, 152.11 (t, $J = 3.2$ Hz), 146.78, 146.10, 145.71, 138.61, 132.82, 130.31, 130.25, 130.19, 124.33, 124.28, 123.98, 119.20, 118.17, 118.13, 115.86 (t, $J = 258$ Hz); m/z (ESI) 438 ([M+Na]$^+$); HRMS (APCI) 416.07177 ([M+H]$^+$) calcd. for $C_{19}H_{13}ClF_2N_5O_2^+$ 416.07204; Anal. Calcd. for $C_{19}H_{12}ClF_2N_5O_2$: C, 54.89; H, 2.91; N, 16.84. Found: C, 55.02; H, 2.53; N, 16.61.

5.6.2 *N*-(3-chloro-2-methylphenyl)-3-(4-(difluoromethoxy)phenyl)-[1,2,4]triazolo[4,3-a]pyrazine-5-carboxamide 21
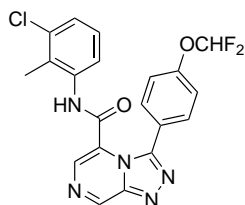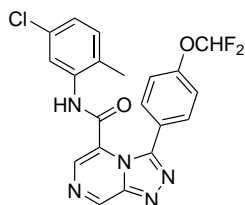
Prepared according to general procedure 4, from **11** (200 mg, 0.46 mmol). Fine pearly white powder (140 mg, 0.33 mmol, 71%); mp 211–212 ℃; ν_{max} (film)/cm^{-1} 1667, 1531, 1462, 1376; δ_H (500 MHz, DMSO−d$_6$) 10.63 (1 H), 9.66 (1 H), 8.38 (s, 1 H), 7.70 (d$_{app}$, J = 8.7 Hz, 2 H), 7.32 (dd, J = 1.0, 8.0 Hz, 1 H), 7.32 (t, J = 73.6 Hz, 1 H), 7.30 (d$_{app}$, J = 8.6 Hz, 2 H), 7.14 (t, J = 8.0 Hz, 1 H), 6.97 (dd, J = 1.2, 8.3 Hz, 1 H), 2.22 (3 H); δ_C (100 MHz, DMSO−d$_6$) 158.01, 152.09 (t, J = 3.5 Hz), 146.83, 146.11, 145.85, 136.09, 133.78, 130.50, 130.47, 130.25 (2 C), 126.91, 126.73, 124.36, 124.31, 123.92, 118.48 (2 C), 115.93 (t, J = 256.9 Hz), 14.93; m/z (ESI) 428.53 ([M−H]−, 100%); HRMS (APCI) 430.08721 ([M + H]$^+$) calcd. for C$_{20}$H$_{15}$ClF$_2$N$_5$O$_2{}^+$ 430.08769; Anal. Calcd. for C$_{20}$H$_{14}$ClF$_2$N$_5$O$_2$: C, 55.89; H, 3.28; N, 16.28. Found: C, 56.36; H, 3.01; N, 16.19.

5.6.3 *N*-(3-chloro-2-fluorophenyl)-3-(4-(difluoromethoxy)phenyl)-[1,2,4]triazolo[4,3-a]pyrazine-5-carboxamide 23
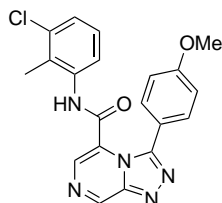
Prepared according to general procedure 4, from **13** (200 mg, 0.46 mmol). Fine pearly white solid (129 mg, 0.29 mmol, 63%); mp 218–219 ℃; ν_{max} (film)/cm^{-1} 1688, 1612, 1543, 1459; δ_H (400 MHz, DMSO−d$_6$) 10.81 (s, 1 H), 9.65 (s, 1 H), 8.28 (s, 1 H), 7.65 (d$_{app}$, J = 8.7 Hz, 2 H), 7.52 (ddd$_{app}$, J = 8.2, 7.2, 1.2 Hz, 1 H), 7.35 (ddd$_{app}$, J = 8.1, 6.9, 1.3 Hz, 1 H), 7.19 (d$_{app}$, J = 8.6 Hz, 2 H), 7.17 (t, J = 73.5 Hz, 1 H), 7.12 (td$_{app}$, J = 8.3, 1.3, 1 H); δ_C (100 MHz, DMSO−d$_6$) 158.01, 152.10 (t, J = 3.2 Hz), 149.09 (d, J = 249.8 Hz), 146.67, 146.05, 145.74, 130.39, 130.33 (2 C), 126.51, 126.01 (d, J = 11.5 Hz), 124.78 (d, J = 4.6 Hz), 124.34, 123.92, 122.26, 119.77 (d, J = 15.8 Hz), 118.26 (2 C), 115.85 (t, J = 258.4 Hz); m/z (ESI) 434 ([M + H]$^+$), 466 ([M + MeOH + H]$^+$); HRMS (APCI) 434.06259 ([M + H]$^+$) calcd. for C$_{19}$H$_{12}$ClF$_3$N$_5$O$_2{}^+$ 434.06261; Anal. Calcd. for C$_{19}$H$_{11}$ClF$_3$N$_5$O$_2$: C, 52.61; H, 2.56; N, 16.15. Found: C, 52.67; H, 2.18; N, 16.02.

5.6.4 *N*-(5-chloro-2-methylphenyl)-3-(4-(difluoromethoxy)phenyl)-[1,2,4]triazolo[4,3-a]pyrazine-5-carboxamide 25
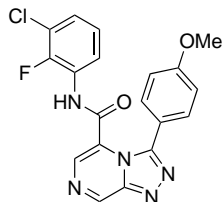
Prepared according to general procedure 4, from **15** (200 mg, 0.46 mmol). White solid (144 mg, 0.33 mmol, 73%); mp 247–248 °C; ν_{max} (film)/cm^{-1} 1686, 1582, 1530, 1462; δ_H (400 MHz, DMSO−d$_6$) 10.42 (s, 1 H), 9.66 (s, 1 H), 8.35 (s, 1 H), 7.70 (d$_{app}$, $J = 8.7$ Hz, 2 H), 7.29 (d$_{app}$, $J = 8.6$ Hz, 2 H), 7.28 (t, $J = 78.5$ Hz, 1 H), 7.24 (d, $J = 8.2$ Hz, 1 H), 7.17 (dd, $J = 8.2, 2.2$ Hz, 1 H), 7.06 (d, $J = 2.1$ Hz, 1 H), 2.19 (s, 3 H); δ_C (100 MHz, DMSO−d$_6$) 157.96, 152.35, 146.76, 146.03, 145.79, 135.78, 131.85, 130.42 (2 C), 130.34, 130.32, 129.82, 125.66, 124.35, 124.10, 123.68, 118.13 (2 C), 118.93 (t, $J = 258.0$ Hz), 17.12; m/z (ESI) 430 ([M + H]$^+$), 462 ([M + MeOH + H]$^+$); HRMS (APCI) 430.08711 ([M + H]$^+$) calcd. for $C_{20}H_{15}ClF_2N_5O_2^+$ 430.08769; Anal. Calcd. for $C_{20}H_{14}ClF_2N_5O_2$: C, 55.89; H, 3.28; N, 16.28. Found: C, 56.01; H, 2.97; N, 16.23.

### 5.6.5 *N*-(3-chloro-2-methylphenyl)-3-(4-methoxyphenyl)-[1,2,4]triazolo[4,3-a]pyrazine-5-carboxamide 22

Prepared according to general procedure 4 from **12** (150 mg, 0.38 mmol). Tan powder (86 mg, 0.22 mmol, 58%); mp 220–221 °C; ν_{max} (film)/cm^{-1} 3230, 2832, 1686, 1612, 1461, 1254; δ_H (400 MHz, DMSO−d$_6$) 10.62 (s, 1 H), 9.63 (s, 1 H), 8.34 (s, 1 H), 7.57 (d$_{app}$, $J = 8.7$ Hz, 2 H), 7.32 (d, $J = 7.6$ Hz, 1 H), 7.16 (t, $J = 8.0$ Hz, 1 H), 7.02 (d$_{app}$, $J = 8.7$ Hz, 2 H), 7.01 (d, $J = 7.6$ Hz, 1 H), 3.77 (s, 3 H), 2.22 (s, 3 H); δ_C (100 MHz, DMSO−d$_6$) 160.61, 158.07, 147.60, 146.10, 145.76, 132.20, 133.80, 130.44, 130.30, 129.84 (2 C), 126.88, 126.76, 124.59, 123.95, 119.54, 114.08 (2 C), 55.36, 15.04; m/z (ESI) 394 ([M + H]$^+$); HRMS (APCI) 394.10644 ([M + H]$^+$) calcd. for $C_{20}H_{17}ClN_5O_2^+$ 394.10653.

### 5.6.6 *N*-(3-chloro-2-fluorophenyl)-3-(4-methoxyphenyl)-[1,2,4]triazolo[4,3-a]pyrazine-5-carboxamide 24

Prepared according to general procedure 4 from **14** (150 mg, 0.38 mmol). Beige solid (78 mg, 0.20 mmol, 58%); mp 229–230 ℃; ν_{max} (film)/cm^{-1} 3175, 3046, 1672, 1525, 1455, 1287; δ_H (400 MHz, DMSO−d$_6$) 10.75 (s, 1 H), 9.61 (s, 1 H), 8.23 (s, 1 H), 7.60 (ddd, J = 8.4, 7.0, 1.5 Hz, 1 H), 7.50 ((d$_{app}$, J = 8.7 Hz, 2 H), 7.35 (ddd, J = 8.3, 6.8, 1.5 Hz, 1 H), 7.14 (td, J = 8.2, 1.4 Hz, 1 H), 6.89 (d$_{app}$, J = 8.7 Hz, 2 H), 3.66 (s, 3 H); δ_C (100 MHz, DMSO−d$_6$) 160.49, 158.12, 148.91 (d, J = 249 Hz), 147.43, 146.01, 145.66, 130.22, 129.91 (2 C), 126.25, 124.80 (d, J = 5.8 Hz), 124.62, 122.07, 119.68 (d, J = 15.4 Hz), 119.17, 113.88 (2 C), 55.17; m/z (ESI) 398 ([M + H]$^+$), 430 ([M + MeOH + H]$^+$), 452 ([M + MeOH + Na]$^+$); HRMS (APCI) 398.08134 ([M + H]$^+$) calcd. for C$_{19}$H$_{14}$ClFN$_5$O$_2{}^+$ 398.08146; Anal. Calcd. for C$_{19}$H$_{13}$ClFN$_5$O$_2$: C, 57.37; H, 3.29; N, 17.61. Found: C, 57.36; H, 3.10; N, 17.19.

### 5.6.7 *N*-(5-chloro-2-methylphenyl)-3-(4-methoxyphenyl)-[1,2,4]triazolo[4,3-a]pyrazine-5-carboxamide 26
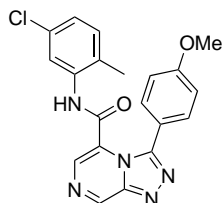
Prepared according to general procedure 4 from **16** (150 mg, 0.38 mmol). White solid (81 mg, 0.21 mmol, 55%); mp 273–274 ℃; ν_{max} (film)/cm^{-1} 3155, 2918, 1674, 1534, 1462, 1303, 1256; δ_H (400 MHz, DMSO−d$_6$) 10.39 (s, 1 H), 9.63 (s, 1 H), 8.29 (s, 1 H), 7.56 (d$_{app}$), J = 8.7 Hz, 2 H), 7.23 (dd, J = 8.3, 0.5 Hz, 1 H), 7.26 (dd, J = 8.2, 2.2 Hz, 1 H), 7.03 (d$_{app}$, J = 8.8 Hz, 2 H), 6.98 (d, J = 2.2 Hz, 1 H), 3.79 (s, 3 H), 2.19 (s, 3 H); δ_C (100 MHz, DMSO−d$_6$) 161.18, 158.43, 147.95, 146.38, 146.12, 136.31, 132.28, 130.76, 130.50 (2 C), 130.44, 130.17, 126.04, 125.06, 124.26, 119.80, 114.48 (2 C), 55.72, 17.62; m/z (ESI) 394 ([M + H]$^+$), 416 ([M + Na]$^+$); HRMS (APCI) 394.10637 ([M + H]$^+$) calcd. for C$_{20}$H$_{17}$ClN$_5$O$_2{}^+$ 394.10653; Anal. Calcd. for C$_{20}$H$_{16}$ClN$_5$O$_2$: C, 61.00; H, 4.10; N, 17.78. Found: C, 61.00; H, 3.90; N, 17.43.

### 5.6.8 *N*-(3-chlorophenyl)-3-(pyridin-2-yl)-[1,2,4]triazolo[4,3-a]pyrazine-5-carboxamide 19
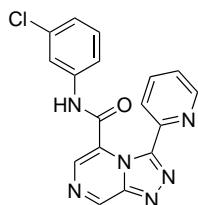
Prepared according to general procedure 4 from **9** (100 mg, 0.28 mmol). Beige powder (56 mg, 0.16 mmol, 57%); mp 222–224 ℃; ν_{max} (film)/cm^{-1} 3055, 2918, 1686, 1591, 1536, 1425, 1310; δ_H (400 MHz, DMSO−d$_6$) 11.21 (s, 1 H), 9.73 (s, 1 H), 8.42 (s, 1 H), 8.29 (ddd, J = 4.9, 1.8, 1.0 Hz, 1 H), 8.15 (dt, J = 7.8, 1.1 Hz, 1 H), 8.02 (td, J = 7.7, 1.7 Hz, 1 H), 7.58 (t, J = 2.3 Hz, 1 H), 7.41 (ddd, J = 7.6, 4.8, 1.2 Hz, 1 H), 7.38–7.36 (m, 2 H), 7.19 ((dt$_{app}$), J = 6.8, 2.1 Hz, 1 H); δ_C (100 MHz, DMSO−d$_6$) 158.56, 148.30, 146.91, 146.53, 146.44, 146.05, 139.58, 137.83, 133.01, 130.97, 130.56, 124.89, 124.61, 124.05, 123.39, 119.16, 118.14; m/z (ESI) 351 ([M+H]$^+$), 373 ([M+Na]$^+$); HRMS (APCI) 351.07547 ([M+H]$^+$) calcd. for C$_{17}$H$_{12}$ClN$_6$O$^+$ 351.07556.

5.6.9 *N*-(3-chlorophenyl)-3-(pyridin-3-yl)-[1,2,4]triazolo[4,3-a]pyrazine-5-carboxamide 20
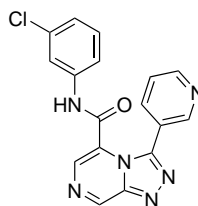
Prepared according to general procedure 5 from **10** (100 mg, 0.28 mmol). Tan powder (50 mg, 0.14 mmol, 50%); mp 196–197 ℃; ν_{max} (film)/cm^{-1} 3058, 1681, 1594, 1542, 1480, 1425, 1313; δ_H (400 MHz, DMSO−d$_6$) 11.07 (s, 1 H), 9.71 (s, 1 H), 8.79 (dd, J = 2.3, 1.1 Hz, 1 H), 8.55 (dd, J = 4.9, 1.6 Hz, 1 H), 8.38 (s, 1 H), 8.01 (dt, J = 7.9, 2.0 Hz, 1 H), 7.42 (dd, J = 5.2, 1.0 Hz, 1 H), 7.41 (t, J = 2.2 Hz, 1 H), 7.40 (dd, J = 5.0, 1.1 Hz, 1 H), 7.31 (t, J = 8.1 Hz, 1 H), 7.21 (ddd, J = 8.2, 1.8, 1.0 Hz, 1 H), 7.18 (ddd, J = 7.9, 2.0, 1.0 Hz, 1 H); δ_C (100 MHz, DMSO−d$_6$) 157.85, 151.10, 149.02, 146.81, 146.45, 145.75, 139.09, 136.30, 133.33, 131.08, 130.87, 124.94, 124.53, 124.45, 123.71, 119.85, 118.78; m/z (ESI) 351 ([M+H]$^+$); HRMS (APCI) 351.07526 ([M+H]$^+$) calcd. for C$_{17}$H$_{12}$ClN$_6$O$^+$ 351.0755.

5.6.10 *N*-(3-chlorophenyl)-3-(4-(trifluoromethoxy)phenyl)-[1,2,4]triazolo[4,3-a]pyrazine-5-carboxamide 18
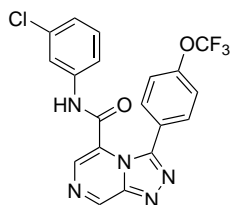
Prepared according to general procedure 4 from **8** (170 mg, 0.39 mmol). Fine white powder (144 mg, 0.33 mmol, 85%); mp 249–250.0 ℃; ν_{max} (film)/cm^{-1} 3222, 3197, 3052, 1673, 1432, 1466, 1313, 1167; δ_H (400 MHz, DMSO−d$_6$) 10.94 (s, 1 H), 9.68 (s, 1 H), 8.33 (s, 1 H), 7.72 (d$_{app}$, $J = 8.7$ Hz, 2 H), 7.44 (t, $J = 2.10$ Hz, 1 H), 7.36 (d$_{app}$, $J = 8.0$ Hz, 2 H), 7.27 (t, $J = 8.1$ Hz, 1 H), 7.17 (dd, $J = 2.9, 2.1$ Hz, 1 H), 7.15 (ddd, $J = 3.4, 2.1, 1.1$ Hz, 1 H); δ_C (100 MHz, DMSO−d$_6$) 157.38, 149.35, 146.51, 146.20, 145.82, 138.64, 132.93, 130.57 (2 C), 130.45, 130.23, 126.55, 124.32, 124.30, 120.86 (2 C), 119.89 (q, $J = 252.9$), 119.03, 118.00; m/z (ESI) ; HRMS(APCI) 434.06242 ([M + H]$^+$) calcd. for C$_{19}$H$_{12}$ClF$_3$N$_5$O$_2^+$ 434.06261; Anal. Calcd. for C$_{19}$H$_{11}$ClF$_3$N$_5$O$_2$: C, 52.61; H, 2.56; N, 16.15. Found: C, 52.02; H, 2.32; N, 15.69.

5.7 Preparation of 6-chloro-2-pyrazine carboxylic acid starting material

5.7.1 Methyl 2-pyrazinecarboxylate 27
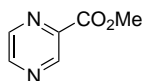
This procedure was taken from the literature[39]. Pyrazine-2-carboxylic acid (15.2 g, 122 mmol) was placed in methanol (130 mL), catalytic sulfuric acid (1 mL) added, and the reaction mixture was stirred at reflux for 24 h. Methanol was removed under reduced pressure, and the crude dried under vacuum to give a tan solid (16.9 g, 122 mmol, 100%) which was carried forward without further purification. NMR shifts were consistent with previously reported values; δ_H (200 MHz, CDCl$_3$) 9.32 (d, $J = 1.4$ Hz, 1 H), 8.77 (d, $J = 2.5$ Hz, 1 H), 8.72 (dd, $J = 2.4, 1.5$ Hz, 1 H), 4.04 (s, 3 H).

### 5.7.2 3-(Methoxycarbonyl)pyrazine 1-oxide 28
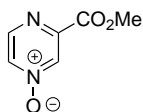
This procedure was taken from the literature[39]. A solution of **27** (17.6 g, 128 mmol, 1 equiv) and *m*-chloroperbenzoic acid (29.0 g, 144 mmol, 85% purity, 1.1 equiv) in dichloroethane (160 mL) was stirred at reflux for 18 h to give a yellow solution containing suspended white solid. The reaction mixture was diluted with CH$_2$Cl$_2$ (400 mL), cooled over ice, then filtered cold to remove precipitated *m*-chlorobenzoic acid. The

solution was concentrated under reduced pressure to give **28** as a pale yellow solid (27.9 g), together with residual *m*-chlorobenzoic acid and some *m*-chloroperbenzoic acid. By ^{1}H NMR integrations, these products were present in a ratio of ∼1:0.74:0.3 respectively, corresponding to 87 mmol, 68% yield of **28**. This crude material was carried forward without further purification. NMR consistent with the literature[39]: δ_H (200 MHz, CDCl$_3$) 8.79 (d, J = 0.6 Hz, 1 H), 8.60 (dd, J = 4.1, 0.7 Hz, 1 H), 8.27 (dd, J = 4.0, 1.7 Hz, 1 H), 4.05 (s, 3 H).

5.7.3   Methyl 6-chloropyrazine-2-carboxylate 29
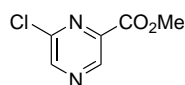
This procedure was adapted from the literature[39]. Crude **28** (27.9 g, as ∼1:1 mixture with *m*-chlorobenzoic acid), 90 mmol) was added to thionyl chloride (90 mL), and heated to 50 ℃ for 16 h. Thionyl chloride was removed under reduced pressure (and quenched in ice water, then neutralised with solid NaOH), and the crude product neutralised with a saturated solution of Na$_2$CO$_3$. The solution was extracted with CH$_2$Cl$_2$ (5 x 200 mL), the combined organic portions washed with brine (2 x 100 mL) and dried over Na$_2$SO$_4$, then concentrated under reduced pressure to give crude **29** as a brown oil (32.2 g). The oil was washed through a silica plug with hexanes to remove the m-chlorobenzoic byproduct remaining (monitored by TLC, ∼2L of solvent), then eluted with 10% EtOAc in hexanes to give **29** as a yellow liquid that slowly congealed at rt. δ_H (200 MHz, CDCl$_3$) 9.13 (d, J = 0.6 Hz, 1 H), 8.73 (d, J = 0.6 Hz, 1 H), 3.98 (s, 3 H).

5.7.4   6-Chloropyrazine-2-carboxylic acid 1
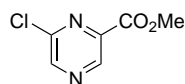
This procedure was adapted from the literature[39]. **29** (2.00 g, 11.6 mmol, 1 equiv.) was dissolved in THF (60 mL), and aqueous NaOH solution (2 M, 10 mL, 2 equiv.) added. The reaction mixture was stirred at rt for 1 h, then acidified with 1 M HCl to pH 3. Water was removed under reduced pressure to give brown flakes, which were dissolved in acetone (to ∼ 0.3 M) with stirring. The solution was dried over anhydrous Na$_2$SO$_4$, filtered, and concentrated under reduced pressure to give **1** as brown flakes (1.66 g, 10.5 mmol, 91%). NMR shifts were consistent with commercially obtained 6-chloropyrazine-2-carboxylate; δ_H (200 MHz, DMSO−d$_6$) 13.98 (s, 1 H), 9.15 (d, J = 0.6 Hz, 1 H), 9.02 (d, J = 0.6 Hz, 1 H) (commercial sample: 14.06, 9.16, 9.04).

5.8 Palladium-free molybdenum mediated carbonylations

This procedure was adapted from the literature[35]. All solvents used were degassed by freeze-thawing, stored over 4 Å molecular sieves, and used within two weeks of preparation. 2-bromonapthalene (207 mg, 1 mmol, 1 equiv.), molybdenum hexacarbonyl (53 mg, 0.2 mmol, 1.2 equiv. CO), tributylamine (204 mg, 1.1 equiv.), and an oxygen nucleophile (phenol: 141 mg, 1.5 mmol, 1.5 equiv.; water: 54 μL, 54 mg, 3 equiv.) were combined in diglyme (10 mL) and heated at 150 ℃ for 12 h in a sealed tube. Diglyme was removed under reduced pressure by azeotroping with water, and the crude product obtained was purified by flash chromatography.

5.9 Palladium-catalysed carbonylations

This procedure was adapted from the literature[31]. All solvents used were degassed by freeze-thawing, stored over 4 Å molecular sieves, and consumed within two weeks of preparation. Anhydrous potassium carbonate was stored in an oven at 150 ℃. Powdered 3 Å molecular sieves were stored in an oven prior to use. Glassware was oven dried for at least 12 h before use. PTFE vial adapters fitted with septa and sealed with PTFE tape were used with 21 mL sample vials in a metal heating block for rapid screening of reaction conditions.
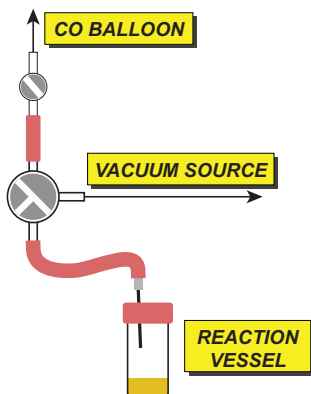

**Figure 5.1:** Apparatus used for safe handling of CO in an inert atmosphere.

Potassium carbonate (207 mg, 1.5 mmol), molecular sieves (powdered, 3 Å, 150 mg), and substrate (1.0 mmol) were placed in a 21 mL sample vial containing a stir bar. A septum-fitted PTFE adapter was attached, and the vial evacuated and refilled with nitrogen several times. The adapter was removed briefly, and palladium acetate (4.5 mg, 0.02 mmol) and dcpp$\cdot$2 HBF$_4$ (24.4 mg, 0.04 mmol) added. The adapter was re-attached, sealed with PTFE tape, and the vial

evacuated and backfilled with nitrogen several times. Solvent (DMF or DMSO, 1 mL) and alcohol (5 mmol: 0.2 mL methanol, or 0.3 mL ethanol) were added by syringe.

Separately, two nested balloons were attached to a short length of vacuum tubing, secured with a cable tie, and sealed with parafilm. The vacuum tubing was attached to a plastic stopcock, allowing the balloon to be sealed. The balloon was flushed three times with CO to remove air, then filled and the stopcock closed. A three-way stopcock was used to connect the balloon and a vacuum source to a short length of tubing terminating in a needle, inserted into the reaction vessel. Using the three-way valve, the vial was evacuated and refilled with CO three times, with the balloon left attached and open to the reaction vessel. The vial was then heated using a metal heating block for a specified time, at a specified temperature. A diagram of the apparatus described above is given in Figure 5.1.

At reaction completion the vial was allowed to cool to rt, and remaining CO dissipated in the fume hood. The reaction mixture was filtered through a short plug of Celite™, and the plug washed with ethyl acetate (~50 mL). The filtrate was then concentrated onto Celite™ under reduced pressure, and the resulting solid used as a dry load for purification by the stated method.

5.9.1 Methyl nicotinate
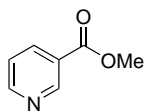
This compound is known to the literature[31]. According to the general procedure, 3-chloropyridine (114 mg, 1 mmol) and methanol (0.2 mL, 5 mmol) were heated in DMF at 100 ℃ for 5 h. Purification by automatic column chromatography (25 to 100% ethyl acetate in hexanes, silica, 1% triethylamine addiditve) gave the title compound (85 mg, 62%) as a herbal-smelling yellow oil. NMR shifts were consistent with the literature[69]; δ_H (500 MHz, CDCl$_3$) 9.22 (d, J = 1.4 Hz, 1 H), 8.77 (dd, J = 4.8, 1.6 Hz, 1 H), 8.29 (dt, J = 7.9, 1.9 Hz, 1 H), 7.39 (ddd, J = 7.9, 4.9, 1.0 Hz, 1 H), 3.96 (s, 3 H); δ_C (126 MHz, CDCl$_3$) 165.92, 153.60, 151.10, 137.18, 126.19, 123.42, 52.56.

5.9.2 Ethyl nicotinate
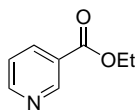
This compound is known to the literature[31]. According to the general procedure, 3-chloropyridine (114 mg, 1 mmol) and ethanol (0.3 mL, 5 mmol) were heated in DMF at 100 ℃ for 5 h. Purification by automatic column chromatography (25 to 100% ethyl acetate in hexanes, silica, 1% triethylamine addiditve) gave the title compound (90 mg, 53%) as a white solid. NMR shifts were consistent with the literature[70]; δ_H (500 MHz,

CDCl$_3$) 9.19 (dd, J = 2.0, 0.7 Hz, 1 H), 8.73 (dd, J = 4.9, 1.7 Hz, 1 H), 8.26 (dt, J = 7.9, 2.0 Hz, 1 H), 7.35 (ddd, J = 7.9, 4.9, 0.8 Hz, 1 H), 4.38 (q, J = 7.1 Hz, 2 H), 1.37 (t, J = 7.2 Hz, 3 H); δ_C (126 MHz, CDCl$_3$) 165.34, 153.39, 150.98, 137.06, 126.41, 123.30, 61.50, 14.33.

## 5.10 General procedure 5: annulation of hydrazinylpyrazines

Hydrazinylpyrazine (1 equiv.), triethyl orthoformate (2 equiv.), and tosylic acid (0.05 equiv.) were dissolved in toluene (to around 0.35 M) and heated at reflux for 24 h. Volatiles were removed under reduced pressure, remaining orthoester was blown off under a gentle stream of nitrogen, and the desired product obtained by the stated method.

5.10.1 2-Chloro-6-hydrazinylpyrazine 32
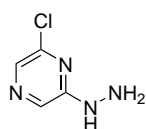
Prepared from 2,6-dichloropyrazine (21 g, 141 mmol) according to general procedure 2, with ethyl acetate/water workup. **32** obtained as a fluffy pale yellow solid (19.13 g, 132 mmol, 94%); δ_H (400 MHz, DMSO−d$_6$) 8.42 (s, 1 H), 8.04 (s, 1 H), 7.71 (s, 1 H), 4.37 (s, 2 H) (consistent with the literature[47]); δ_C (100 MHz, DMSO−d$_6$) 157.19, 145.77, 128.94, 128.61.

5.10.2 5-Chloro-[1,2,4]triazolo[4,3-a]pyrazine 33
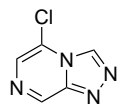
Prepared from **48** (8.00 g, 55.3 mmol) according to general procedure 5. Purified by automatic column chromatography (20 to 100% ethyl acetate in hexanes, 1% triethylamine additive; λ_{max} ∼ 295 nm) to give **33** as a pale yellow solid (5.30 g, 35.4 mmol, 62%); mp 164–167 (lit mp 167–172[47]; δ_H (400 MHz, DMSO−d$_6$) 9.69 (d, J = 0.7 Hz, 1 H), 9.45 (t, J = 0.6 Hz, 1 H), 8.17 (t, J = 0.6 Hz, 1 H); δ_C (100 MHz, DMSO−d$_6$) 145.66, 141.76, 135.97, 127.74, 121.19; m/z (ESI) 155 ([M+H]$^+$).
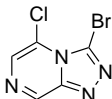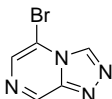
5.10.3 [1,2,4]Triazolo[4,3-a]pyrazine 39
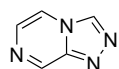
This compound is known to the literature[48]. Prepared from hydrazinylpyrazine (1.5 g, 13.6 mmol) according to general procedure 5. Purified by automatic column chromatography (20 to 100% ethyl acetate in hexanes, 1% triethylamine additive; λ_{max} ∼ 295 nm) to give **39** as yellow flakes (345 mg, 2.9 mmol, 29%); mp 194–195 (lit. mp 194–195[48];

δ_{H} (300 MHz, CDCl$_3$) 9.40 (d, $J = 2.0$ Hz, 1 H), 8.96 (s, 1 H), 8.11 (dd, $J = 4.8$, 1.7 Hz, 1 H), 7.94 (d, $J = 4.8$ Hz, 1 H).

5.10.4 3-Bromo-5-chloro-[1,2,4]triazolo[4,3-a]pyrazine 34

33 (1 g, 6.49 mmol) and N-bromosuccinimide (2 g, 11.2 mmol, 1.7 equiv.) were placed in chloroform (50 mL) and refluxed for 24 h. The reaction mixture was then diluted with chloroform (50 mL), washed with sodium carbonate solution (15 mL), and the aqueous layer re-extracted with chloroform (2 x 20 mL). The combined organic portions were concentrated under reduced pressure to give **34** as a yellow solid (884 mg, 3.80 mmol, 58%); mp 122–124 ℃; ν_{max} (film)/cm^{-1} 3096, 1612, 1512, 1486, 1281, 1207; δ_{H} (500 MHz, CDCl$_3$) 9.25 (s, 1 H), 7.87 (s, 1 H); δ_{C} (126 MHz, CDCl$_3$) 148.27, 143.14, 130.49, 121.90, 120.27; m/z (APCI) 233, 235, 237 ([M + H]$^+$); HRMS 232.92229 (largest peak of isotopic pattern) ([M + H]$^+$) calcd. for C$_5$H$_3$BrClN$_4^+$ 232.92241.

5.10.5 5-Bromo-[1,2,4]triazolo[4,3-a]pyrazine 38

This procedure was adapted from the literature[47]. To a solution of **39** (150 mg, 1.25 mmol) in glacial acetic acid (6 mL) was added bromine (65 μL, 200 mg, 1.25 mmol, 1 eq), causing a yellow solid to precipitate. The solid was collected by filtration, dissolved in CH$_2$Cl$_2$ (15 mL), washed with sodium carbonate solution (5 mL), and the aqueous portion re-extracted with CH$_2$Cl$_2$ (2 x 25 mL) to give **49** as a greenish-yellow solid (230 mg, 1.21 mmol, 97%); mp 192–193 (lit. mp 214–217[47]; δ_{H} (400 MHz, CDCl$_3$) 9.32 (s, 1 H), 9.04 (s, 1 H), 8.04 (s, 1 H); δ_{C} (100 MHz, CDCl$_3$) 145.71, 142.37, 136.42, 131.80, 109.14.

References

[1] WHO | Malaria, 2014. URL http://www.who.int/mediacentre/factsheets/fs094/en/. Accessed: 2014-10-23.

[2] P. B. Bloland, E. M. Lackritz, P. N. Kazembe, J. B. O. Were, R. Steketee, and C. C. Campbell. Beyond chloroquine: implications of drug resistance for evaluating malaria therapy efficacy and treatment policy in Africa. *J. Infect. Dis.*, 167:932–937, 1993. doi: 10.1093/infdis/167. 4.932.

[3] N. J. White and P. L. Olliaro. Strategies for the prevention of antimalarial drug resistance: rationale for combination chemotherapy for malaria. *Parasitol. Today*, 12:399–401, 1996. doi: 10.1016/0169-4758(96)10055-7.

[4] Friedrich, M. J. Artemisinin-resistant malaria. *J. Am. Med. Assoc.*, 307:2017–2017, 2012. doi: 10.1001/jama.2012.5079.

[5] Malaria - strategy overview, 2014. URL http://www.gatesfoundation.org/What-We-Do/ Global-Health/Malaria. Accessed: 2014-10-23.

[6] OpenSourceMalaria:FAQ - OpenWetWare, 2014. URL http://openwetware.org/wiki/ OpenSourceMalaria:FAQ. Accessed: 2014-10-24.

[7] Open source malaria lab notebook, 2014. URL http://malaria.ourexperiment.org/. Accessed: 2014-10-24.

[8] F.-J. Gamo, L. M. Sanz, J. Vidal, C. de Cozar, E. Alvarez, J.-L. Lavandera, D. E. Vanderwall, D. V. S. Green, V. Kumar, S. Hasan, J. R. Brown, C. E. Peishoff, L. R. Cardon, and J. F. Garcia-Bustos. Thousands of chemical starting points for antimalarial lead identification. *Nature*, 465:305–310, 2010. doi: 10.1038/nature09107.

[9] OSM ELN. A new triazolopyrazine series for OSM - series 4, 2013. URL http: //malaria.ourexperiment.org/osdd_malaria_shared/7949/A_New_Triazolopyrazine_ Series_for_OSM__Series_4.html. Accessed: 2014-10-23.

[10] MMV. Potential new class of antimalarials now open source | MMV, 2013. URL http://www. mmv.org/newsroom/news/potential-new-class-antimalarials-now-open-source. Accessed: 2014-10-15.

[11] E. Vitaku, D. T. Smith, and J. T. Njardarson. Analysis of the structural diversity, substitution patterns, and frequency of nitrogen heterocycles among U.S. FDA approved pharmaceuticals. *J. Med. Chem.*, 2014. doi: 10.1021/jm501100b.

[12] A. H. Gordon, D. E. Green, and V. Subrahmanyan. Liver aldehyde oxidase. *Biochem. J.*, 34: 764–774, 1940.

[13] C. Stubley, J. G. P. Stell, and D. W. Mathieson. The oxidation of azaheterocycles with mammalian liver aldehyde oxidase. *Xenobiotica*, 9:475–484, 1979. doi: 10.3109/00498257909087261.

[14] D. C. Pryde, D. Dalvie, Q. Hu, P. Jones, R. S. Obach, and T.-D. Tran. Aldehyde oxidase: an enzyme of emerging importance in drug discovery. *J. Med. Chem.*, 53:8441–8460, 2010. doi: 10.1021/jm100888d.

[15] E. Garattini and M. Terao. The role of aldehyde oxidase in drug metabolism. *Expert Opin. Drug Metab. Toxicol.*, 8:487–503, 2012. doi: 10.1517/17425255.2012.663352.

[16] F. O'Hara, A. C. Burns, M. R. Collins, D. Dalvie, M. A. Ornelas, A. D. N. Vaz, Y. Fujiwara, and P. S. Baran. A simple litmus test for aldehyde oxidase metabolism of heteroarenes. *J. Med. Chem.*, 57:1616–1620, 2014. doi: 10.1021/jm4017976.

[17] A. Hantzsch. Condensationsprodukte aus aldehydammoniak und ketonartigen verbindungen. *Ber. Dtsch. Chem. Ges.*, 14:1637–1638, 1881. doi: 10.1002/cber.18810140214.

[18] E. Fischer and F. Jourdan. Ueber die hydrazine der brenztraubensäure. *Ber. Dtsch. Chem. Ges.*, 16:2241–2245, 1883. doi: 10.1002/cber.188301602141.

[19] E. Fischer and O. Hess. Synthese von indolderivaten. *Ber. Dtsch. Chem. Ges.*, 17:559–568, 1884. doi: 10.1002/cber.188401701155.

[20] L. Knorr. Synthese von pyrrolderivaten. *Ber. Dtsch. Chem. Ges.*, 17:1635–1642, 1884. doi: 10.1002/cber.18840170220.

[21] W. Marckwald and E. Meyer. Ueber das α-chinolylhydrazin und seine derivate. *Ber. Dtsch. Chem. Ges.*, 33:1885–1895, 1900. doi: 10.1002/cber.19000330272.

[22] K. Sonogashira, Y. Tohda, and N. Hagihara. A convenient synthesis of acetylenes: catalytic substitutions of acetylenic hydrogen with bromoalkenes, iodoarenes and bromopyridines. *Tetrahedron Lett.*, 16:4467–4470, 1975. doi: 10.1016/S0040-4039(00)91094-3.

[23] R. F. Heck and J. P. Nolley. Palladium-catalyzed vinylic hydrogen substitution reactions with aryl, benzyl, and styryl halides. *J. Org. Chem.*, 37:2320–2322, 1972. doi: 10.1021/jo00979a024.

[24] A. O. King, N. Okukado, and E.-i. Negishi. Highly general stereo-, regio-, and chemo-selective synthesis of terminal and internal conjugated enynes by the Pd-catalysed reaction of alkynylzinc reagents with alkenyl halides. *J. Chem. Soc., Chem. Commun.*, pages 683–684, 1977. doi: 10.1039/C39770000683.

[25] D. Milstein and J. K. Stille. A general, selective, and facile method for ketone synthesis from acid chlorides and organotin compounds catalyzed by palladium. *J. Am. Chem. Soc.*, 100: 3636–3638, 1978. doi: 10.1021/ja00479a077.

[26] A. Schoenberg, I. Bartoletti, and R. F. Heck. Palladium-catalyzed carboalkoxylation of aryl, benzyl, and vinylic halides. *J. Org. Chem.*, 39:3318–3326, 1974. doi: 10.1021/jo00937a003.

[27] A. Schoenberg and R. F. Heck. Palladium-catalyzed formylation of aryl, heterocyclic, and vinylic halides. *J. Am. Chem. Soc.*, 96:7761–7764, 1974. doi: 10.1021/ja00832a024.

[28] C. F. J. Barnard. Palladium-catalyzed carbonylation—a reaction come of age. *Organometallics*, 27:5402–5422, 2008. doi: 10.1021/om800549q.

[29] A. Brennführer, H. Neumann, and M. Beller. Palladium-catalyzed carbonylation reactions of aryl halides and related compounds. *Angew. Chem., Int. Ed.*, 48:4114–4133, 2009. doi: 10.1002/anie.200900013.

[30] J. R. Martinelli, T. P. Clark, D. A. Watson, R. H. Munday, and S. L. Buchwald. Palladium-catalyzed aminocarbonylation of aryl chlorides at atmospheric pressure: the dual role of sodium phenoxide. *Angew. Chem., Int. Ed.*, 46:8460–8463, 2007. doi: 10.1002/anie.200702943.

[31] D. A. Watson, X. Fan, and S. L. Buchwald. Carbonylation of aryl chlorides with oxygen nucleophiles at atmospheric pressure. Preparation of phenyl esters as acyl transfer agents

and the direct preparation of alkyl esters and carboxylic acids. *J. Org. Chem.*, 73:7096–7101, 2008. doi: 10.1021/jo800907e.

[32] S. Korsager, R. H. Taaning, and T. Skrydstrup. Effective palladium-catalyzed hydroxycarbonylation of aryl halides with substoichiometric carbon monoxide. *J. Am. Chem. Soc.*, 135: 2891–2894, 2013. doi: 10.1021/ja3114032.

[33] L. Odell, F. Russo, and M. Larhed. Molybdenum hexacarbonyl mediated CO gas-free carbonylative reactions. *Synlett*, 23:685–698, 2012. doi: 10.1055/s-0031-1290350.

[34] W. Ren and M. Yamane. Mo(CO)6-mediated carbamoylation of aryl halides. *J. Org. Chem.*, 75:8410–8415, 2010. doi: 10.1021/jo101611g.

[35] W. Ren, A. Emi, and M. Yamane. Molybdenum hexacarbonyl mediated alkoxycarbonylation of aryl halides. *Synthesis*, 2011:2303–2309, 2011. doi: 10.1055/s-0030-1260060.

[36] W. Ren and M. Yamane. Carbamoylation of aryl halides by molybdenum or tungsten carbonyl amine complexes. *J. Org. Chem.*, 75:3017–3020, 2010. doi: 10.1021/jo1002592.

[37] OpenSourceMalaria:triazolopyrazine (TP) series - OpenWetWare, 2014. URL `http://openwetware.org/wiki/OpenSourceMalaria:Triazolopyrazine_(TP)_Series`.

[38] Thomson, Patrick. Series 4: Synthetic route to amides · issue #101 · OpenSourceMalaria/OSM_to_do_list, 2013. URL `https://github.com/OpenSourceMalaria/OSM_To_Do_List/issues/101`. Accessed: 2014-10-15.

[39] M. J. C. Scanio, L. Shi, W. H. Bunnelle, D. J. Anderson, R. J. Helfrich, J. Malysz, K. K. Thorin-Hagene, C. E. Van Handel, K. C. Marsh, C.-H. Lee, and M. Gopalakrishnan. Structure–activity studies of diazabicyclo[3.3.0]octane-substituted pyrazines and pyridines as potent α4β2 nicotinic acetylcholine receptor ligands. *J. Med. Chem.*, 54:7678–7692, 2011. doi: 10.1021/jm201045m.

[40] A. El-Faham and F. Albericio. Peptide coupling reagents, more than a letter soup. *Chem. Rev. (Washington, DC, U. S.)*, 111:6557–6602, 2011. doi: 10.1021/cr100048w.

[41] A. K. Sadana, Y. Mirza, K. R. Aneja, and O. Prakash. Hypervalent iodine mediated synthesis

of 1-aryl/hetryl-1,2,4-triazolo[4,3-a] pyridines and 1-aryl/hetryl 5-methyl-1,2,4-triazolo[4,3-a]quinolines as antibacterial agents. *Eur. J. Med. Chem.*, 38:533–536, 2003. doi: 10.1016/S0223-5234(03)00061-8.

[42] O. R. Thiel, M. M. Achmatowicz, A. Reichelt, and R. D. Larsen. Palladium-catalyzed coupling of aldehyde-derived hydrazones: Practical synthesis of triazolopyridines and related heterocycles. *Angew. Chem., Int. Ed.*, 122:8573–8576, 2010. doi: 10.1002/ange.201001999.

[43] R. E. Desjardins, C. J. Canfield, J. D. Haynes, and J. D. Chulay. Quantitative assessment of antimalarial activity in vitro by a semiautomated microdilution technique. *Antimicrob. Agents Chemother.*, 16:710–718, 1979.

[44] M. C. Sanguinetti and M. Tristani-Firouzi. hERG potassium channels and cardiac arrhythmia. *Nature*, 440:463–469, 2006. doi: 10.1038/nature04710.

[45] J. T. Milnes, O. Crociani, A. Arcangeli, J. C. Hancox, and H. J. Witchel. Blockade of hERG potassium currents by fluvoxamine: incomplete attenuation by s6 mutations at f656 or y652. *Br. J. Pharmacol.*, 139:887–898, 2003. doi: 10.1038/sj.bjp.0705335.

[46] Williamson, Alice E. Compounds sent for evaluation against the hERG ion channel at AstaZeneca, 2014. URL http://malaria.ourexperiment.org/biological_data/11081/Compounds_sent_for_evaluation_against_the_hERG_ion_channel_at_AstraZeneca.html. Accessed: 2014-10-23.

[47] J. Bradac, Z. Furek, D. Janezic, S. Molan, I. Smerkolj, B. Stanovnik, M. Tisler, and B. Vercek. Heterocycles. 167. telesubstitution and other transformations of imidazo[1,2-a]- and s-triazolo[4,3-a]pyrazines. *J. Org. Chem.*, 42:4197–4201, 1977. doi: 10.1021/jo00862a005.

[48] P. J. Nelson and K. T. Potts. 1,2,4-triazoles. VI.1 the synthesis of some s-triazolo[4,3-a]pyrazines. *J. Org. Chem.*, 27:3243–3248, 1962. doi: 10.1021/jo01056a061.

[49] G. G. Chilov and I. Y. Titov. Protein kinase inhibitors (variants), use thereof in treating oncological diseases and a pharmaceutical composition based thereon, 2013. WO2012173521 (A3).

[50] J. E. Baldwin. Rules for ring closure. *J. Chem. Soc., Chem. Commun.*, pages 734–736, 1976. doi: 10.1039/C39760000734.

[51] J. E. Baldwin, R. C. Thomas, L. I. Kruse, and L. Silberman. Rules for ring closure: ring formation by conjugate addition of oxygen nucleophiles. *J. Org. Chem.*, 42:3846–3852, 1977. doi: 10.1021/jo00444a011.

[52] H. B. Bürgi, J. D. Dunitz, J. M. Lehn, and G. Wipff. Stereochemistry of reaction paths at carbonyl centres. *Tetrahedron*, 30:1563–1572, 1974. doi: 10.1016/S0040-4020(01)90678-7.

[53] H. B. Bürgi, J. D. Dunitz, and E. Shefter. Geometrical reaction coordinates. II. nucleophilic addition to a carbonyl group. *J. Am. Chem. Soc.*, 95:5065–5067, 1973. doi: 10.1021/ja00796a058.

[54] S. D. Friis, T. Skrydstrup, and S. L. Buchwald. Mild Pd-catalyzed aminocarbonylation of (hetero)aryl bromides with a palladacycle precatalyst. *Org. Lett.*, 2014. doi: 10.1021/ol502014b.

[55] N.-F. K. Kaiser, A. Hallberg, and M. Larhed. In situ generation of carbon monoxide from solid molybdenum hexacarbonyl. A convenient and fast route to palladium-catalyzed carbonylation reactions. *J. Comb. Chem.*, 4:109–111, 2002. doi: 10.1021/cc010085f.

[56] H. Finkelstein. Darstellung organischer jodide aus den entsprechenden bromiden und chloriden. *Ber. Dtsch. Chem. Ges.*, 43:1528–1532, 1910. doi: 10.1002/cber.19100430257.

[57] J. Liu, Z. Janeba, and M. J. Robins. SNAr iodination of 6-chloropurine nucleosides: an aromatic finkelstein reactions at temperatures below -40 °C. *Org. Lett.*, 6:2917–2919, 2004. doi: 10.1021/ol048987n.

[58] A. Klapars and S. L. Buchwald. Copper-catalyzed halogen exchange in aryl halides: an aromatic finkelstein reaction. *J. Am. Chem. Soc.*, 124:14844–14845, 2002. doi: 10.1021/ja028865v.

[59] J. Albaneze-Walker, C. Bazaral, T. Leavey, P. G. Dormer, and J. A. Murry. Improved carbonylation of heterocyclic chlorides and electronically challenging aryl bromides. *Org. Lett.*, 6:2097–2100, 2004. doi: 10.1021/ol0498287.

[60] M. J. Waring and C. Johnstone. A quantitative assessment of hERG liability as a function of lipophilicity. *Bioorg. Med. Chem. Lett.*, 17:1759–1764, 2007. doi: 10.1016/j.bmcl.2006.12.061.

[61] J. Hartwig, M. Jorgensen, and S. Lee. Catalytic method to convert aryl compounds to aryl amines, 2003. WO03006420 (A1).

[62] M. Todd and C. Swain, 2014. URL `https://github.com/OpenSourceMalaria/OSM_To_Do_List/issues/214`. Accessed: 2014-11-2.

[63] A. E. Williamson, P. Thomson, and J. Garfunkle. PIDA cyclisation · issue #97 · OpenSourceMalaria/OSM_to_do_list, 2013. URL `https://github.com/OpenSourceMalaria/OSM_To_Do_List/issues/97`. Accessed: 2014-10-15.

[64] C. Swain. Predicting sites of metabolism, 2014. URL `http://malaria.ourexperiment.org/triazolopyrazine_se/10460/Predicting_sites_of_metabolism.html`. Accessed: 2014-11-2.

[65] J. R. Dunetz, Y. Xiang, A. Baldwin, and J. Ringling. General and scalable amide bond formation with epimerization-prone substrates using T3P and pyridine. *Org. Lett.*, 13:5048–5051, 2011. doi: 10.1021/ol201875q.

[66] M. Dolezal, R. Vicik, M. Miletín, and K. Kralova. Synthesis and antimycobacterial, antifungal, and photosynthesis-inhibiting evaluation of some anilides of substituted pyrazine-2-carboxylic acids. *Chem. Pap.*, 54:245–248, 2000.

[67] M. Dolezal, J. Zitko, Z. Osicka, J. Kunes, M. Vejsova, V. Buchta, J. Dohnal, J. Jampilek, and K. Kralova. Synthesis, antimycobacterial, antifungal and photosynthesis-inhibiting activity of chlorinated n-phenylpyrazine-2-carboxamides. *Molecules*, 15:8567–8581, 2010. doi: 10.3390/molecules15128567.

[68] T. Curtius and A. Lublin. Ueber nitrobenzalhydrazine. *Ber. Dtsch. Chem. Ges.*, 33:2460–2466, 1900.

[69] L. Kaganovsky, D. Gelman, and K. Rueck-Braun. Trans-chelating ligands in palladium-catalyzed carbonylative coupling and methoxycarbonylation of aryl halides. *J. Organomet. Chem.*, 695:260–266, 2010. doi: 10.1016/j.jorganchem.2009.10.001.

[70] R. Shang, Y. Fu, J.-B. Li, S.-L. Zhang, Q.-X. Guo, and L. Liu. Synthesis of aromatic esters via Pd-catalyzed decarboxylative coupling of potassium oxalate monoesters with aryl bromides and chlorides. *J. Am. Chem. Soc.*, 131:5738–5739, 2009. doi: 10.1021/ja900984x.
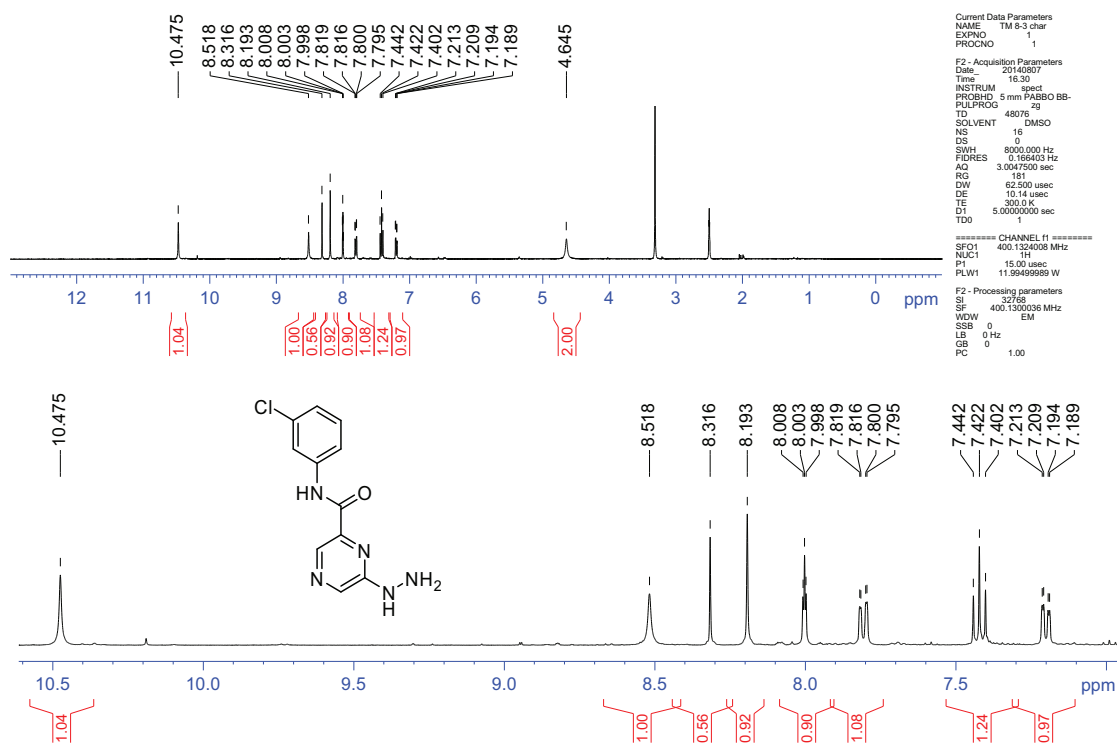
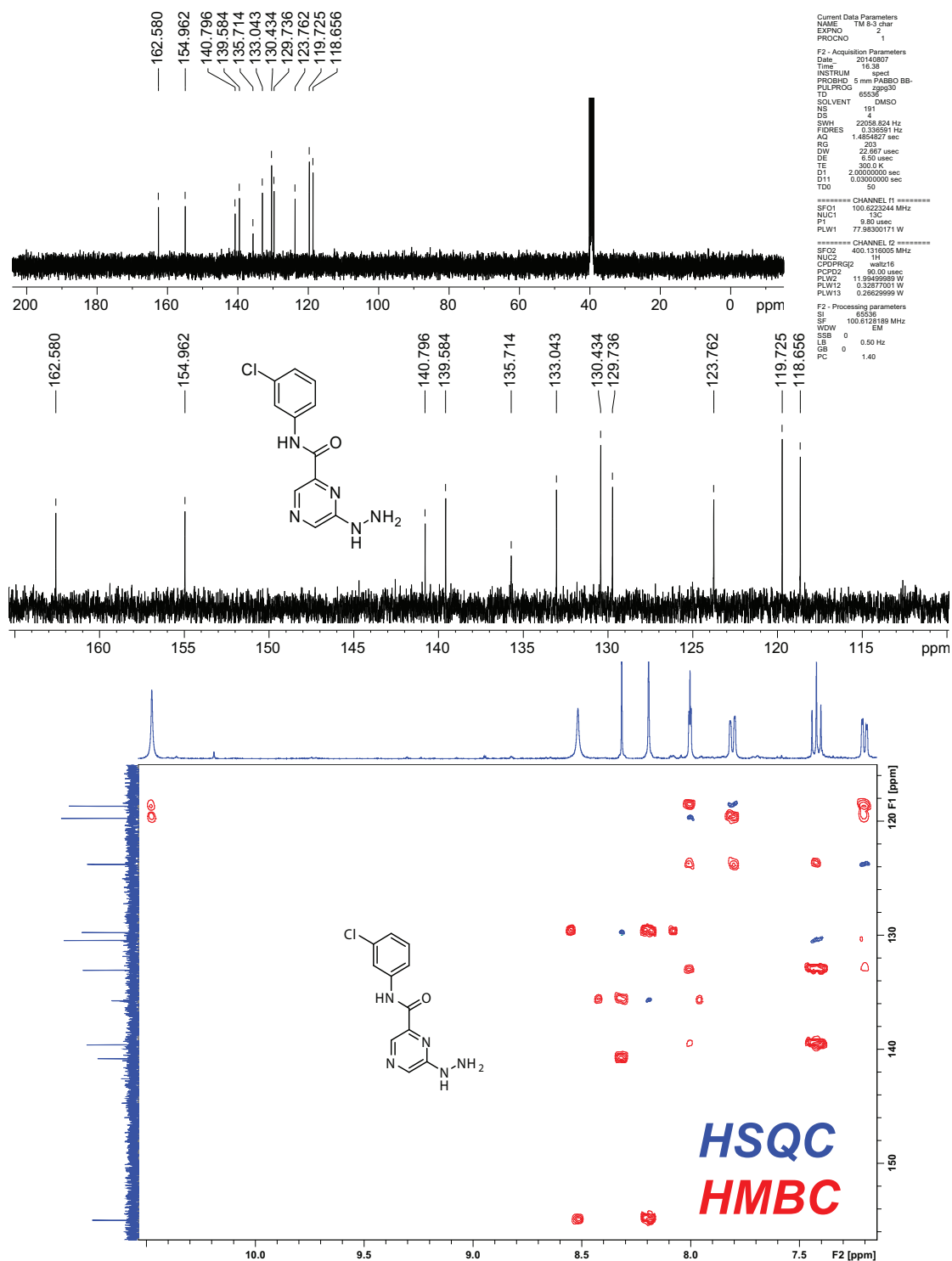# Appendix A

Supporting NMR data of selected compounds

A.1   6-Chloro-N-(3-chlorophenyl)pyrazine-2-carboxamide 2
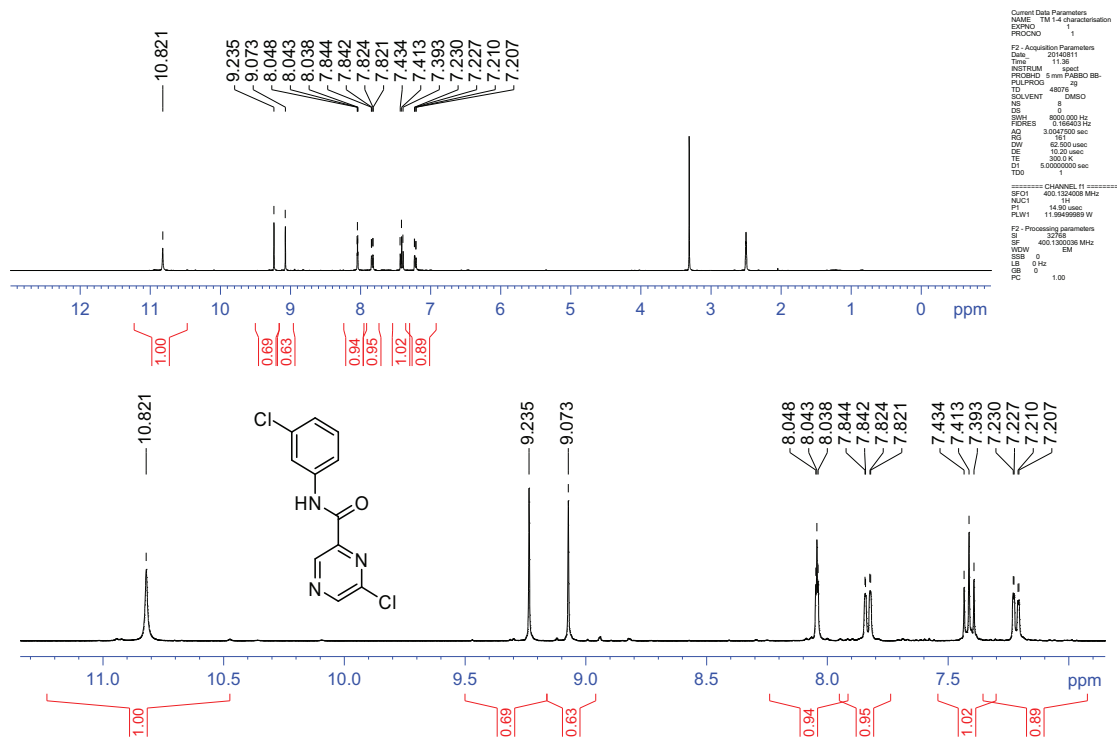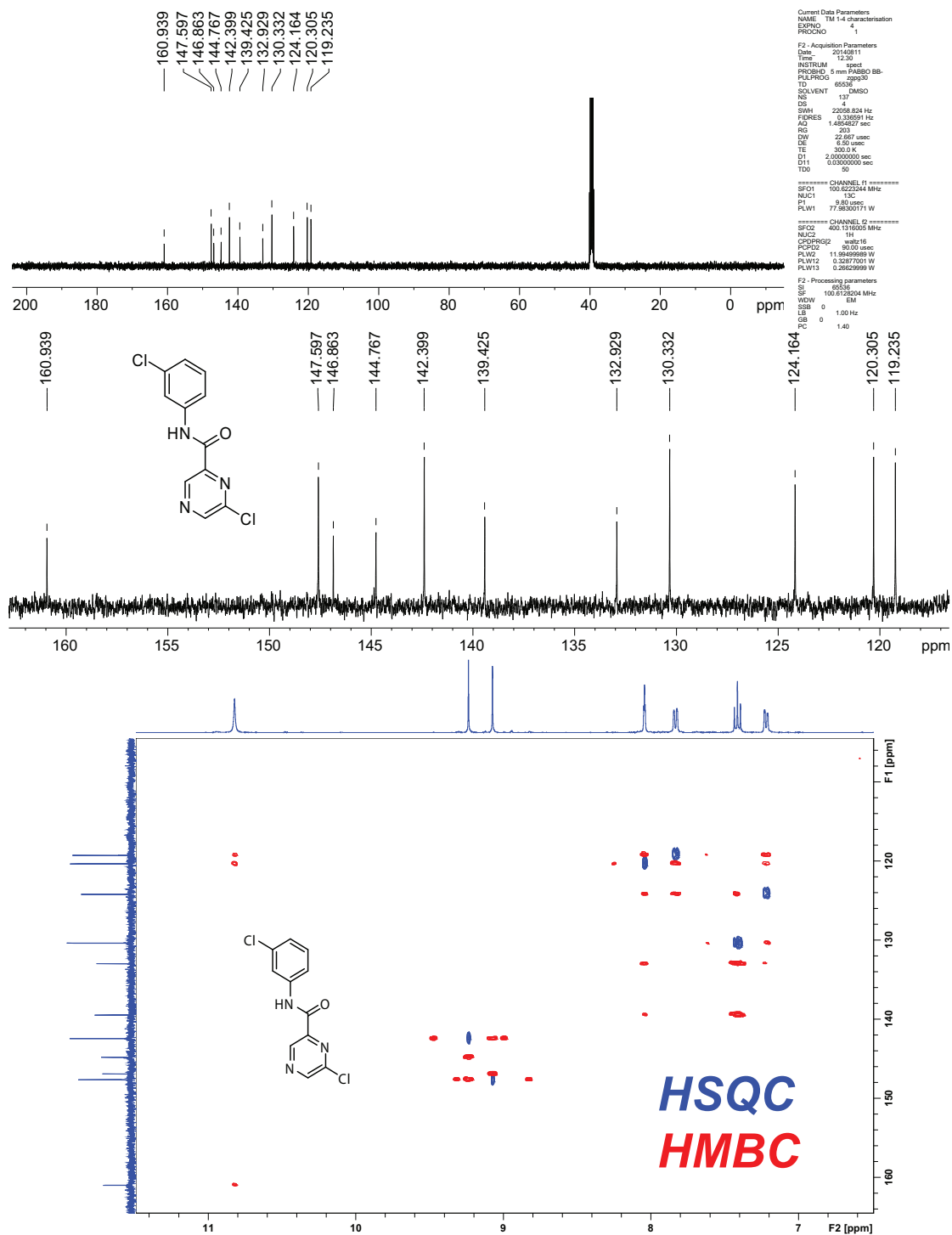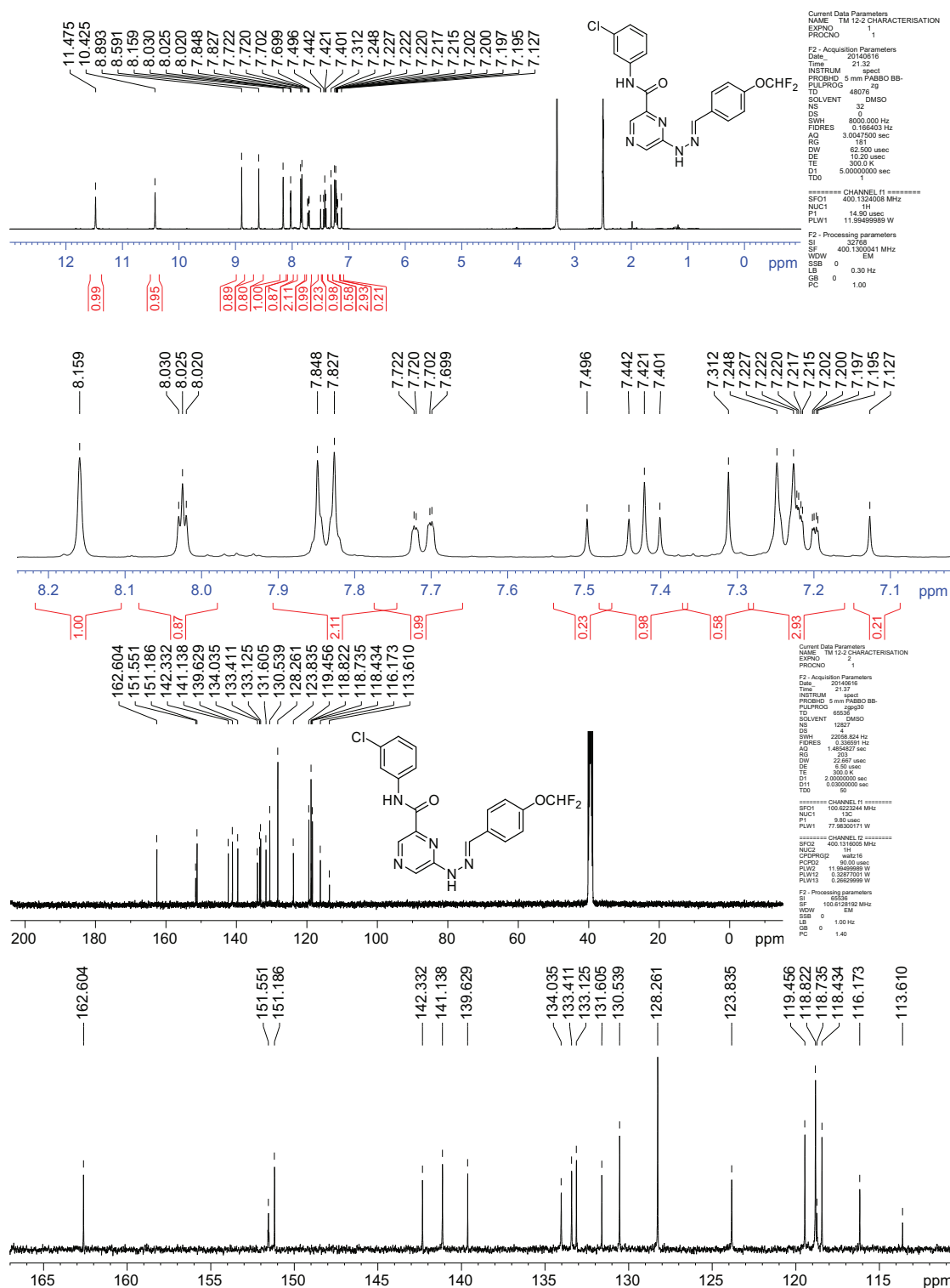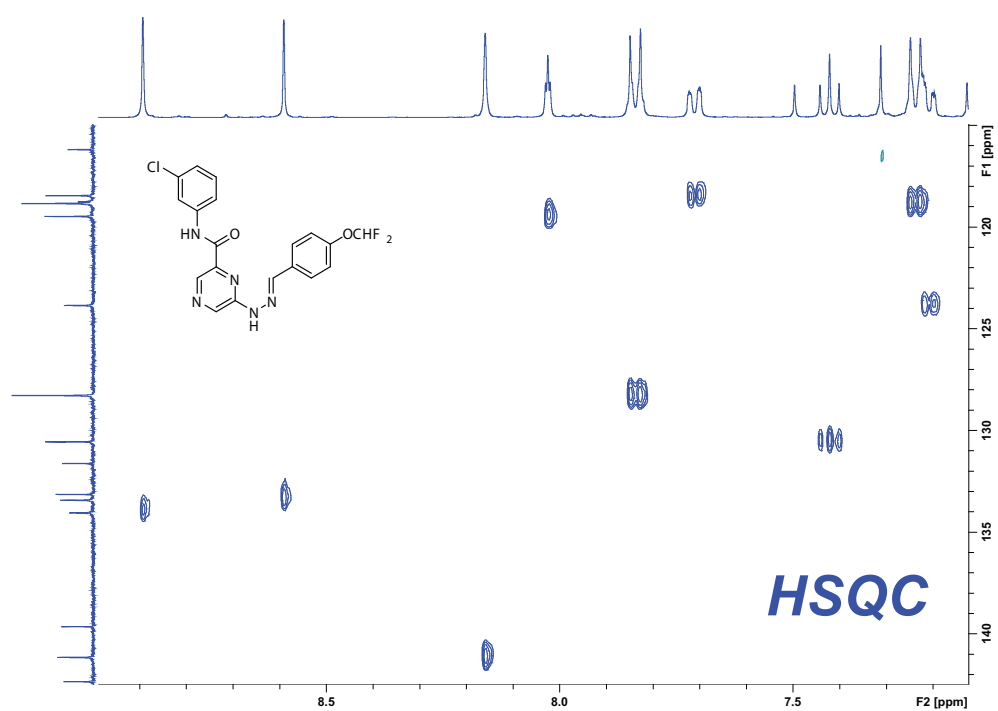
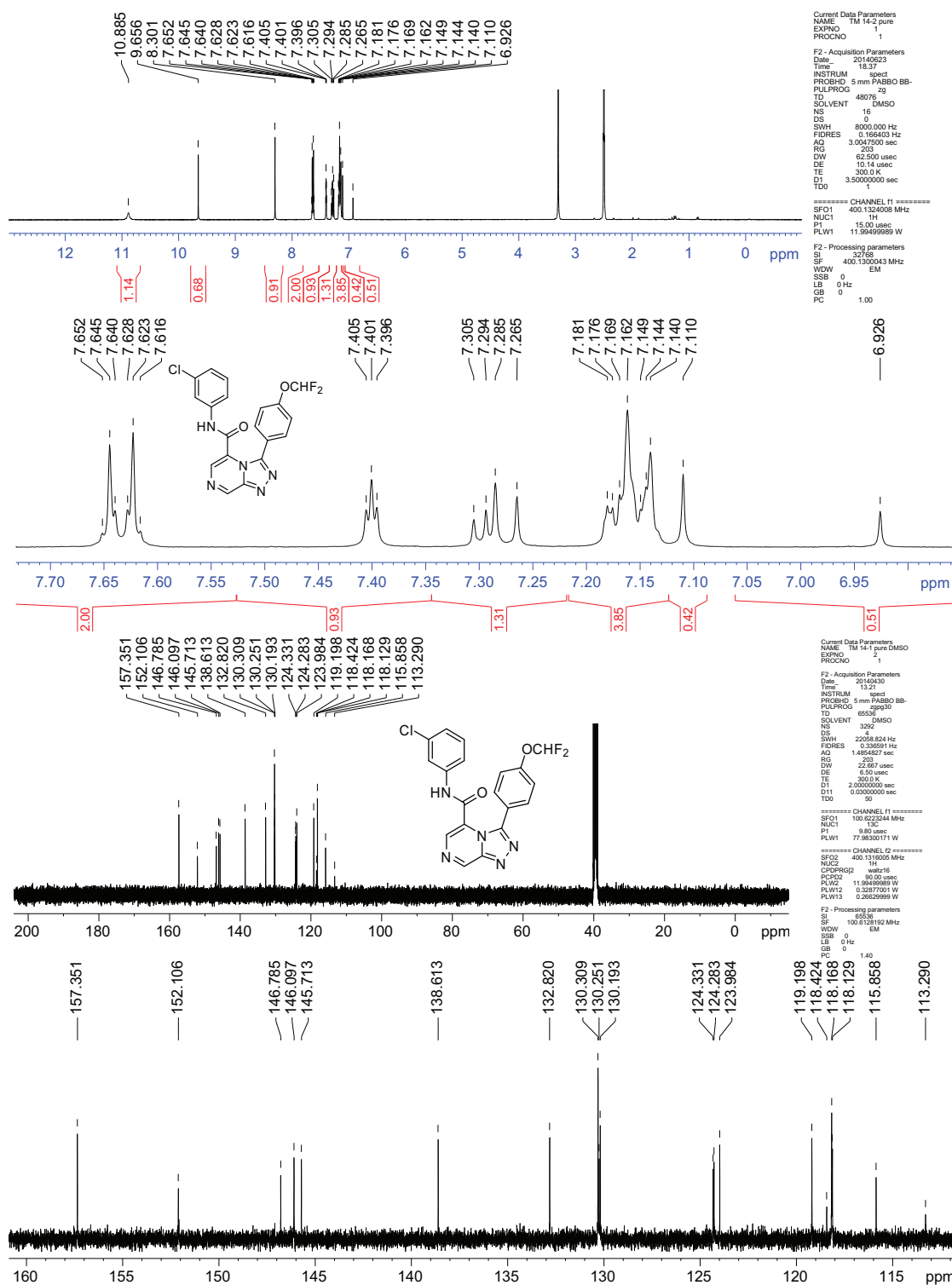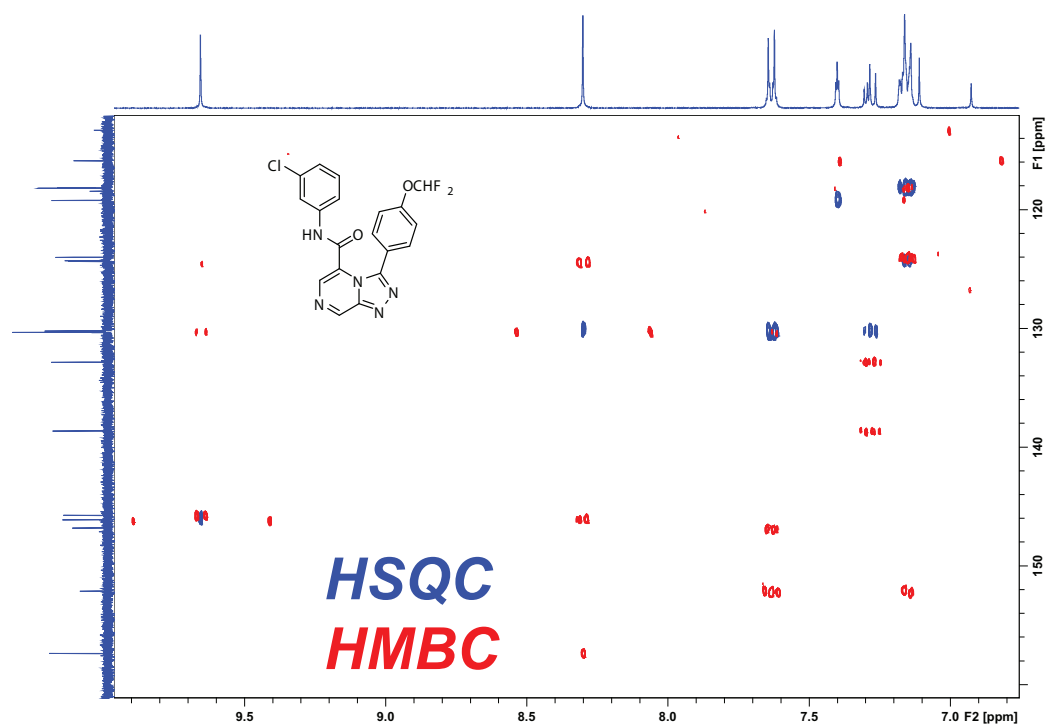## A.2   *N*-(3-chlorophenyl)-6-hydrazinylpyrazine-2-carboxamide 6

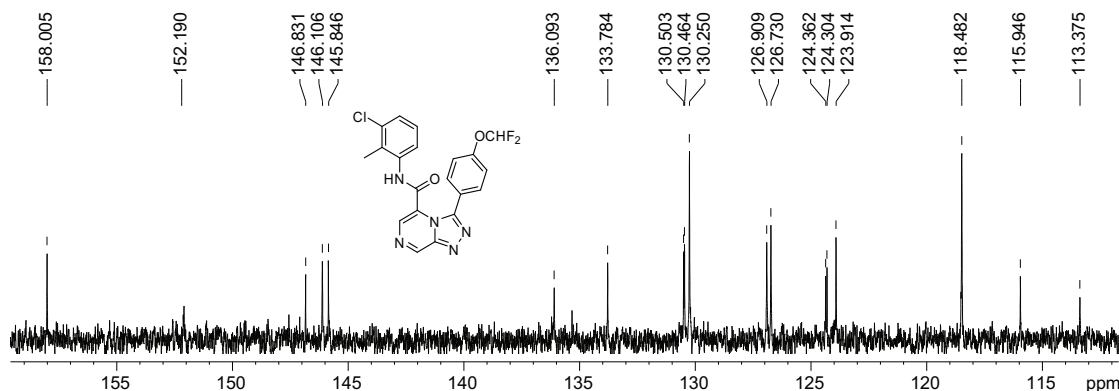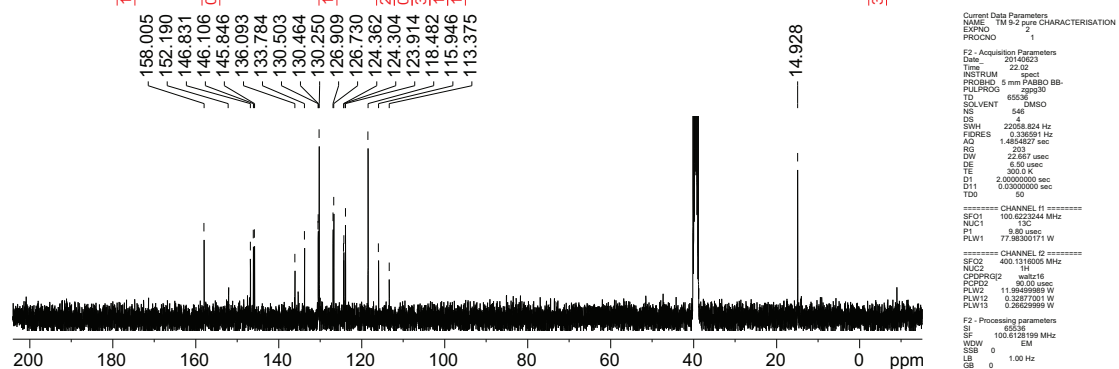## A.3 *N*-(3-chlorophenyl)-6-(2-(4-(difluoromethoxy)benzylidene) hydrazinyl)pyrazine-2-carboxamide 7
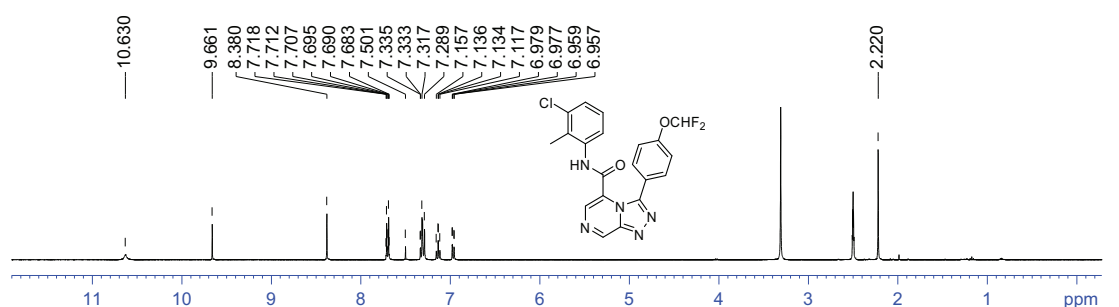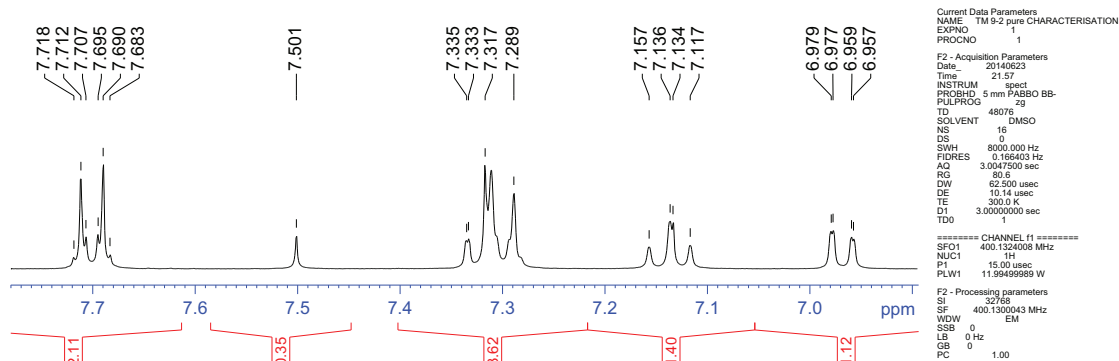
A.4 *N*-(3-chlorophenyl)-3-(4-(difluoromethoxy)phenyl)-[1,2,4]triazolo[4,3-a]pyrazine-5-carboxamide 17
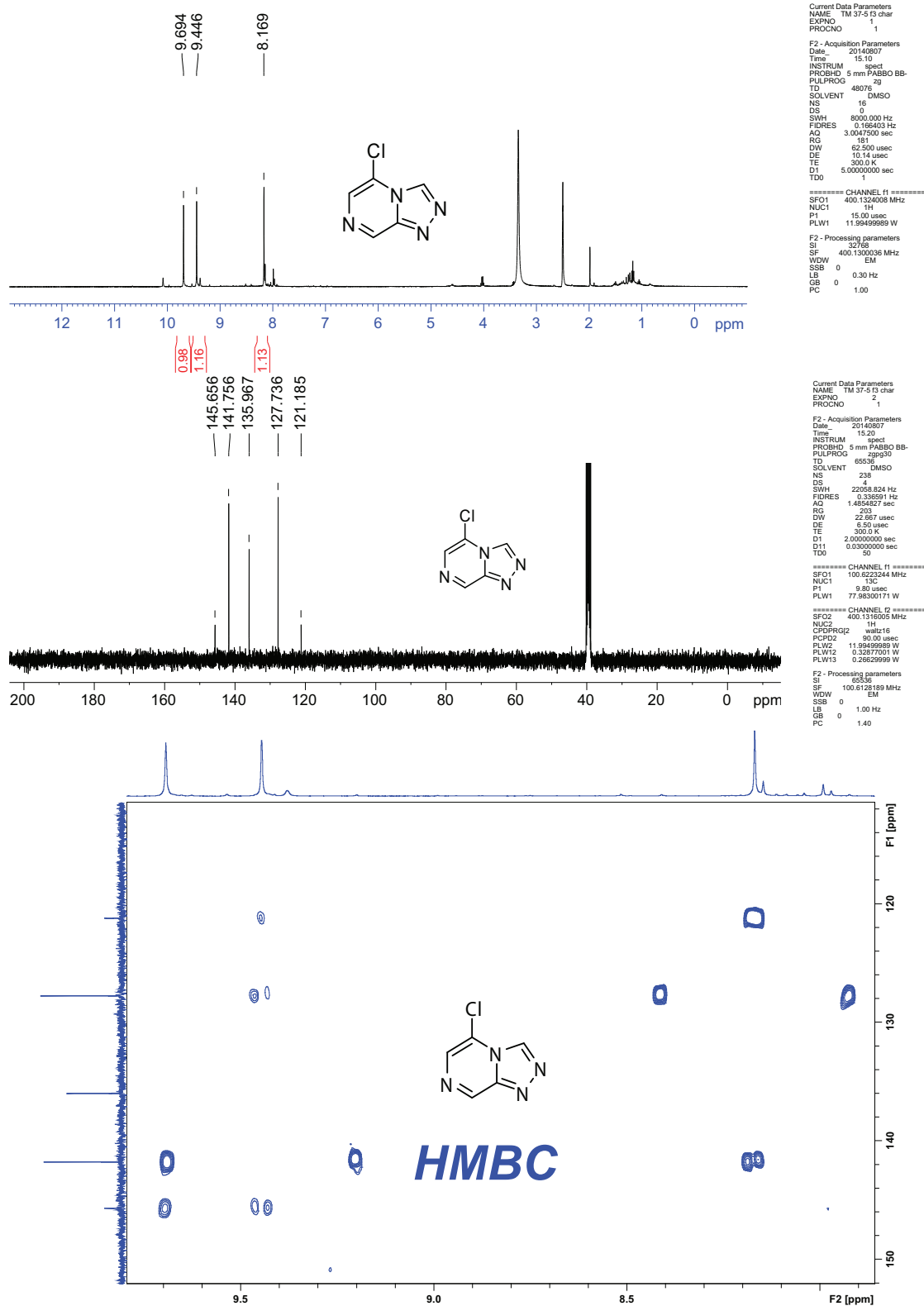
HSQC
HMBC

A.5 *N*-(3-chloro-2-methylphenyl)-3-(4-(difluoromethoxy)phenyl)-

[1,2,4]triazolo[4,3-a]pyrazine-5-carboxamide 21

A.6　5-Chloro-[1,2,4]triazolo[4,3-a]pyrazine 33

A.7   3-Bromo-5-chloro-[1,2,4]triazolo[4,3-a]pyrazine 34